Technische Universität München
Lehrstuhl für Biotechnologie der Nutztiere

Immunodeficient pigs for biomedical research

Marina Đurković

Vollständiger Abdruck der von der Fakultät Wissenschaftszentrum Weihenstephan für Ernährung, Landnutzung und Umwelt der Technischen Universität München zur Erlangung des akademischen Grades eines

Doktor der Naturwissenschaften

genehmigten Dissertation.

Vorsitzende(r): Univ.-Prof. Dr. S. Scherer

Prüfer der Dissertation:

1. Univ.-Prof. A. Schnieke, Ph.D.
2. Univ.-Prof. Dr. E. Wintermantel

Die Dissertation wurde am 20.03.2012 bei der Technischen Universität München eingereicht und durch die Fakultät Wissenschaftszentrum Weihenstephan für Ernährung, Landnutzung und Umwelt am 05.06.2012 angenommen.

Marina Đurković. *Immunodeficient pigs for biomedical research.* Dissertation, Technische Universität München, Munich, Germany, 2012.

Contents

Abstract

In biomedical research fields, such as regenerative medicine or cancer research, immunodeficient mice have provided an invaluable tool. They allow the examination of engrafted human cells under *in vivo* conditions without putting humans at risk. However, the pig is considered a better animal model as it resembles humans more closely than the mouse in regards of size and physiology. In humans, natural mutations leading to inactivation of the Interleukin-2 receptor γ chain (IL2RG) or the Janus kinase 3 (JAK3) genes cause severe combined immunodeficiency (SCID). This disease is characterised by lack or dysfunction of T, B and natural killer cells, as both genes are influencing the function of immunomodulatory cytokines critical in immune response.

This work describes the progress towards an immunodeficient pig model by knock out of IL2RG or JAK3. The targeting vectors used in this study were based on a positive selection approach combined with a visual marker in order to enrich correct events and exclude random integrations. They were also designed with different extents of homology and thus allowed to assess the influence of homology length on gene targeting frequencies. Vectors carrying long homology arms were based on bacterial artificial chromosomes (BAC). The IL2RG targeting BAC produced knock out cells, but these were not viable. The shorter JAK3 conventional vector triggered HR in kidney fibroblasts, bone marrow (BM) and adipose tissue mesenchymal stem cells (MSCs) with frequencies up to 16%. Genetically modified BM-MSCs were used for SCNT and heterozygous JAK3 knock out piglets were born.

JAK3$^{-/-}$ will establish immunodeficiency and phenotype analysis will reveal their potential to engraft human cells and to study their performance under *in vivo* conditions. The results from this study elucidate new approaches, which will be of interest also for the generation of other gene targeted pigs.

Zusammenfassung

Immundefiziente Mäuse sind für die biomedizinische Forschung von unschätzbarem Wert, zum Beispiel auf den Gebieten der regenerative Medizin oder der Krebsforschung. Sie ermöglichen es transplantierte menschliche Zellen unter *in vivo* Bedingungen zu untersuchen ohne dabei Menschen zu gefährden. Das Schwein wird jedoch als besseres Modelltier angesehen, da es dem Menschen im Bezug auf Größe und Physiologie ähnlicher ist als die Maus. Schwere kombinierte Immundefizienz wird beim Menschen durch natürliche Mutationen im Interleukin-2 Rezeptor γ (IL2RG) oder der Janus Kinase 3 (JAK3) ausgelöst. Diese Krankheit ist gekennzeichnet durch ein Fehlen oder die Fehlfunktion der T, B und der natürlichen Killerzellen, da beide Gene für die Funktion immunmodulatorischer Zytokinen in der Immunantwort eine zentrale Rolle spielen.

Diese Arbeit beschreibt die Fortschritte zu einem immundefizienten Schweinemodell, welches durch den Knock-out von IL2RG oder JAK3 erreicht werden sollte. Die Targetingvektoren in dieser Studie, basieren auf Positivselektion kombiniert mit einem sichtbaren Marker. Dies ermöglichte eine Annreicherung korrekter Klone unter Ausschluss von zufälligen Integrationen. Die Vektoren enthielten verschieden lange Homologien um deren Einfluss auf die Häufigkeit von *gene targeting* einschätzen zu können. Vektoren mit langen Homologien basierten auf bakteriellen künstilchen Chromosomen (BACs). Der IL2RG BAC erzeugte Knock-out Zellen, jedoch waren diese nicht überlebensfähig. Der kürzere konventionelle JAK3 Vektor ermöglichte homologe Rekombination in Nierenfibroblasten und mesenchymalen Stammzellen aus Knochenmark (BM-MSC) und Fettgewebe mit bis zu 16% Effizienz. Genetisch modifizierte BM-MSCs wurden für den somatischen Kerntransfer verwendet und JAK3 Knock-out Ferkel wurden geboren.

JAK3$^{-/-}$ Schweine werden immundefizient sein und die Analyse ihres Phenotyps wird ihre Eignung zur Transplantation und Untersuchung menschlicher Zellen unter *in vivo* Bedingungen aufzeigen. Die Ergebnisse aus dieser Studie erläutern des Weiteren neue Ansätze, welche für die Erzeugung anderer genetisch modifizierter Schweine von Interesse sein werden.

1. Introduction

Pre-clinical *in vivo* studies are essential in biomedical research as intensive risk-benefit pre-assessment has to precede any testing of therapies in human patients. Immunodeficient mice have provided an invaluable tool for cell-based studies in basic and application-oriented research. This is based on the fact that they facilitate engraftment of – potentially modified – human cells or tissues and their study within the context of a whole organism. For example, immunodeficient mice are intensively used for the study of fate, function and safety of human stem cell based therapies and thus provide a means for bridging the gap between *in vitro* results and clinical studies (Figure 1.1) [1]. Besides regenerative medicine research, study of basic immunological processes can be performed, e.g. of haematopoiesis with injection of human haematopoietic stem cells into immunodeficient mice [2, 3]. A human immune system established by immune cell injection further allows the investigation of infectious diseases, which normally do not occur in mice, such as acquired immunodeficiency syndrome (AIDS) or Dengue [4–6]. The engraftment of human tumour cells permits the investigation of carcinogenesis, potential therapies and the improvement of imaging techniques for diagnosis in cancer research [7–10].

The high value of mice for basic research cannot be questioned, but correct translation of pre-clinical study results from mice to humans did not always prove to be possible. The pig resembles humans more closely in terms of physiology and has been been suggested as a more suitable animal for some research applications [11–14].

This thesis deals with the generation of immunodeficient pigs in order to meet the need for a better model in biomedical research. This introduction outlines the defects that underlie immunodeficiency in humans and immunodeficient mouse strains currently available. Then suitability of pigs as animal models in biomedical research and methods for the generation of gene targeted large animals will be discussed.

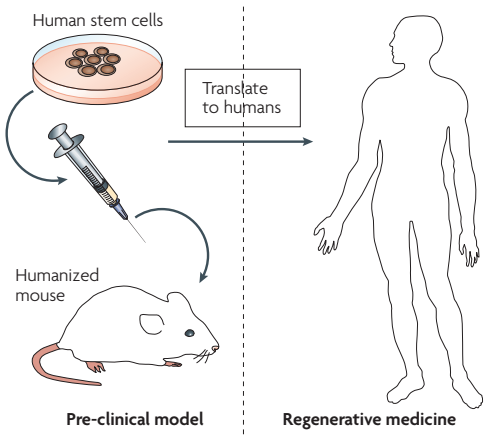

Figure 1.1.: The use of immunodeficient mice in translational biomedical research
Immunodeficient mice engrafted with human cells, e.g. stem cells, bridge the gap between basic *in vitro* studies and the clinic. They are a means for pre-clinical *in vivo* evaluation of the therapeutic potential provided by the engrafted cell [1].

1.1. Severe combined immunodeficiency

In the 20^{th} century, some infants were found to suffer frequently from infections due to impaired immune reaction, which was caused by abnormal numbers of T, B and natural killer (NK) cells. Early death of these young patients motivated the study of this disease, which is today known as severe combined immunodeficiency (SCID).

Glanzmann and Riniker observed immune system impairment in a boy in Zurich in 1950, which is today considered to be the first reported case of human SCID [15]. Although this disease was diagnosed more often in the following years, it was not until 1975 that the world health organisation officially termed it "SCID". The terms "severe" and "combined" imply high lethality rates and the impairment of both cell-mediated and humoral immunity. Intensive effort was put in the search for the genetic cause of SCID during the last decades. Finally, not one single but a broad range of different genetic defects has been associated with immunodeficiency [16–25]. They can be classified according to the underlying, affected mechanism: these are for example, impaired cytokine-mediated signaling, defective V(D)J recombination, impaired pre-T cell receptor signaling and others. Table 1.1 summarises the SCID subtypes, the corresponding defective genes and the T, B and NK cell phenotype regarding the cell number. Depending on the gene's role in immunity, a patient's immune cells can be affected in number and/or in functionality [26].

Today the overall incidence of SCID is about 1 in 40,000 to 75,000 infants. Although the disease is a prenatal disorder as lymphopoiesis starts early in the human embryo, most patients

appear normal at birth. The average time of diagnosis is 4 to 7 months and often takes place only after a manifestation of unusual symptoms, e.g. skin graft versus host disease, already occurred [26].

As early diagnosis, prevention of infections and timely therapy is absolutely necessary for complete healing, SCID is considered a pediatric emergency [27]. Patients can be cured to full recovery of immunity by allogenic bone marrow transplantation from a histoidentical donor as was shown in the first trial in 1968 [28]. This therapy enables survival in up to 97% of patients [29–31]. To overcome the requirement for a suitable donor, gene correction by retrovirus-based gene therapy has been repeatedly and successfully tested [32–34]. However, severe safety problems caused by retrovirus vector integration lead to the death of some patients. If this approach is to become standard therapy for the treatment of SCID, these risks have to be eliminated.

Table 1.1.: Classification of genetic defects in SCID
Different subtypes of SCID can be distinguished depending on the underlying, impaired mechanism. The mutant phenotype with lack (-) or presence (+) of T, B or NK cells is listed, but does not indicate whether immune cell are functional. Adapted from Cossu *et al.* (2010) [26].

Prevalent mechanism/ disease	**Gene**	**T/B/NK**
Impaired cytokine-mediated signaling		
Common γ chain defect	IL2RG	$T^-B^+NK^-$
JAK3 defect	JAK3	$T^-B^+NK^-$
IL7Rα chain defect	IL7RA	$T^-B^+NK^+$
Defects in the pre-T cell receptor		
Defects in V(D)J recombination		
RAG1 defect	RAG1	$T^-B^-NK^+$
RAG2 defect	RAG2	$T^-B^-NK^+$
Artemis defect	DCLRE1C	$T^-B^-NK^+$
DNA-PKcs defect	PRKDC	$T^-B^-NK^+$
DNA ligase IV defect	LIG4	$T^-B^-NK^+$
Cernunnos/XLF defect	NHEJ1	$T^-B^-NK^+$
Impaired signaling through the pre-T cell receptor		
CD3δ defect	CD3D	$T^-B^+NK^+$
CD3ϵ defect	CD3E	$T^-B^-NK^+$
CD3ζ defect	CD3Z	$T^-B^-NK^+$
CD3γ defect	CD3G	$T^-B^-NK^+$
CD45 defect	PTPRC	$T^-B^-NK^{-/+}$
ZAP-70 defect	ZAP70	$T^+B^+NK^+$
p56lck defect	LCK	$T^-B^+NK^+$

Table 1.1 – continued from previous page

Prevalent mechanism/ disease	Gene	T/B/NK
Increased lymphocyte apoptosis		
Reticular dysgenesis	AK2	$T^-B^-NK^-$
ADA-SCID	ADA	$T^-B^-NK^-$
PNP-SCID	PNP	$T^-B^-NK^-$
Defects in thymus embryogenesis		
Nude/SCID Syndrome	WHN	$T^-B^+NK^+$
Complete DiGeorge Anomaly		
DiGeorge Syndrome	>35 genes	$T^-B^+NK^+$
CHARGE	CHD7	$T^-B^+NK^+$
Diabetic mother embryopathy		$T^-B^+NK^+$
Impaired calcium flux		
ORAI1 defect	ORAI1	$T^+B^+NK^+$
STIM1 defect	STIM1	$T^+B^+NK^+$
Other mechanisms		
Coronin-1A defect	CORO1A	$T^-B^+NK^+$
MHC Class II defect	CIITA, RFXANK, RFX5, RFXAP	$T^+B^+NK^+$
Cartilage hari hypoplasia	RMRP	$T^-B^+NK^+$
Hoyeraal-Hreidarsson Syndrome	DKC1, TERT, TINF2, DCLRE1B	$T^+B^-NK^-$
Hereditary folate malabsorption	SLC46A1	$T^+B^+NK^+$

1.2. Impaired cytokine-mediated signaling in immunodeficiency

The majority of SCID cases in humans is caused by impaired cytokine-mediated signaling in immune cells. The so-called γ_C cytokines are of central importance in this context. Two genes are essential for functionality of γ_C signal transduction from the cell surface to the nucleus: the interleukin-2 receptor γ subunit (IL2RG) and janus kinase 3 (JAK3) [35].
In the following section general information about the role of these two genes in SCID are presented. A brief outline of T, B and NK cell activation and details about γ_C cytokine function and signaling will highlight the effects of impaired cytokine-mediated signaling in immunodeficiency.

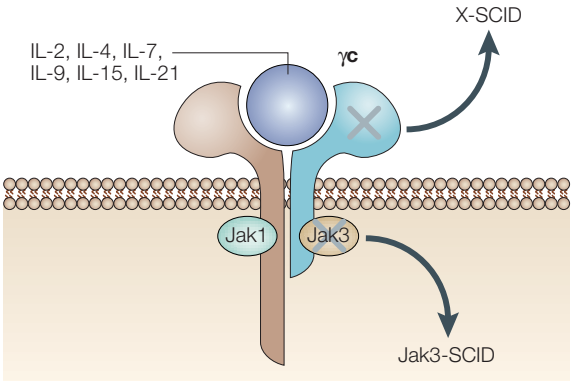

Figure 1.2.: The interplay of γ_C and JAK3 in SCID
The involvement of γ_C and JAK3 in the same signaling pathway leads to equal phenotypes. The defect is inherited in a X-linked recessive or autosomal recessive way, respectively. [49]

1.2.1. Interleukin-2 receptor γ and janus kinase 3 defects

Impaired cytokine signaling caused by mutations in IL2RG results in the most common form of severe combined immunodeficiency and accounts for approximately 50% of cases [35–37]. As the gene is encoded on the X-chromosome, IL2RG deficiency is also referred to as X-SCID or X-linked SCID [16, 37]. Most X-SCID patients are male and exhibit a $T^-B^+NK^-$ phenotype. However, because of random X-chromosome inactivation, females only have reduced numbers of functional T, B and NK cells [38].

The IL2RG gene is approximately 4.2 kb in size and organised in 8 exons. It encodes a 369 amino acid and 64 kD protein containing a fibronectin type 3 domain and an erythropoietin receptor, ligand binding region [39–41]. The protein is termed P64 or CD132, but the more common name IL2RG originates from its first identified binding partner interleukin-2 (IL-2). However, it is shared by several cytokines, including interleukin-2, -4, -7, -9, -15 and -21 [42–49]. Due to this fact, IL2RG is often referred to as the common γ chain or γ_C. The progressive identification of γ_C cytokines and their function revealed that IL2RG mutations affect a broad range of crucial immunological processes.

JAK3 is the sole cytosolic binding partner of IL2Rγ and a critical component of the γ_C cytokine signaling pathway (Section 1.2.4). Thus, mutations in JAK3 cause SCID with a phenotype identical to X-SCID (Figure 1.2) [49]. However, JAK3-based SCID affects both male and female patients equally since it is inherited in an autosomal recessive mode. Its overall incidence is lower and causes approximately 7% to 14% of SCID cases [17, 50–54].

JAK3 is a member of the human janus kinase protein family including also JAK1, JAK2 and TYK2, which have been identified in mammals, birds and fish based on sequence homology [55–59]. Expression analysis proved differential regulation of the JAK proteins. In contrast to

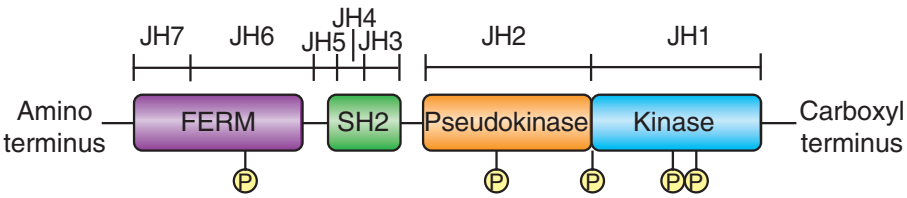

Figure 1.3.: Schematic protein structure of JAK3
The C-terminal kinase domain JH1 is homologous to other kinases and located next to the pseudo-kinase domain, which is responsible for catalytic activity regulation. Src homology 2 (SH2) function is not known. Band-4.1, ezrin, radixin, moesin (FERM) binds cytokine receptors and regulates kinase activity. Phosphorylation sites are indicated. Modified from Yamaoka *et al.* (2004) [59].

JAK1, JAK2 and Tyk2, which are constitutively and ubiquitously expressed, JAK3 expression is inducible and predominantly found in hematopoietic cells [60–62]. The human JAK3 gene is located on chromosome 19 and spans a 23 kb region organised in 24 exons [63, 64]. The 1124 amino acid protein, with a molecular weight of 125 kDa , can be divided in seven janus homology domains JH1 to JH7 (Figure 1.3) [59, 60]: The C-terminal kinase domain JH1 is highly similar to other protein kinases and is located next to the pseudokinase or kinase-like domain JH2. Artificial mutations within this protein domain and patient-derived mutations elucidated its crucial regulatory function, although it does not have catalytic activity. This unique structural feature with these two domains gives JAK kinases their name as it reminds of Janus, the two-faced Roman god. The N-terminal Band-4.1, ezrin, radixin, moesin (FERM) homology domain (JH6-JH7) is responsible for receptor interaction with γ_C, whereas src homology 2 (SH2-like domain, JH3-JH4) function is not fully understood [59].

1.2.2. Activation of NK, T and B cell mediated immunity

The T, B and NK cell phenotype is affected differently in SCID patients depending on the genetic defect. Impairment of cytokine signaling in X-SCID and JAK3-based SCID causes a lack of mature NK and T cells and non-functionality of B cells [27].

NK cells are cytotoxic cells, which kill infected and malignant cells and represent one of the main effector cell types of the innate immune system. They release proteins like perforin and granzyme from cytoplasmic granules and induce apoptosis. NK cells represent early effectors of immunity and confine an infection until a specialised response is triggered by adaptive immunity. After T and B cell activation, NK cells can act concertedly with immunoglobulins in antibody-dependent cell-mediated cytotoxicity. They bind the constant region of antibodies and induce killing of the affected cell. Development and activation of NK cells are dependent on interferons and cytokines including γ_C cytokines (see 1.2.3) [65].

Pathogens capable of avoiding death by the innate immune system require specialised attacks

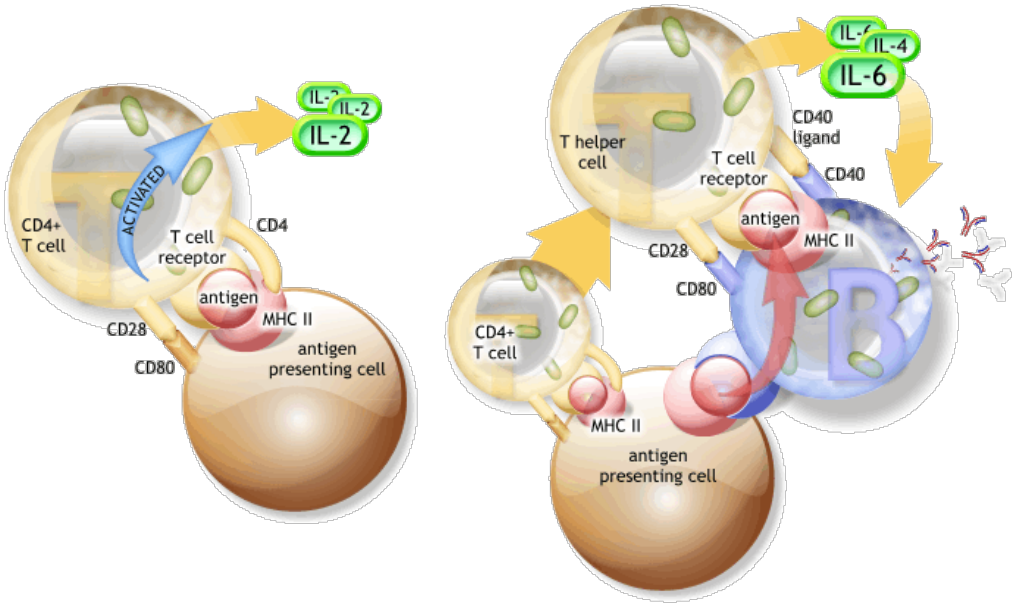

Figure 1.4.: T cell and B cell activation
Recognition of MHC II specific antigen complexes by circulating naive T cells and CD28-CD80 co-stimulation lead to expression of IL-2 and its receptor. $CD4^+$ T helper cells induce B cell activation through direct contact and cytokine secretion [72].

by adaptive immunity. In healthy individuals most circulating lymphocytes in the blood are quiescent. Rapid clonal expansion of specific, resting T cells and differentiation into armed effector and memory cells only takes place upon encounter of the corresponding antigen in the periphery [66, 67]: Initially, infectious particles are taken up by antigen presenting cells (APCs), such as dendritic cells (DCs) and are processed into small antigen peptides. These are transported to and presented at the cell surface via major histocompatibility complex II (MHC II) molecules [68, 69]. Recognition of the presented complexes by the corresponding $CD4^+$ T cell, supported by co-stimulation via CD28-CD80, leads to expression of interleukin-2 and its receptor (Figure 1.4) [70]. IL-2 functions in an autocrine-paracrine manner and induces T cell proliferation and expression of different essential cytokines. As B cells require specific $CD4^+$ T cell help through receptor binding and secretion of activating cytokines, humoral immunity is directly dependent on T cell activation (Figure 1.4) [71].

1.2.3. Function of γ_C cytokines in immunity

Some representatives of the group of γ_C cytokines are of central importance for adaptive immunity activation and maintenance. Whether they induce activating or repressing effects depends on the immune cell types expressing the cytokine and its receptor, which are summarised in

Figure 1.5. The function of the γ_C cytokines was mostly elucidated by study results in knock out mice. Details about the function of γ_C cytokines are given below and, if known, differences between humans and mice are indicated.

Interleukin-2 – also known as T cell growth factor TCGF – promotes proliferation of T cells and stimulates immunoglobulin production by B cells [73–75]. It is responsible for the development of regulatory T cells (T_{reg}) and for regulation of apoptosis [76]. Moreover, it was found to increase natural killer cell cytolytic activity and influence Th_2-type T cell differentiation (Figure 1.5) [75, 77, 78]. Although IL-2 deficient mice show normal lymphoid development, abnormal T cell responses to polyclonal stimuli and increased autoimmune symptoms were reported for aging animals [75, 79].

Signals essential for T cell development and homeostasis, including survival, proliferation and T cell receptor (TCR) rearrangement require regulation via **interleukin-7 (IL-7)**. As a consequence IL-7 receptor α (IL7Rα) deficient mice show reduced thymocyte and peripheral T cell numbers and abnormal response of T cells to polyclonal stimuli. B cells remain present in these mice but early development is defective at the pre-pro stage, indicating its key role in murine B cell maturation [80]. Species-specific differences in IL-7 function have been found between humans and mice. Human patients with SCID have reduced thymic cell numbers, whereas mice have normally developing thymic T cells. Possibly, significant numbers of $CD4^+$ cells result from the murine alternative IL7R ligand thymic stromal lymphopoietin (TSLP) [81].

Interleukin-4 (IL-4) is a key cytokine for $CD4^+$ T helper 2 (Th_2) cells. It plays a central role in regulating the differentiation of antigen-stimulated naive $CD4^+$ cells by induction of expression of IL-4 itself and a series of other cytokines including IL-5, IL-6, IL-9, IL-10 and IL-13 [7, 8]. Th_2 mediated immune responses are linked to development of asthma and allergy. Furthermore, IL-4 suppresses the appearance of interferon γ producing $CD4^+$ T helper 1 (Th_1) cells and is also involved in immunoglobulin class switching to IgG1 and IgE [82]. Mice deficient for IL-4 or IL-4Rα show severely compromised Th_2 differentiation and decreased IgG1 and IgE serum levels [83, 84].

In cooperation with IL-4, **Interleukin-21 (IL-21)**, which is the γ_C cytokine identified most recently, regulates Ig production [85]. Furthermore, it controls Th_1 differentiation, but the underlying mechanisms are still poorly understood [86, 87].

Interleukin-15 (IL-15) is involved in regulation of NK cell development and memory cell homeostasis. It shares not only the receptor γ chain with IL-2, but also the receptor β subunit [47]. Although *in vitro* many of its biological functions, such as T cell proliferation induction, are similar to IL-2, its influence on NK cells *in vivo* is very different: For example, IL-2 and IL2Rα deficient mice generally show normal T cell and NK cell development, whereas IL2Rβ deficient mice have highly decreased NK cell and γ/δ T cell numbers [88, 89]. Moreover, IL-15 or IL15Rα deficient mice show a lack of NK cells, decreased numbers of $CD8^+$ T cells and almost complete lack of

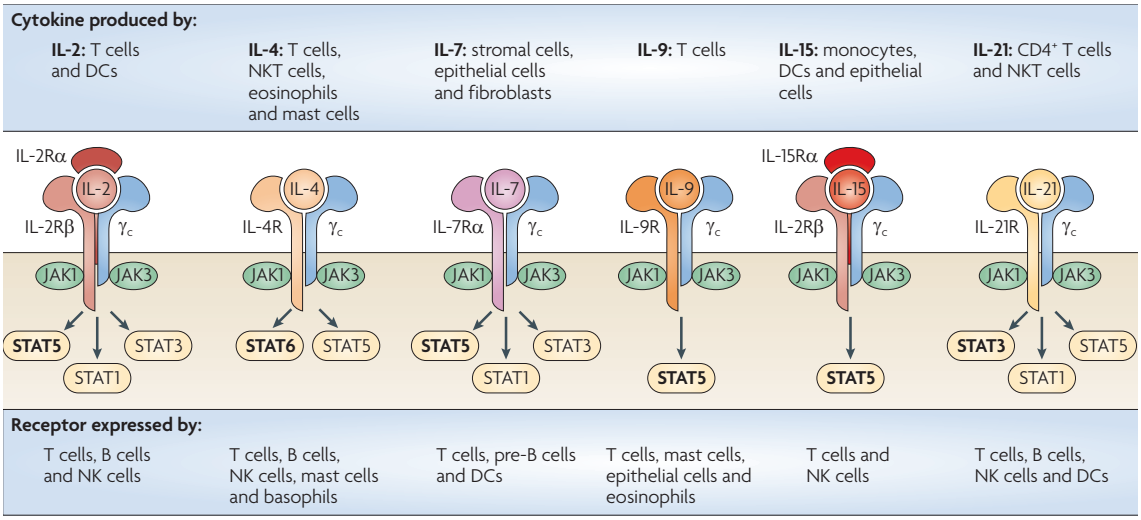

Figure 1.5.: Expression, signaling and target cells of γc cytokines
γc cytokines and their receptors are expressed by different immune cell types and signal via different JAK and STAT molecules. [92].

memory $CD8^+$ T cells. These results indicate that *in vivo* IL-15 is responsible for the development and differentiation of NK and $CD8^+$ memory T cells [90, 91].

Interleukin 9 (IL-9) is a late acting T cell and a mast cell growth factor. Hence, IL-9 deficient mice generally develop normally, but show excessive mucus.

Taken together, the $T^-B^+NK^-$phenotype found in X-SCID patients can be attributed mainly to defective signaling of IL-7, IL-15, IL-4 and IL-21. Proper T cell function requires IL-7. IL-15 defects are responsible for NK cell dysfunction and the combination of IL-4 and IL-21 defective signaling causes an intrinsic B cell defect. The interplay of these cytokines in survival, clonal expansion and differentiation of immune cells is summarised in Figure 1.6.

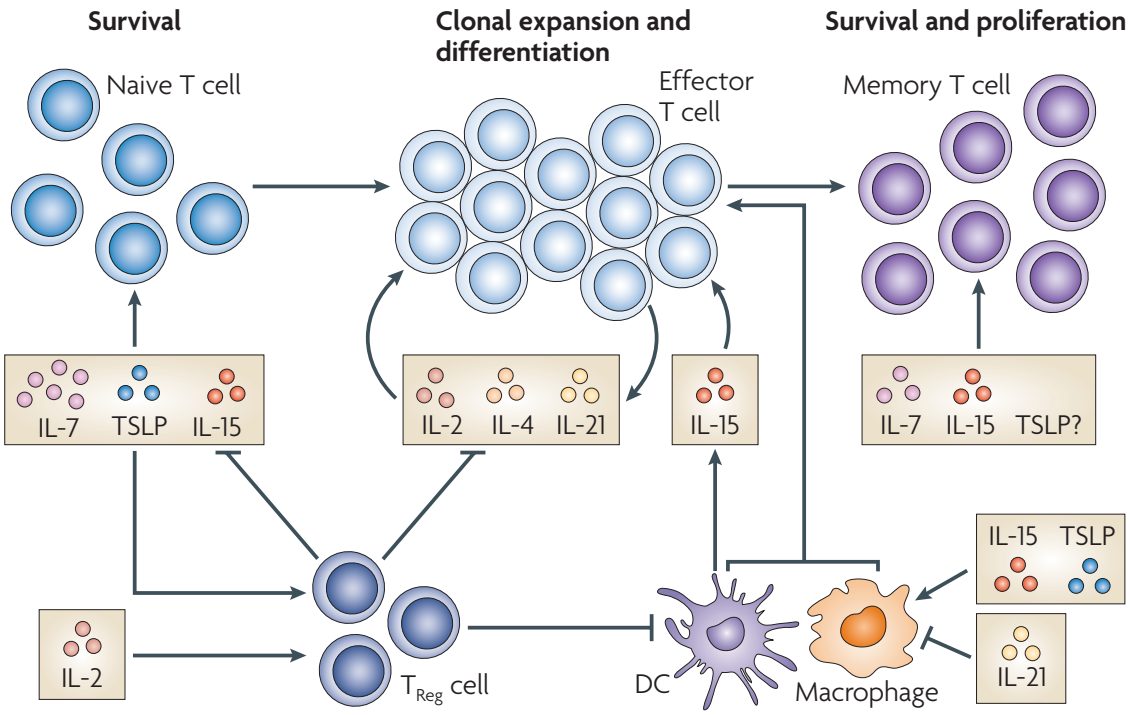

Figure 1.6.: γ_C cytokines in immunity regulation
γ_C cytokines regulate the complex network of immune cell survival, activation, homeostasis and differentiation. IL-7 and IL-15 exhibit a positive effect on naive and memory T cell survival. IL-2, -4, -15 and -21 are involved in clonal expansion and differentiation of effector T cells. Regulatory T are regulated by IL-2 and are responsible for naive and effector T cell homeostasis. IL-21 and IL15 act as counterparts in macrophage regulation [92].

1.2.4. Signaling pathway of γ_C cytokines

Signaling via IL2Rγ chain has been studied first for IL-2 based signal transduction initiation that requires the formation of a quaternary complex by the three receptor subunits α, β, γ and the cytokine IL-2. This quaternary complex formation takes place in three steps. The β and γ subunits have very low or no detectable binding affinity for IL-2, respectively [93, 94]. As IL-2 concentrations increase to high levels after T cell activation (see 1.2.2), β and γ together form an intermediate affinity receptor (Kd$\approx$1 nM). The α subunit is a low affinity receptor [95] that is neither physically bound to the other two subunits, nor directly involved in signal transduction. However, it is postulated to possibly induce a conformational change in IL-2 and to stabilise the tertiary complex [94]. Finally, complex formation involving all three subunits results in a high affinity receptor (Kd$\approx$10 pM) detectable on activated T cells.

Heterodimerisation of the cytoplasmic regions of IL2Rβ and IL2Rγ is necessary and sufficient for effective signal cascade initiation [96]. It results in activation of three different signaling pathways: the Ras-mitogen activated protein kinase (MAPK) pathway, Phosphoinositide 3- kinases (PI3K-Akt) pathway and – of central importance – the JAK-STAT pathway [97–100].

Janus kinase 3, a cytoplasmic tyrosine kinase associated with IL2Rγ, initiates the JAK-STAT signaling cascade. IL2Rβ associated JAK1 and IL2Rγ associated JAK3 dimerise in the cytosol upon formation of the quaternary IL-2 receptor complex (Figure 1.7). They activate each other and phosphorylate the receptor. Signal transducers and activators of transcription (STATs) can bind to the receptor phosphorylation sites and are subsequently phosphorylated by the tyrosine kinases themselves. The activated STATs dimerise, translocate into the nucleus and induce transcription of immunemodulatory genes, such as interferon γ (IFNγ) and tumour necrosis factor alpha (TNFα). Which of the seven known STAT protein family members is activated after γ_C induced signaling, depends on the signaling cytokine and the affected cell type as listed in Figure 1.5 [101, 92].

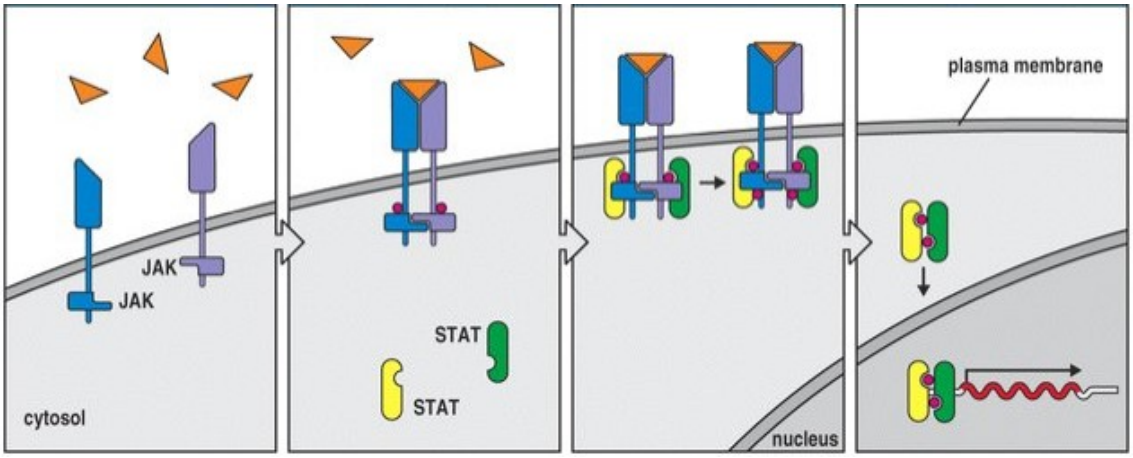

Figure 1.7.: The JAK-STAT signaling pathway
Formation of the quaternary IL-2 complex leads to dimerisation and phosphorylation of JAK1 and JAK3 in the cytosol. In turn the JAK proteins phosphorylate STAT proteins, which subsequently dimerise and translocate into the nucleus. There STATs function as transcription factors for various immunity involved genes, such as TNFα or IFNγ. [65].

1.3. V(D)J recombination defects in immunodeficiency

For the recognition of a huge diversity of antigens by the adaptive immune system, a large repertoire of specific T cell receptors and immunoglobulins is required. Due to limited space in the genome, immune cell receptors are encoded by a few hundred gene segments, which can be combined to a high variety of possible receptors [102]. This takes place in the process of V(D)J recombination during early lymphocyte development. Defects in several genes involved in this receptor rearrangement have been associated with SCID. Patients thereby show a $T^-B^-NK^+$ phenotype [19, 103].

1.3.1. V(D)J recombination

The immune receptor gene segments encoded in multiple variants and arranged to a single immune receptor are named variable (V), diversity (D) and joining (J) segments (Figure 1.8). For this reason the process of receptor rearrangement is also named V(D)J recombination. Thereby, DJ recombination is carried out first, followed by VDJ joining [102]

The key factor for VDJ recombination is the RAG recombinase, which is a protein complex built by the recombination activating genes 1 and 2 (RAG1 and RAG2) and takes place in two phases (Figure 1.9). They bind to specific recombination signal sequences (RSS) that flank V, D and J segments. 12RSS and 23RSS are distinguished according to the base pair length of the RSS spacer region between conserved heptamer and nonamer elements. After the binding

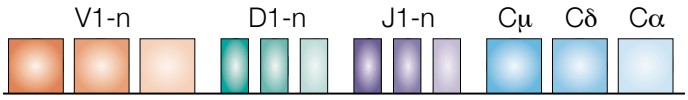

Figure 1.8.: V, D and J segments
Multiple variants for V, D and J receptor gene segments are encoded before early lymphocyte development and are recombined during V(D)J recombination. Constant regions (C) are recombined in a later phase. Modified from [102].

of one RSS by RAG, second RSS capture and paired complex formation takes place during so-called synapsis. The double strand breaks between gene segments and RSS are rejoined: either by non-template nucleotide addition or by nucleotide loss caused by non-homologous end joining DNA repair factors or terminal deoxynucleotidyl transferase, respectively. During DNA cleavage RAG recombinase first catalyses phosphodiester bond hydrolysis by introduction of a single strand DNA nick. The 3' hydroxyl group is then free to attack the opposite DNA strand and to lead to formation of a hairpin-sealed coding end and a blunt signal end [104].

1.3.2. RAG1 and RAG2 deficiency in SCID

As listed in Table 1.1, several genetic defects can cause impaired V(D)J recombination. The RAG recombinase was determined as a SCID candidate gene relatively early and RAG1 and RAG2 genetic defects account for approximately 3.5% of cases [35]. Briefly, the two genes are located close to each other on chromosome 11 in humans and have a size of 11.7 kb (RAG1) and 6.3 kb (RAG2) [105, 106]. The 1040 amino acid RAG1 protein has domains responsible for the binding of RSS heptamers and nonamers, RAG2 binding and DNA cleavage activity. RAG2 (527 amino acids) has no DNA binding affinity itself, but enhances DNA binding affinity and specificity of the RAG recombinase. Furthermore, it has cleavage activity and a domain for catalytic activity improvement of the RAG recombinase [107, 104]. Consequently, mutations preventing RSS or DNA binding and DNA cleavage can lead to impaired function of the RAG complex.

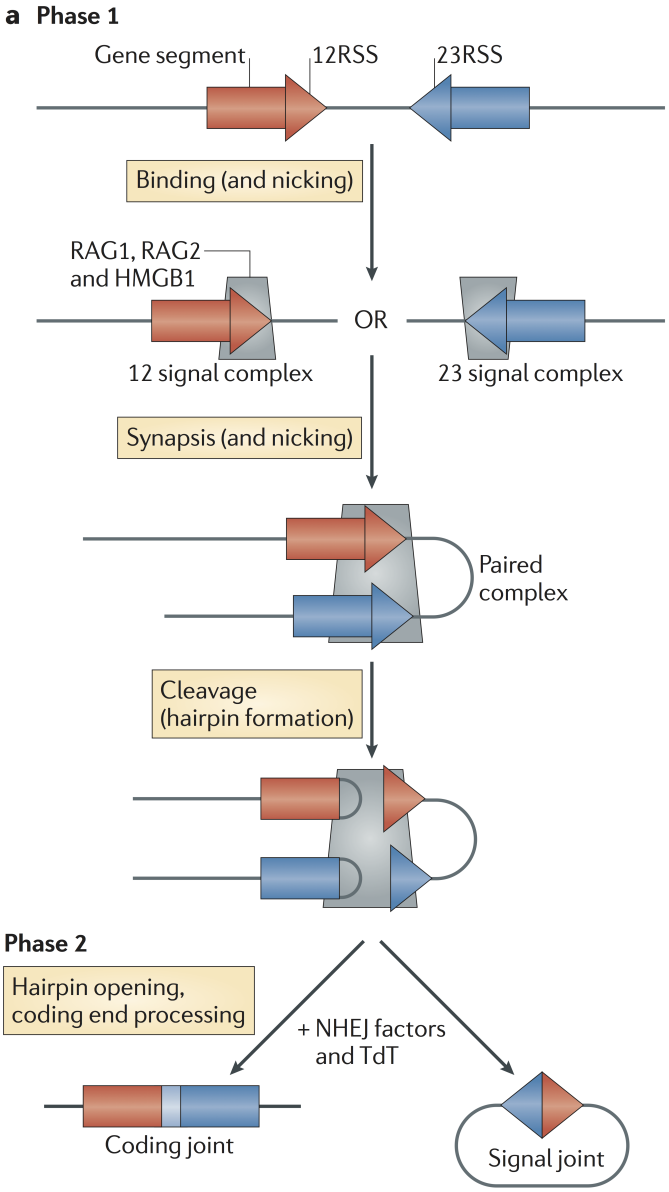

Figure 1.9.: V(D)J recombination
A: RAG1 and RAG2 proteins bind the gene segment flanking recombination signal sequences (RSS) 12 signal complex or the 23 signal complex, respectively. They induce formation of a paired complex and produce double strand breaks between the gene segments and the RSSs. Nucleotides are lost under involvement of non homologous end joining (NHEJ) DNA repair factors or non-template nucleotides are added (light blue rectangle) by terminal deoxynucleotidyl transferase (TdT). Modified from [104].

1.4. Immunodeficient mice for cell-based biomedical research

Immunodeficient mice are intensively used in biomedical research fields, such as oncology or regenerative medicine as the study of human cells under *in vivo* conditions is essential in these areas. Early immunodeficient mouse strains have been constantly optimised regarding the suitability for human to mouse xenotransplantation. The currently available strains differ in the type of mutation and genetic background. Both factors influence the level of human cell engraftment, residual activity of NK cells and innate immunity [1]. Table 1.2 gives an overview of the most important immunodeficient mouse strains and their characteristics discussed below.

The starting point for human to mouse xenotransplantation was the discovery and characterisation of a spontaneous mutation of protein kinase, DNA activated, catalytic polypeptide (Prkdc) in CB17 mice [108]. This strain - referred to as CB17-SCID - was used for transplantation of human peripheral blood mononuclear cells (PBMCs) [109], fetal liver and thymic tissue [110] and hematopoietic stem cells (HSCs) [111]. However, poor performance with low levels of engraftment and high residual immune activity required further optimisation [111]. NOD-scid (non-obese scid) mice resulting from crossing of CB17-scid and NOD mice functioned better in both aspects [112]. However, offspring defective for Prkdc in general showed reduced lifespan due to high radiosensitivity as the gene is involved in DNA repair [113]. This presented a major drawback, especially for long-term studies requiring extended observation.

To overcome this problem, recombination activating genes 1 or 2 (RAG1, RAG2) deficient animals were established. RAG$^{-/-}$ animals do not develop mature T or B cells, but residual NK cell activity and innate immunity remains [114]. The combination of RAG deficiency with other modifications, e.g. knock out of perforin or β-microglobulin reduced this problem, but other complications, such as rapid thymic lymphoma development, were reported [115, 116]. Finally, most of the drawbacks of immunodeficient mouse strains developed earlier were resolved with one major improvement: Targeted mutation of IL2RG lead to severe defects in T and B cell development and to a lack of NK cells. IL2RG$^{-/-}$ mouse strains were independently generated by several groups in parallel and differ mostly in terms of the genetic modification, e.g. with expression of a truncated IL2Rγ protein or no protein expression at all [117, 3, 1]. The potential of IL2RG$^{-/-}$ strains to engraft human cells exceeded all previously developed strains and was further improved by further crossbreeding, e.g. with RAG2 deficient animals [118, 119].

Table 1.2.: Immunodeficient mouse strains
Mutated genes and main characteristics are listed. Prkdc: protein kinase, DNA activated, catalytic polypeptide, NOD: non-obese SCID, Prf1: Perforin 1, BALB: Bagg Albino. Adapted from [1].

Mutant allele	Common strain name	Advantages and Disadvantages
Prkdc^{scid}	CB17-scid	No mature T and B cells Radiation sensitive High level of innate immunity and NK-cell function Leaky Very low level of engraftment of human cells
Prkdc^{scid}	NOD-scid	No mature T and B cells Low but present NK-cell activity Decreased but residual innate immunity Increased engraftment of human HSCs and PBMCs Radiation sensitive Decreased lifespan owing to thymic lymphomas
Rag1^{tm1Mom}	NOD-Rag1$^{-/-}$	Lack of mature T and B cells Radiation resistant Low but present NK-cell activity Residual innate immunity Low and variable level of engraftment
Rag1^{tm1Mom} Prf1^{tm1Sdz}	NOD-Rag1$^{-/-}$ Prf1$^{-/-}$	Lack of mature T and B cells Radiation resistant Very low NK-cell cytotoxicity Lack of perforin High level of engraftment of human PBMCs Very low NK-cell killing but NK cells still present Limited engraftment of human HSCs
Rag2^{tm1Fwa} Il2rg^{tm1Sug}	BALB/c-Rag2$^{-/-}$ Il2rg$^{-/-}$	No mature T and B cells NK cells absent Further reduction in innate immunity Higher level of human cell engraftment Development of functional human immune system Radiation resistant Seem to lack some human-specific cytokines required for human cell development and survival Lack appropriate MHC molecules for T cell selection in the mouse thymus

1.5. Pigs in biomedical research

Rodents, especially mice, are commonly used as animal models in research. Their size makes them easy to handle and inexpensive to keep. Mice also reproduce rapidly, due to early sexual maturity and large litter size. Early availability of the complete genomic sequence and a broad range of genetic manipulation technologies provided a strong basis for the study of basic genetics and genetic disorders. However, there is an urgent need for a model organism that resembles the human body more closely as significant differences between mouse and man restrict correct translation of pre-clinical study results into human therapy.

The common pig, *Sus scrofa*, represents a suitable animal model in many regards. Remarkable similarities are found between pigs and humans in terms of anatomical, physiological, immunological, metabolic and nutritional characteristics. Breeding and keeping is cost-effective and well established for pigs as they present the main source of meat in the industrial world. Breeding is also fast, due to litter sizes of 10 to 12 piglets and a short gestation period of 114 to 115 days. Sexual maturity is reached after 5 to 8 months and more than two litters can be obtained per sow and year [120–122].

Due to these characteristics, pigs are already used as standard animal models in some biomedical research fields: For example, in immunological studies regular collection of sufficient blood volumes is not restricted in pigs as compared to mice. Other anatomical aspects, such as body weight, organ size and orientation, are important parameters especially in regenerative medicine. For example, bone and joint regeneration require correct physiological pressure as key regulatory factor not given in mice [123]. Nearly identical heart size and rates, mean arterial pressure and myocardial blood flow in humans and pigs make them interesting for the study of cardiovascular conditions, such as arteriosclerosis and myocardial infarction [124, 125].

Furthermore, transgenic porcine animals are available today. One example are α-1,3-galactosyltransferase (GGTA1) gene targeted pigs, which are important in xenotransplantation. In this field transplantation of porcine organs into humans is investigated to overcome donor organ shortage. The GGTA1 knock out pigs do not express the galactose-α(1,3)-galactose (Gal) protein epitope on blood vessel epithelium, which is also not expressed in humans. As it causes hyperacute rejection of the donor organ by antibody recognition, elimination of this protein is essential for xenotransplantation [126, 127].

.

1.6. Generation of transgenic animals

First animal models for human disease were obtained by identification of spontaneously occurring mutations leading to a phenotype of interest. Today, various technologies for the generation

of transgenic animals are available. They can be grouped in precise and non-precise genetic modification methods and are briefly outlined in the following section.

1.6.1. Non-precise genetic modification

The introduction of specific exogenous sequence information was rendered possible in the 1980s, after random mutagenesis had been used for years. Methods established for this purpose were virus injection into the blastocoel cavity of the blastocyst, sperm-mediated transgenesis and microinjection of foreign DNA into the male pro-nucleus of a fertilized oocyte [128–130]. Initial experiments in mice were soon followed by transgenic livestock, e.g. pigs, sheep and rabbits generated by DNA microinjection [131] and lentiviral transduction of oocytes [132].

Despite the success of these studies, there are important drawbacks in the application of the mentioned techniques. They all have a non-precise character leading to unpredictable transgene expression due to random and multiple copy integration [133]. Restriction of these techniques to exogenous gene addition inspired scientists to develop methods for precise modification of endogenous sequence information referred to as gene targeting.

1.6.2. Precise genetic modification

Gene targeting methods allow precise genetic modification, such as gene knock out, knock in or gene replacement. They are based on the mechanism of homologous recombination (HR) taking place between exogenous modified DNA introduced into a target cell and a homologous target locus on the chromosome.

In mammalian cells the first gene targeting experiment of an endogenous gene was performed in 1985 by Smithies *et al.* [134]. For this and many following experiments the previously established protocols for isolation and cultivation of pluripotent embryonic stem cells (ES cells) were of central importance [**? ?**]. Mouse ES cells are characterised by self-renewal capacity and the ability to differentiate into tissue derived from all three germ layers including the germ line. They empowered scientists to genetically manipulate and inject these cells directly into the blastocyst. ES cells taking part in the development of the animal lead to the generation of chimeric mice [135, 136].

However, despite various attempts, definitive ES cells have not been isolated from livestock, such as cattle, pig and sheep, but only from human, rat, rabbit, goat and monkey [137–143]. To circumvent this problem, the somatic cell nuclear transfer (SCNT) was established as an alternative method for the generation of transgenic animals. A genetically modified somatic donor cell is injected into and electrofused with an enucleated oocyte (Figure 1.10). Culture to blastocyst stage and embryo transfer into a hormonally stimulated foster mother leads to the birth of transgenic, non-chimeric offspring [144]. Originally, suitable donor cells for nuclear transfer in

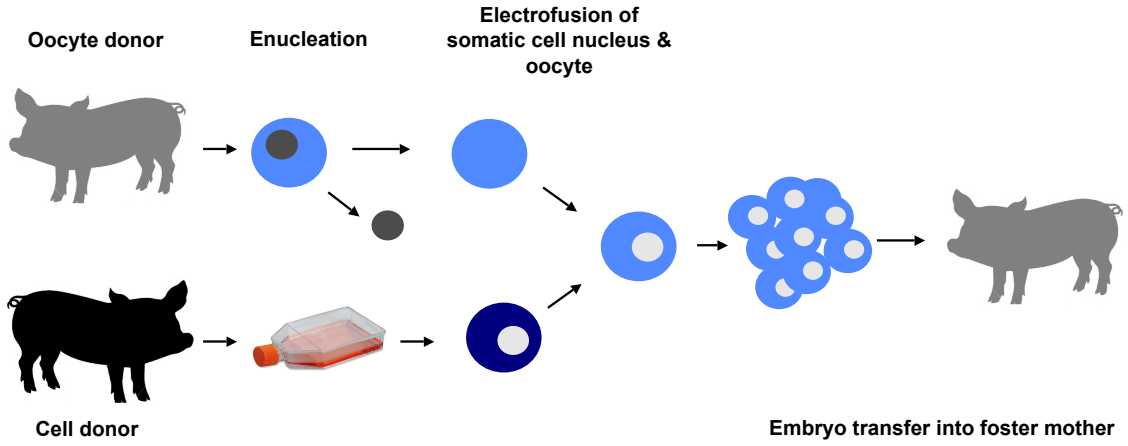

Figure 1.10.: Generation of transgenic livestock by SCNT
A genetically modified somatic cell is fused with a enucleated oocyte. After culture to blastocyst stage, transfer of blastocyst into the uterus of a hormonally stimulated foster mother is performed.

mice and large animals were restricted to embryonic blastomeres [145, 146]. However, with the establishment of SCNT a broad range of cell types became applicable. For example, thus far SCNT has been conducted with mammary epithelial cells, fetal fibroblasts, cumulus and muscle cells [147–150]. That way also different transgenic livestock species, e.g. sheep, pig, cow and goat have been generated [132, 148, 151–154]. However, efficiencies for transgenic livestock generation are still poor and different optimisation steps, which are discussed in the following section, have to be considered.

Optimisation of transgenic livestock generation

Generation of transgenic mice with mES gene targeting and subsequent blastocyst injection is very effective, due to high HR rates and the simplicity of the techniques used. HR efficiency in ES cells ranges between 10^{-5} and 10^{-9} and is reported to be two orders of magnitude higher than in somatic cells [155]. However, as long as ES cells have not been isolated from livestock, the success rate for generation of transgenic large animals can only be improved by optimisation of parameters involved. Henceforward, the main goals are the increase of targeting efficiency by optimised targeting vector design, the choice of suitable target cells and the optimisation of SCNT conditions.

Target cell choice and culture conditions The target cell chosen for a gene targeting experiment has to fulfill certain criteria as the cell critically influences both targeting efficiency and SCNT success. Proliferative capacity is an essential factor as gene targeting experiments involve

a long process of transfection, selection and analysis. Time in culture has to be reduced as far as possible since early senescence of nuclear donor cells can limit their application in SCNT [127]. For example a total number of approximately 45 population doublings has been estimated for fetal tissue cells [156]. Currently, strategies to prolong cell life spans and thus to improve gene targeting and NT efficiencies suggest the usage of early passage cells. Methods further increasing the lifespan of cultured cells, e.g. by addition of proliferation improving agents to the culture medium or culture at low oxygen tensions are also considered [157, 158]. Moreover, suitable transfection methods have to be available. Electroporation, lipofection and other systems, including viral delivery, are commonly used, but have to be optimised for each vector and cell type [136].

Beside supporting successful gene targeting, the chosen cell type is also required to be suitable for production of healthy animals by SCNT. During nuclear transfer the somatic cell nucleus has to be set back to the developmental status of an embryo, a process called reprogramming. Although different cell types have been used for SCNT successfully, generation of gene targeted large animals remains difficult. Even in SCNT with non-modified cells, only 0% to 4% of reconstructed embryos develop to surviving young animals [159].

Targeting vector design Random integration of the targeting vector in the genome occurs 30,000-40,000 times more frequently than HR [160]. To overcome this problem different vector designs can be used for enrichment of HR events schematically depicted in Figure 1.11.

First, promoter-driven positive markers flanked by homology sequences are classically used to select for stably transfected cells. The most common markers are antibiotic resistance genes, such as neomycine, hygromycine, blasticidine and puromycin. Negative selection of random integration events can be achieved by a promoter-driven negative selection marker. Located on the targeting vector backbone it is only expressed after random vector integration [161]. The most prominent negative selection markers used are *herpes simplex virus* thymidine kinase (HSV-TK) and *diphteria* toxin A [162]. Enrichment up to 10,000 fold was reported for the most effective vector design – the promoter-trap. Hereby, a promoter-less positive selection marker comes under expression control of the endogenous target gene promoter after correct HR. Gene targeting efficiencies in this early study ranged between 9% and 32% [163]. However, this method requires the promoter to be active and hence target gene expression. For cases with inactive target gene methods for expression induction are discussed. However, if available, somatic target cells should be chosen that do express the gene of interest.

Targeting efficiency correlates with the extent of homology between targeting vector and target gene locus. In mouse ES cells it was reported to positively correlate with HR efficiency. Total homology length of approximately 14 kb with minimum 1 kb continuous homology was reported to be most efficient in mice ES cells [165, 166]. For somatic cells only little is known about vector

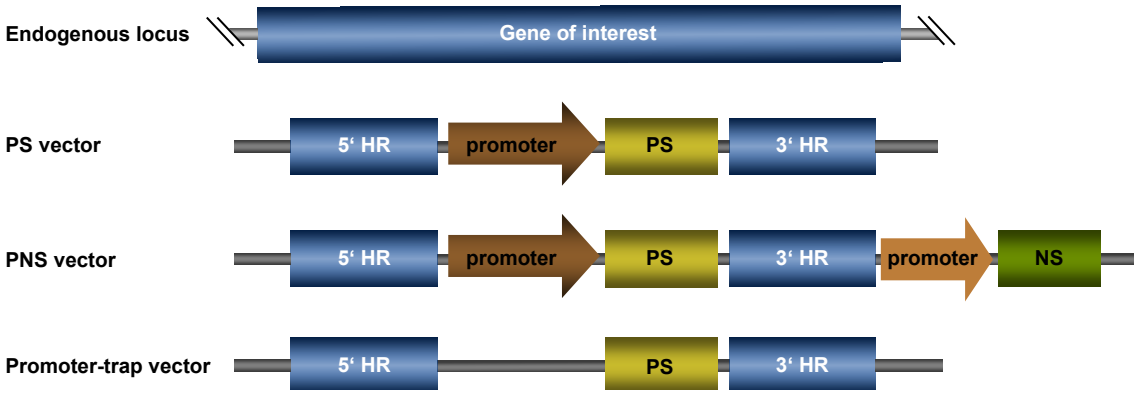

Figure 1.11.: Targeting vector design
Simple positive selection by constitutive promoter driven expression can be performed alone or combined with a negative selection marker. With HR the marker is lost, whereas for random integration gene expression leads to cell killing. The promoter trap vector contains a selective marker without a promoter. Those cells survive in which the vector was placed behind an endogenous active promoter. PS: positive selection, PNS: positive-negative selection. Adapted from [164].

size requirements. Most vectors range between approximately 6 and 12 kb, but even sizes down to 0.75 kb have been used for one homology arm. However, sequence homology below 1 kb was reported to lead to decrease in correct HR with rearrangements and multiple integrations [164]. In general, homology arms are often constructed in a way to enable PCR based screening across the short arm. Targeting vectors based on bacterial artificial chromosomes (BACs) can be constructed. However, their design and cloning is often more complicated compared to conventional targeting vectors and will be discussed in Section 1.6.3.

Beside the discussed strategies, the use of a viral nuclear localisation signal (NLS) and cell synchronisation were reported to boost targeting efficiency. The NLS triggers active transport of the vector into the nucleus. Thus, nuclear envelope breakdown during cell division is not required. Combination of positive selection, the NLS approach and cell synchronisation in S phase prior to transfection further improved results, since HR mainly takes place in late S/G2 phase. In this study gene targeting efficiency was increased from 0% with positive selection alone to 32% with the combined approach [167].

High efficiency homologous recombination is possible with induction of site-specific double strand breaks (DSB) introduced by custom designed zinc finger nucleases (ZFN). ZFNs contain three to four DNA-binding zinc finger proteins coupled to a FokI restriction endonuclease. Each zinc finger protein is designed to recognise a specific DNA triplet. The combination of two ZFNs, which bind on complementary strands of a locus, permit DNA break induction by dimerisation of FokI. The cellular repair machinery is activated with the recognition of a DSB that can be repaired by HR [168]. Alternatively, non-homologous end joining (NHEJ) can take place and cause loss

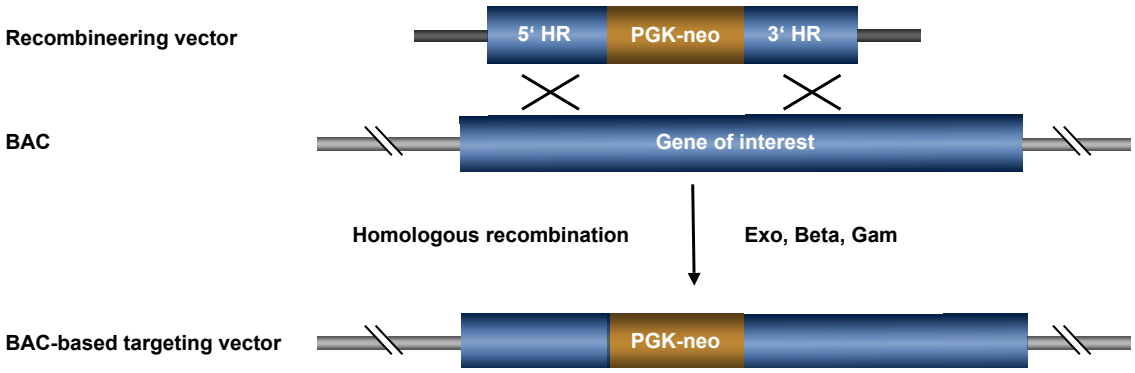

Figure 1.12.: Recombineering
BAC modification during recombineering takes place by homologous recombination in *E. coli*. Therefore, both BAC and a small, linear recombineering vector containing the desired modification is introduced into the bacteria. HR screening is performed by selection and PCR.

or addition of bases in the process of strand rejoining. HR can be triggered by additional delivery of a targeting vector homologous to the 5' and 3' flanking regions of the DSB. Hence, defined genomic alterations can be specifically introduced by using this mechanism, e.g. specific gene knock out by simultaneous introduction of a selectable marker [169]. Thus far, ZFN based gene targeting has been successfully demonstrated to work for generation of transgenic rats, rabbits, pigs and zebrafish [170–173].

1.6.3. Production of BAC-based targeting vectors by recombineering

Homologous recombination efficiency correlates with the length of homology between the targeting vector and the genomic region to be modified. Thus, for gene targeting approaches with efficiencies expected to be very low, application of vectors with longer homologous arms is preferable. This is the case, for example, when the target gene is not expressed in the target cell type and hence, a promoter trap approach cannot be used for HR enrichment. For this purpose bacterial artificial chromosomes (BACs) can be used as gene targeting vectors. In contrast to plasmids, BACs can carry large inserts up to approximately 300 kb [174].

However, due to their large size, modification of BACs by conventional cloning techniques is difficult as unique restriction sites are often lacking. In order to overcome this drawback and to be able to introduce selectable markers or mutations into a BAC-based targeting vector, the technique of recombineering was developed. Recombineering (recombination-mediated genetic engineering) is based on the principle of BAC-DNA modification by homologous recombination in *E.coli*. HR takes place between the BAC and a linear DNA fragment carrying the desired modification flanked by short (50 to 500 bp) homologous arms (Figure 1.12) [174].

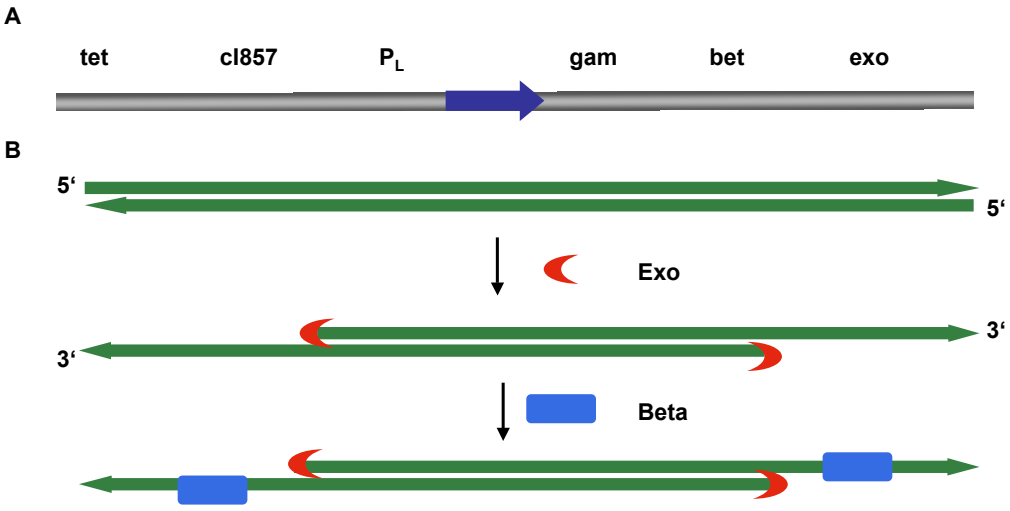

Figure 1.13.: The bacteriophage λ recombineering system
A: The defective prophage (blue) is integrated into the *E.coli* chromosome and phage genes exo, bet and gam are expressed under the control of the P_L promoter and the temperature-sensitive repressor cI857. Exposure to 42°C for 15 minutes induces gene expression and enables HR. B: The 5'-3' exonuclase exo binds linear, dsDNA and cleaves to form 3' overhangs. Beta binds the single stranded 3' overhangs and promotes HR between the linear recombineering vector and the BAC to be modified. Adapted from [174].

Today different recombineering systems have been developed. The λ-encoded Red system is used very often. In this case successful HR is driven by the λ phage encoded genes gam, exo and bet. In order to prevent degradation of the linear DNA targeting cassette, gam inhibits *E.coli* RecBCD exonucleases (Figure 1.13 B). Exo is a 5'-3' exonuclase itself, which produces 3' overhangs from the introduced linear dsDNA. After binding of the resulting single-stranded 3' overhangs by bet – a pairing protein – annealing and HR between the complementary DNA sequences is triggered [175].

In some recombineering-systems the λ Red genes are expressed from multicopy plasmids. Alternatively, a defective prophage, stably integrated into the *E.coli* host genome is used (Figure 1.13 A). Tight repression of gam gene expression is essential as RecBCD defectiveness causes decreased cell viability and plasmid stability. Rapid gene expression induction is mediated by the strong phage promoter pL, which is controlled by the temperature-sensitive repressor CI857. Bacteria are cultured at 32°C to maintain an active repressor. Repressor inactivation and very high levels of HR can be achieved quickly within only 15 minutes of culture at 42°C [176]. Screening for successful recombination is easy when selectable markers applicable in *E.coli* are introduced into the BAC. Selection for neo is possible with G418 or kanamycin in eukaryotes and bacteria, respectively [177].

1.7. Objective of the study

The objective of this study was the generation of immunodeficient pigs for biomedical research. For that purpose one of the two most common genes causing human immunodeficiency — interleukin-2 receptor gamma chain and Janus kinase 3 — had to be knocked out by gene targeting. For this purpose different vector types had to be constructed: For IL2RG a BAC-based targeting vector, for JAK3 a BAC-based and a conventional targeting vector were designed and transfected into porcine mesenchymal stem cells and kidney fibroblasts. For the screening of successful homologous recombination of transfected clones, suitable screening methods had to be optimised for each of the different vectors. Targeted clones had to be identified and used for application in somatic cell nuclear transfer. Finally, piglets born had to be analysed for correct transgenesis.

2. Material and Methods

2.1. Biochemicals and chemicals

Acetic acid	Fluka Laborchemikalien GmbH, Seelze, Germany
Anti-digoxigenin-AP Fab fragments	Roche Diagnostic GmbH, Mannheim, Germany
Ascorbic acid-2-phosphate	Sigma-Aldrich Chemie GmbH, Steinheim, Germany
Blocking reagent for Southern Blot	Roche Diagnostic GmbH, Mannheim, Germany
Boric acid	Fluka Laborchemikalien GmbH, Seelze, Germany
Bovine serum albumin (BSA) (100×)	New England Biolabs, Frankfurt, Germany
Bovine serum albumin, pH 7.0	PAA Pasching, Austria
5-Bromo-4-chloro-3-inolyl-β-D-galactopyranosid	Sigma-Aldrich Chemie GmbH, Steinheim, Germany
Bromphenol blue	Sigma-Aldrich Chemie GmbH, Steinheim, Germany
Calcium Chloride	Merck KGaA, Darmstadt, Germany
CDP Star	Roche Diagnostic GmbH, Mannheim, Germany
Chloroform	Sigma-Aldrich Chemie GmbH, Steinheim, Germany
Chondroitin-6-Sulphate	Sigma-Aldrich Chemie GmbH, Steinheim, Germany
Dexamethasone	Sigma-Aldrich Chemie GmbH, Steinheim, Germany
4',6'-Diamidino-2'-phenylindole-dihydrochloride (DAPI)	Roche Diagnostics GmBH, Mannheim
1,9-Dimethyl-methylen blue	Sigma-Aldrich Chemie GmbH, Steinheim
Dimethyl sulfoxide (DMSO)	Sigma-Aldrich Chemie GmbH, Steinheim
DIG Easy Hyb Granules	Roche Diagnostic GmbH, Mannheim, Germany
Digoxygenin-11-2'-deoxy-uridine-5'-triphosphate,	Roche Diagnostic GmbH, Mannheim, Germany
DNA marker (100 bp, 1 kb)	New England Biolabs, Frankfurt, Germany
DNA marker (1 kb)	Invitrogen, Karlsruhe, Germany
DNA marker VII, digoxigenin-labeled	Roche Diagnostic GmbH, Mannheim, Germany
Dithiotreitol (DTT)	Omnilab Life Science OLS, Bremen, Germany
Ethanol 96%	Riedel-de-Haen, Seelze, Germany
Ethidium bromide (10 mg/ml)	Sigma-Aldrich Chemie GmbH, Steinheim, Germany
Ethylenediamintetraacetic acid (EDTA)	Sigma-Aldrich Chemie GmbH, Steinheim, Germany

Formalin 10%	Sigma-Aldrich Chemie GmbH, Steinheim, Germany
Formamid (deionized)	Sigma-Aldrich Chemie GmbH, Steinheim, Germany
GenAgarose L.E.	Genaxxon Bioscience GmbH, Biberach, Germany
Glacial acetic acid	Fluka Laborchemikalien GmbH, Seelze, Germany
Glutaraldehyd	Fluka Laborchemikalien GmbH, Seelze, Germany
Glycerol 99%	Carl Roth GmbH, Karlsruhe, Germany
Glycine	Carl Roth GmbH, Karlsruhe, Germany
Heparin disodium salt	Sigma-Aldrich Chemie GmbH, Steinheim, German
Hydrochloric acid 37%	Merck KGaA, Darmstadt
Indomethacine	Sigma-Aldrich Chemie GmbH, Steinheim, Germany
Isopropyl-β-D-thiogalactopyranosid	Omnilab Life Science OLS, Bremen, Germany
Isopropanol	Carl Roth GmbH, Karlsruhe, Germany
Kanamycin (Kana)	Sigma-Aldrich Chemie GmbH, Steinheim, Germany
Loading dye (5$\times$)	Sigma-Aldrich Chemie GmbH, Steinheim, Germany
β-Mercaptoethanol	Sigma-Aldrich Chemie GmbH, Steinheim, Germany
Methanol	Sigma-Aldrich Chemie GmbH, Steinheim, Germany
MidRange DNA marker II	New England Biolabs, Frankfurt, Germany
N-Acetyl-Cystein	Sigma-Aldrich Chemie GmbH, Steinheim, Germany
Oil Red O	Sigma-Aldrich Chemie GmbH, Steinheim, Germany
Potassium acetate	Riedel-de HaÎn, Seelze
Potassium hexacyanoferrat (III)	AppliChem, Darmstadt, Germany
Potassium hexacyanoferrat (II)-trihydrat	AppliChem, Darmstadt, Germany
Proline	Sigma-Aldrich Chemie GmbH, Steinheim, Germany
Silver nitrate	Sigma-Aldrich Chemie GmbH, Steinheim, Germany
Sodium dodecyl sulfate (SDS)	Sigma-Aldrich Chemie GmbH, Steinheim, Germany
Sodium acetat	Roth, Karlsruhe, Germany
Sodium hydroxide	Riedel-de Haen GmbH, Seelze, Germany
Sodium chloride	Sigma-Aldrich Chemie GmbH, Steinheim, Germany
Sodium pyruvate	PAA Pasching, Austria
Sucrose	Sigma-Aldrich Chemie GmbH, Steinheim, Germany
Trizima base (Tris base)	Sigma-Aldrich Chemie GmbH, Steinheim, Germany
Trizol	Invitrogen, Karlsruhe, Germany
Tris hydrochloid (Tris HCl)	Sigma-Aldrich Chemie GmbH, Steinheim, Germany
Trypan blue solution (0.4%)	Sigma-Aldrich Chemie GmbH, Steinheim, Germany
Tween 20	Sigma-Aldrich Chemie GmbH, Steinheim, Germany

2.2. Enzymes

Antarctic Phosphatase	New England Biolabs, Frankfurt, Germany
DNA polymerase I, large (Klenow) fragment	New England Biolabs, Frankfurt, Germany
GoTaq DNA polymerase	Promega GmbH, Mannheim, Germany
Herculase DNA polymerase	Agilent Technologies
OmniTaq DNA polymerase	Omnilab Life Science OLS, Bremen, Germany
Papain (28 U/mg)	Sigma-Aldrich Chemie GmbH, Steinheim, Germany
PCR Extender System	5Prime GmbH, Hamburg, Germany
Phusion High Fidelity DNA polymerase	New England Biolabs, Frankfurt, Germany
Proteinase K	Sigma-Aldrich Chemie GmbH, Steinheim, Germany
Restriction endonucleases	New England Biolabs, Frankfurt, Germany
RNase A solution	Sigma-Aldrich Chemie GmbH, Steinheim, Germany
T4 DNA Ligase	New England Biolabs, Frankfurt, Germany

2.3. Kits

Mammalian Genomic DNA Miniprep Kit	Sigma-Aldrich Chemie GmbH, Steinheim, Germany
NucleoBond Xtra Plasmid Purification	Macherey-Nagel GmbH and Co. KG, Dueren, Germany
pGEM-T Easy Vector System	Promega, Mannheim, Germany
SuperScriptIII One-Step RT PCR, with Platinum Taq	Invitrogen, Karlsruhe, Germany
TaqMan GeneExpression Assay	Applied Biosystems, Foster City, USA
Turbo DNA-free	Ambion, huntingdon, UK
Wizard SV Gel and PCR Clean-up System	Promega, Mannheim, Germany

2.4. Cells

2.4.1. Bacterial strains

E. Coli DH10B ElectroMAX	Invitrogen, Karlsruhe, Germany

Genotype	F$^-$ *mcr*A Δ(*mrr-hsd*RMS-*mcr*BC) Φ80lacZΔM15 Δ*lac*X74 *rec*A1 endA1 *ara*D139 Δ(*ara, leu*)7697 *gal*U *gal*K λ^- *rps*L *nup*G
E. Coli SW106	Prof. Dr. Wolf, Gene Center LMU, Munich, Germany
Genotype	DH10B *cI*857, (cro-bioA)<>araC-P_{BAD} Cre, gal490, gal$^+$, ΔgakK DH10B *cI*857, (cro-bioA)<>araC-P_{BAD} Cre, gal490, gal$^+$, ΔgakK

2.4.2. Eukaryotic cells

pAD-MSC1101	Isolated during this project
pAD-MSC1702	Isolated during this project
pBM-MSC0303	Isolated during this project
pBM-MSC1702	Isolated during this project
pBM-MSC0902	Isolated during this project
pBM-MSC1101	Isolated during this project
HT1080	Laboratory stock
pKDNF2109	Prof. Dr. Wolf, Gene Center LMU, Munich, Germany
ST007	Laboratory stock

2.5. Primers

All primers have been acquired on biomers.net GmbH (Ulm, Germany) or by Sigma-Aldrich Chemie GmbH (Steinheim, Germany).

Primer name	Sequence	Annealing [°C]
Amp_F	GGTCTGACAGTTACCATGCTT	60
Amp_R	GCGGAACCCCGATTTGTTTA	
BB_F	CCGTAGTGAGAGTGCGTTCA	59
BB_F	GTCACTATGGCGTGCTGCTA	
HR1_F	TAGCATTTCCATCCCAAACC	
HR1_R	ATAAGGGCTGGAGAGGGTGT	
HPRT_F	CTGTTCTTGCCTTTCATTTCT	59
HPRT_R	TCATCACTTCTGTTCTTTCC	
HPRT_probe_VIC	AAAGAGATGGGAGGCCAT	
HR2b_R	CCTCCTTGCAGAAGAAGTGC	60

HR2b_F	ATGAGCAGAAGAGGGGTTGA	
IL2Rg_HR_F IL2Rg_HR_R	TGAGTGAGTGGGAACAGCAG CTGATTGTTCCTTGGGGAGA	58
IL2Rg_genseq_ri_1f IL2Rg_genseq_rl_2r	CTGGTTACTGAATATCATGGGAAC CGACTTTCTTGGCTTCTTGG	60
JAK3_targscreen_F2 JAK3_targscreen_R2	ATCCCTTGTCAGTCGATCGATTCAT TTACGCCACTGACTTGCTTG	58
JAK3_targscreen_F3	TGTCCCATTCTGTGGGTTGT	59
JAK3_Ex2/3_F JAK3_Ex3/4_R	GCTAAGGCCAGTGGTATCCT GAAGTAAAAGCGGAGCCTGT	60
JAK3_endo_R JAK3_probe_6-FAM	TTACGCCACTGACTTGCTTG ACGTCAAGATCG	58
JAK3_HR1b_F JAK3_HR1b_F	TAGCATTTCCATCCCAAACC ATAAGGGCTGGAGAGGGTGT	60
Long_F Long_R	GGGAGGATTGGGAAGACAAT TGGAGATGGGAAAACTGAGG	59
NLS_F NLS_R	ACGCGTGCTGTGGAATGTGTGTCAGTTAG ACGCGTGGAGTTAGGGGCGGGACTA	60
Neo_seq_f1	ACGACAAGGTGAGGAACTAAAC	60
P1_F P1_R	GGGGTACCGAGACACCCTTGATC GGAATTCCAGCTCCCACCAGTC	60
Short_F	GGGGATCCCCTTGTCAGTCGATTCATT	60

2.6. Vectors

2.6.1. Bacterial Artificial Chromosomes

CH242-331C1	Children's Hospital Oakland Research Institute, USA
CH242-317A24	Children's Hospital Oakland Research Institute, USA
CH242-6A14	Children's Hospital Oakland Research Institute, USA
CH242-118B2	Children's Hospital Oakland Research Institute, USA

2.6.2. Plasmids

pBluescriptIISK+	Stratagene, La Jolla, USA
pCAGGS-Cherry	Laboratory stock
pGEM-T Easy Vector System I	Promega, Mannheim, Germany

pJET1.2/blunt	Invitrogen, Karlsruhe, Germany
pL452	Prof. Dr. Wolf, Gene Center LMU, Munich, Germany
pSL1180 Amersham	Amersham Bioscience, Piscataway, New Jersey, USA

2.7. Tissue culture and microbiology buffers, media and supplements

Difco LB Agar Miller (Luria-Bertrani)	Becton Dickinson, Erembodegem-Aalst, Belgium
rhBMP-2	R&D Systems, Inc., Minneapolis, USA
bFGF	PromoCell, Heidelberg, Germany
Amphotericin B solution	PAA Pasching, Austria
Ampicillin (Amp)	Sigma-Aldrich Chemie GmbH, Steinheim, Germany
Blasticidin S (BS)	InvivoGen, San Diego, USA
Advanced DMEM	Gibco BRL, Paisley, UK
β-Glycerol phosphate	Sigma-Aldrich Chemie GmbH, Steinheim, Germany
Chicken serum	PAA, Pasching, Austria
Chloramphenicol (Cam)	Sigma-Aldrich Chemie GmbH, Steinheim, Germany
Dulbecco's modified Eagel's medium (DMEM)	PAA, Pasching, Austria
Fetal Bovine Serum	PAA, Pasching, Austria
Hank's buffered salt solution (HBSS), w/o Phenol red, with Ca and Mg	PAA, Pasching, Austria
Hypoosmolar buffer	Eppendorf, Hamburg, Germany
Insulin	Roche Diagnostics GmbH, Mannheim
ITS$^+$ liquid medium supplement (100$\times$)	Sigma-Aldrich Chemie GmbH, Steinheim, Germany
Lipofectamine 2000	Invitrogen, Karlsruhe, Germany
Lymphocyte separation medium LSM 1077	PAA, Pasching, Austria
G418	PAA, Pasching, Austria
GlutaMAX	Gibco BRL, Paisley, UK
3-Methyl-isobutylxanthine (MIX)	Sigma-Aldrich Chemie GmbH, Steinheim, Germany
Dulbecco's phosphate buffered saline (PBS) 1$\times$, w/o Ca and Mg	PAA, Pasching, Austria
Penicillin/ Streptomycin	Sigma-Aldrich, Deisenhofen

(10,000 U, 10 µg/µlin 0.9% NaCl)	
LB Agar	BD, Sparks, USA
Opti-MEM	Gibco BRL, Paisley, UK
Trypsin/ EDTA (1 ×, 10×)	PAA, Pasching, Austria
X-Gal (5-Bromo-4-chloro-3-indolyl-β-D-galactopyranoside)	Sigma-Aldrich Chemie GmbH, Steinheim, Germany

2.8. Buffers and solutions

DMMB stock solution	16 mg DMMB dissolved O/N in 5 ml 100% EtOH
	2.37 g NaCl and 3.04 g glycine dissolved in 975 ml water
	0.69 ml 11.6 M HCl added
	solutions were combined
	pH was adjusted to 3.0 with 1 M HCl
	absorption should be about 0.3 at 525 nm (blank: H_2O)
Gel loading buffer (5×)	5 ml Glycerol
	4 ml EDTA (0.5 M)
	point of a spatula Bromphenol blue
	filled up with ddH2O to 10 ml
Miniprep solution I	5 mM sucrose
	TRIS (pH 8.0)
	10 mM EDTA
Miniprep solution II	1% SDS
	0.2 N NaOH
Miniprep solution III	3 M sodium acetate (pH 5.3)
Oil Red O stock solution	0.3 g Oil Red O in 100 ml isopropanol (99%),
	stable at room temperature
Oil Red O working solution	6 ml Oil Red O stock solution
	4 ml ddH_2O
	left for 10 minutes at room temperature,
	filtered through Whatman filter (stable for 1-2 hours)
Staining solution (β-Gal)	5 mM $K_4Fe(CN)_6$
	5 mM $K_3Fe(CN)_6$
	5 mM $MgCl_2$
	in PBS
	addition of X-Gal to final concentration of 1 mg/ml
TAE buffer (50×)	2 M Trisbase

	50 mM EDTA (0.5 M)
	57.1 ml Glacial acetic acid
	filled up with ddH2O to 1l
	autoclaved
TBE buffer (10×)	0.9 M Tris
	20 mM EDTA (0.5 M)
	0.9 M boric acid
	filled up with ddH2O to 1l
	autoclaved
TAE buffer (1×)	0.04 M Tris acetate
	0.01 M EDTA
X-Gal solution	100 mg X-Gal
	1 ml N,N-Dimethylformamid (DMF)

2.9. Laboratory equipment

ABI 377 automatic sequencer	Applied Biosystem, Foster City, USA
Bio Imaging System Gene Genius	Syngene, Cambridge, UK
Centrifuges:	
Minispin and Centrifuge 5810	Eppendorf, Hamburg, Germany
Laboratory centrifuges 4K15C, 1-15	Sigma, Osterode, Germany
Cooling Units:	
freezer -20°C	Liebherr International, Bulle, Switzerland
freezer -80°C	Thermo Electron GmbH , Dreieich, Germany
Digital Graphic Printer UP D895MD	Syngene, Cambridge, UK
Electroporation apparatus:	
Multiporator	Eppendorf, Hamburg, Germany
Gene Pulser II	Bio-Rad Laboratories GmbH, Munich, Germany
Gel Electrophoresis apparatus:	
Classic CSSU78 and CSSU1214	Thermo Electron GmbH, Dreieich, Germany
HE 33 Mini Submarine Unit	GE Healthcare Europe GmbH, Freiburg, Germany
Glassware (bottles, flasks)	Marienfeld GmbH, Lauda-Königshofen, Germany
Incubators:	
Incubator	Binder GmbH, Tuttlingen, Germany
Forma orbital shaker	Thermo Electron Corporation, Dreieich, Germany
Ice maker	Eurfrigor, Lainate (MI), Italy

Microwaves:	
MDA MW12M706-AU	MHA Haushaltswaren GmbH, Barsbüttel, Germany
NN-E202W	Panasonic
PCR Device: DNA Engine Dyad Cycler (PTC 220)	Bio-Rad Laboratories GmbH, Munich, Germany
Pipets:	
Rainin Pipet-Lite LTS (2, 20, 200, 1000 µl)	Mettler Toledo GmbH, Giessen, Germany
Handy Step multi pipet	Brand, Wertheim, Germany
Pipetman P20, P200 and P1000	Gilson, Bad Camberg, Germany
Pipettus	Hirschmann Laborgeräte, Eberstadt, Germany
Power Supply:	
EC 105 Power Supply	Thermo Electron GmbH, Dreieich, Germany
Power PAC 300	Bio-Rad Laboratories GmbH, Munich, Germany
Precision Balances 440-33N	Kern, Balingen-Frommern, Germany
Safety Cabinets HERAsafe Type HSP	Heraeus Instruments, Munich, Germany
Spectrophotometer: BioPhotometer	Eppendorf, Hamburg, Germany
Vortex Mixer	VELP Scientifica srl, Milano, Italy
Water bath: Haake C10-K15 open-bath circulator	Thermo Fisher Scientific (former: Thermo Electron Corporation), Karlsruhe, Germany
Accu-Jet	Brand, Dietenhofen
Biofuge fresco, #3324 rotor	Heraeus Instruments, Hanau
Cell counting chamber	Neubauer, Marienfeld, Lauda-K^nigshofen
Centrifuge J2-HS with rotors JA-10 und JA-20	Beckman Coulter GmbH, Krefeld
CO_2 incubator	Forma Scientific Inc., Marietta, Ohio, USA
Cryo freezing device Qualifreeze	Qualilab, Olivet, France
Digital camera for microscope AxioCam MR with image processing software Axiovision 4.2	Carl Zeiss Jena GmbH, Jena
Electroporation cuvettes (0.1, 0.2 mm)	PEQLAB Biotechnologie GmbH, Erlangen, Germany
Fluorescence activated cell sorter with CELLQuest software	Becton Dickinson, Heidelberg
Fluorescence microscope Axiovert 135	Carl Zeiss Jena GmbH, Jena
Hera Safe clean bench	Heraeus Instruments/Kendro, Hanau
Inverse microscope Axiovert 25	Carl Zeiss Jena GmbH, Jena

Megafuge 2.0R, #8160G rotor	Heraeus Instruments, Hanau
Single-channel pipettes	Eppendorf, Wesseling-Berzdorf
TaqMan 7900 HT Sequence Detection System 2.2	Applied Biosystems, Foster City, USA
UV-Photometer DU-640	Beckman Coulter GmbH, Krefeld
Varifuge 3.0 R	Heraeus Instruments, Hanau
Vortex laboratory mixer	IKA® Werke GmbH & Co. KG, Staufen

2.10. Consumables

Reaction tubes (1.5 ml, 2 ml)	Brand GmbH & Co. KG, Wertheim, Germany
Round-Bottom Tubes (14 ml)	Becton Dickinson, Sparks, USA
Cell culture flasks (25, 75, 150 cm^2)	Corning Inc., New York, USA
Cell culture plates (6-, 12-, 24-, 96-well)	Corning Inc., New York, USA
Conical bottom centrifuge tubes (15, 50 ml)	Corning Inc., New York, USA
Cuvettes for photometer (UVette)	Eppendorf, Hamburg, Germany
Disposable pipet tips (normal and filtered tips)	Brand GmbH & Co. KG, Wertheim, Germany
Electroporation cuvettes (2, 4 mm)	peqlab Biotechnologie GmbH, Erlangen, Germany
Glassware	Marienfeld GmbH, Landa-KOEngishofen, Germany
Hybond-N+ positively charged nylon transfer membrane 0.45 µmpore size	Amersham Bioscience, Freiburg
Multiscreen filtration plates MAHVN4510	Millipore, Eschborn, Germany
Petri dishes (10 cm)	Brand GmbH & Co. KG, Wertheim, Germany
Rainin pipette tips (2, 20, 200, 1000 µl) (normal und filtered tips)	Mettler Toledo GmbH, Dreieich, Germany
Sephadex G-50 Fine	Sigma-Aldrich Chemie GmbH, Deisenhofen, Germany
Sterile plastic pipets 1-25 ml	Corning Inc., New York, USA
Canula BD Microlance™ 3	Becton Dickinson, Sparks, USA
Cryo Tube TM vials 1.8 ml	Nunc, Wiesbaden-Biebrich, Germany
Rotilabo R Blotting paper (1 mm)	Carl Roth, Karlsruhe, Germany
Syringes (BD Discardit™)	Becton Dickinson GmbH, Sparks, USA
Sterile filter 0.22 µmStericup	Millipore GmbH, Schwalbach
Sterile pipettes	Corning Inc., New York, USA

Tissue culture flasks	Corning Inc., New York, USA
Tissue culture dishes (6, 10, 15 cm)	Corning Inc., New York, USA

All culture dishes, plates and flasks are tissue culture-treated, gamma sterilized, free from pyrogenics, RNA, DNA, RNases and DNases

2.10.1. Software

AxioVision	Zeiss AG, Oberkochen, Germany
Enzyme and Double Digests Finder	NEB, http://www.neb.com
FinchTV	Geospiza Inc. from www.geospiza.com/finchtv
primer3 (v. 0.4.0)	http://fokker.wi.mit.edu/primer3/input.htm
Vector NTI Advance 10, ContigExpress and AlingX	Invitrogen, Karlsruhe, Germany

2.11. Molecular biology methods

2.11.1. Isolation of nucleic acids

Isolation of plasmid and BAC DNA

Isolation of plasmid and BAC DNA was, depending on the required amount, performed with different protocols. A single bacterial colony was picked and transferred into LB medium with appropriate antibiotics for selection and shaken in an orbital shaker at 37°C at 230 rpm for 7 to 16 hours.

Miniprep Bacterial cells for miniprep DNA preparation were obtained from a 5 ml LB over night culture. 2 ml of the solution were centrifuged for 1 minute at 14,000 g. The supernatant was removed and the cell pellet was resuspended in 100 µl of miniprep solution I by vortexing. Alkaline lysis was induced by addition of 200 µl of solution II and careful mixing. After incubation at room temperature for 3 minutes, the reaction was stopped by addition of 150 µl of solution III and mixing by inverting the tube once. Incubation for 30 minutes on ice was followed by pelleting of cell debris and genomic DNA by centrifugation at 14,000 g for 5 minutes. The supernatant containing plasmid or BAC DNA was transferred to a new 1.5 ml reaction tube, precipitated with 1 ml of 95% EtOH and spun at 14,000 g for 15 minutes. Washing was repeated twice: with 500 µl of 80% EtOH and with 500 µl of 95% EtOH. Between the washing steps, centrifugation was conducted

at 14,000 g for 10 minutes. After removal of EtOH, the DNA pellet was dried and resuspended in 50 µl of ddH_2O supplemented with RNase.

Midiprep Medium-scale plasmid DNA preparation was performed with 50 ml to 150 ml over night culture. The DNA isolation was performed with NucleoBond Xtra Midi kit according to the manufacturer's "high-copy plasmid protocol".

Maxiprep Large-scale plasmid DNA preparation was performed with 100 ml to 300 ml over night culture, whereas BAC preparation was performed from 600 ml to 1000 ml. The DNA isolation was conducted with the NucleoBond Xtra Maxi kit according to the manufacturer's "high-copy plasmid protocol" for plasmid and according to the "low-copy plasmid protocol" for BAC DNA.

Isolation of genomic DNA from mammalian cells

Genomic DNA from mammalian cells was isolated with the GenElute Mammalian Genomic DNA Miniprep Kit accoding to the manufacturer's protocol. DNA was eluted with 150 µl of elution buffer.

Isolation of RNA

Isolation and handling of RNA was performed with RNase-free materials and pipette tips with filters. Cleaning of required laboratory surfaces was done with RNase Away. Cells cultivated for RNA isolation in a 6-well plate were washed with PBS. Per well 1 ml of Trizol were incubated for 5 minutes at room temperature. After complete cell lysis, the supernatant containing the cells was transferred to a 2 ml reaction tube and stored at -80°C.

For RNA isolation 200 µl chloroform were added after thawing of the lysed cells. Shaking for 15 seconds and incubation for 3 minutes at room temperature were followed by pelleting for 15 minutes at 12,000 g and 4°C. The clear, upper phase containing RNA was transferred to a new 1.5 ml reaction tube and precipitated with 500 µl ice-cold isopropanol. After thorough mixing, the solution was incubated for 10 minutes and spun at 12,000 g and 4°C for 10 minutes. The supernatant was removed to wash the RNA pellet with 1 ml 75% ethanol. Then, it was centrifuged for 5 minutes at 7,500 g and 4°C. The pellet was dried under a laminar flow at room temperature or at 55°C for 5 minutes. It was dissolved in 50 µl RNase-free ddH_2O. To remove DNA from preparation, the Turbo DNA-free kit was used according to the manufacturer's protocol. RNA was stored at -80°C.

RNA integrity was determined according to Masek *et al.* (2005) [178]. 5 µl of RNA sample were mixed with 5 µl of 5× loading dye and 15 µl of deionised formamid. The solution was incubated at 65°C for 5 minutes and on ice for another 5 minutes. It was loaded onto a 1.2%

TAE agarose gel. High quality RNA produces two bands from 18 S and 28 S ribosomal RNA. The 28 S RNA band should contain the double amount of RNA.

Photometric concentration determination of nucleic acids

Nucleic acid concentration determination was conducted photometrically with the BioPhotometer 6131. Depending on the expected concentration, samples were diluted 1:35 to 1:150 and optical density (OD) was measured at 260 nm against water. DNA and RNA concentrations were calculated according to the following equation:

$$\text{DNA } [\mu g/\mu l] = (OD_{260} \times 50 \times \text{dilution factor})/\ 1000$$
$$\text{RNA } [\mu g/\mu l] = (OD_{260} \times 40 \times \text{dilution factor})/\ 1000$$

2.11.2. DNA manipulation

Adenylation of blunt end PCR products

Blunt end PCR products obtained by the use of Phusion DNA polymerase needed to be adenylated before subcloning into the pGEM-T Easy via TA cloning. For this purpose, 5 U of OmniTaq or GoTaq DNA polymerase were added to the tube after PCR. The solution was incubated at 72°C for 30 minutes and was subsequently used for ligation.

Cleavage of DNA with restriction endonucleases

Analytical digests to verify DNA constructs generated by molecular cloning was conducted with 1 to 3 µgof DNA. For preparative digests up to 80 µgDNA were used. Table 2.3 shows the experimental setups for both, analytical and preparative restriction digests. After incubation for 1 to 3 hours, enzyme heat inactivation was performed according to the manufacturer's instructions.

Table 2.3.: Analytical and preparative DNA restriction digests

Component	Analytical digest	Preparative digest
DNA	2 µl miniprep	5-8 µg
Enzyme	5 U	2-3 U/ µgDNA
10× NEB buffer	1×	1×
100× BSA	1×	1×
H_2O	add up to 20 µl	add up to final volume

Blunting of DNA fragments

Some restriction digest products had overhangs, which had to be removed or filled for further cloning steps. This blunting was performed with DNA Polymerase I, large (Klenow) fragment. It forms blunt ends by removing 3' overhangs and filling in 5' overhangs. For the reaction, up to 5 µgDNA were combined with water, 1× T4 ligase buffer, 0.1 mM dNTPs and 1 µl Klenow enzyme to a final volume of 25 µl. The reaction was stopped by adding EDTA to a final concentration of 10 mM and heating at 75°C for 20 minutes.

Dephosphorylation of cleaved DNA

To avoid re-ligation of plasmid, vector backbone digests producing compatible DNA ends were dephosphorylated. For the reaction 5 U of Antarctic Phosphatase were mixed to the heat inactivated restriction digest supplemented with Antarctic Phosphatase buffer. After incubation at 37°C for 30 minutes, the enzyme was heat inactivated according to protocol.

Ligation

For ligation of DNA fragments with compatible ends, T4 DNA Ligase mediated the formation of phosphodiester groups between the 3'-OH and 5' phosphate group. The reaction was prepared according to the manufacturer's protocol. The ligation mix was incubated for 1 to 2 hours at room temperature. For higher efficiency, the reaction was continued at -4°C over night.

Agarose gel electrophoresis

For separation of DNA fragments and subsequent analysis of their respective sizes, agarose gel electrophoresis was performed.

Standard gel electrophoresis was performed with 1× TAE or TBE buffered systems for DNA fragments between 100 bp and 18 kb. For this purpose 0.6 to 1.5% agarose gels containing ethidium bromide were casted. Prior to running the gel, samples were mixed with 5× DNA loading dye and loaded to the gel together with 1 kb or 100 bp DNA markers to compare band sizes. The gels were run for 45 minutes to 2 hours at 80 to 120 V depending on gel volume and expected fragments' sizes. Visualisation of DNA under UV light (366 nm) took place with the Bio Imaging System Gene Genius.

Pulsed field gel electrophoresis with 0.5× TBE buffered 1% gels was performed with BAC DNA. Midrange marker II and 1 kb DNA marker allowed analysis of fragment sizes. Samples were prepared as described above. The gel was run for at 6 V for 16 hours with 1-30 s switch time at 12°C. For visualisation of DNA, the gel was stained in 0.5× TBE supplemented with ethidium bromide.

Isolation of DNA fragments from agarose gels

For isolation of DNA fragments from the gel, DNA bands were visualised on a UV table. Fragments were cut with a clean scalpel and purified with the Wizard SV Gel and PCR Clean-Up System according to the manufacturer's protocol.

Phenol chloroform extraction

To produce pure BAC DNA for transfection of cells, phenol chloroform extraction was conducted. Therefore, DNA samples were filled up to 700 µl with ddH_2O, combined with 700 µl phenol chloroform isoamylalcohol (25:24:1) solution and inverted 20 times. After incubation at room temperature for 10 minutes, the organic and aqueous phases were separated by centrifugation at 14,000 g for 10 minutes. The aqueous phase was transferred to a new 1.5 ml reaction tube, combined with an equal volume of chloroform and spun again. The transfer of the aqueous phase was repeated and DNA was precipitated with sodium chloride and ethanol.

DNA precipitation with sodium chloride and ethanol

Precipitation of DNA for subsequent utilisation in transfections was conducted according to the following protocol. Samples were combined with 0.1 volume a 3 M NaCl solution and mixed. Plasmid samples could be vortexed, whereas BAC samples had to be mixed by careful inversion. After addition of 2 volumes of 100% ice-cold ethanol, incubation at -20°C was carried out over night. The next day, DNA was pelleted for 10 minutes at 14,000 g and the supernatant was discarded. The pellet was washed with 1 ml 70% sterile ethanol under a laminar flow hood, centrifuged at 14,000 g for 5 minutes and left to dry. It was resuspended in 50 to 100 µl of Tris-low EDTA or ddH_2O. BAC DNA required 5 days to dissolve completely, as vigorous mixing was not possible. To avoid shearing, the DNA was incubated at 55°C for 30 minutes and then left at 4°C. Plasmid DNA could be vortexed and further used the following day.

2.11.3. Polymerase Chain Reaction

Specific amplification of DNA fragments from plasmid, BAC or genomic DNA was conducted with polymerase chain reaction (PCR). GoTaq DNA polymerase was used for analytical PCRs, except for the JAK3 conventional targeting screening, which was performed with Herculase. Phusion is a high-fidelity DNA polymerase with proof-reading function. It was applied for amplifications preceding cloning or sequencing steps. The JAK3 targeting vector long arm was generated by long range PCR with 5Prime DNA polymerase. Table 2.4 summarises the master mix set ups and cycling conditions for the different polymerases used.

Table 2.4.: PCR reaction set ups and cycling conditions

Component	Final concentration	Step	°C	Time	Cycles
Phusion PCR					
DNA		Initial			1
5× HF buffer	1×	denaturation	98	30 s	
dNTPs	200 µM each	Denaturation	98	5 s	
Forward primer	0.2-0.5 µM	Annealing	57-64	30 s	25-30
Reverse primer	0.2-0.5 µM	Elongation	72	20 s/kb	
Phusion	0.4 U	Final elongation	72	10 min	1
H_2O	up to 20 µl	Final hold	4	forever	
GoTaq PCR					
DNA		Initial			1
10× green buffer	1×	denaturation	95	2 min	
dNTPs	200 µM each	Denaturation	95	1 min	
Forward primer	0.2-0.5 µM	Annealing	57-64	30 s	25-40
Reverse primer	0.2-0.5 µM	Elongation	72	1 min/kb	
GoTaq	1.25 U	Final elongation	72	5 min	1
H_2O	up to 50 µl	Final hold	4	forever	
5Prime PCR					
DNA		Initial			1
10× tuning buffer	1×	denaturation	92	30 s	
dNTPs	500 µM each	Denaturation	92	12 s	
Long_F	0.2 µM	Annealing	60	13 min	8
Long_R	0.2 µM	Elongation	66	12 min	
$MgCl_2$	2.75 µM	Final elongation	66	7 min	1
OmniTaq	2 U	Final hold	4	forever	
Enzyme mix	2 U				
H_2O	up to 50 µl				
Herculase PCR					
DNA		Initial			1
5× buffer	1×	denaturation	95	2 min	
dNTPs	250 µM each	Denaturation	95	20 s min	
JAK3_screen_F2	0.25 µM	Annealing	61	20 s	35
JAK3_screen_R2	0.25 uM	Elongation	72	1 min 35 s	
Herculase	1.25 U	Final elongation	72	4 min	1
H_2O	up to 50 µl	Final hold	4	forever	

Colony PCR

Fast screening of intermediate molecular cloning products or recombineering steps was conducted with PCRs on DNA obtained directly from transformed bacterial colonies. Single colonies were picked from an agar plate with a sterile pipette tip and suspended in 50 µl of ddH_2O. The solution was heated to 99°C for 5 minutes and spun down at 14,000 g for 5 minutes. 2 µl of supernatant were inserted as a template for a standard PCR reaction.

PCR from tissue culture clones

Screening of IL2RG-neo-CCN BAC transfected single-cell clones was performed directly on cellular material. Half of a 90% confluent 12-well was detached with Accutase, aliquoted and frozen (-20°C). After centrifugation at 14,000 g for 2 minutes, 6 µl of supernatant were used as DNA template.

2.11.4. Reverse transcriptase polymerase chain reaction

Reverse transcriptase polymerase chain reaction (RT-PCR) was carried out with the SuperScriptIII One-Step RT-PCR with Platinum Taq Kit, according to the manufacturer's protocol. PCR controls were carried out with Platinum Taq without the cDNA synthesis step, to exclude contamination with genomic DNA.

2.11.5. Sequencing

Sequencing was performed by MWG Eurofins Operon (Ebersberg, Germany). Samples and primers were prepared according to the company's guidelines.

2.11.6. Southern blot analysis

Preparation of DIG labelled probes

Probes for the detection of JAK3 and neo internal sequences were prepared by GoTaq PCR with digoxigenin-11-2'-deoxy-uridine-5'-triphosphate (20 µM). 10 pg of JAK3 conventional targeting vector were used as template and the concentration of dNTPs was reduced to 40 µM. A control reaction without DIG labelled UTPs was set up to compare the size shift of the probe DNA after agarose gel electrophoresis. Due to the higher molecular weight of DIG-labelled dUTPs, the probes were expected to be slightly larger than the control.

Dot blot

Binding efficiency of probe to its target DNA was estimated with a dot blot. JAK3 TV CCN was pipetted drop wise onto a Hybond-N+ membrane in amounts ranging from 0.1 to 500 pg. The membrane was baked at 120°C for 30 minutes to link DNA. Subsequently, the Southern blot procedure listed below was performed with 1 and 2 µl of probe per millilitre of hybridisation solution.

Southern blot

For Southern blot analysis, 12 µgof genomic DNA were digested with the appropriate enzymes and seperated by agarose gel electrophoresis with a 1% TBE gel. To avoid high background, ethidium bromide was not added. To control the fragment sizes and the progress of separation, 4 µl of DIG labelled molecular weight marker VII and 6 µl of 1 kb marker were loaded, as well as samples mixed with 5× DNA loading dye. The gel was run at 40 V for 16 hours and additional 12 hours at 80 V. The 1 kb marker gel lane was cut off and stained with ethidium bromide for 30 minutes and visualised with UV light. Gel parts with DNA fragment sizes, which were not of interest for analysis, were determined by comparison to marker bands and cut off. The gel was incubated in 250 mM HCl for 10 minutes for DNA depurination and rinsed with water. Denaturation was performed under UV light for 5 minutes and twice in denaturation solution (0.5 M sodium hydroxide, 1.5 M sodium chloride) for 15 minutes. After rinsing with water, the gel was neutralised twice in neutralisation solution (0.5 M Tris-HCl (pH 7.5), 1.5 M sodium chloride) for 15 minutes. Equilibration in 20×SSC (3.0 M sodium chloride, 0.3 M sodium citrate, adjust with 1.0 M HCl to pH 7.0) took place for 10 minutes. All steps were carried out with gentle shaking.

The capillary blot was assembled according to protocol. After DNA blotting onto the membrane, it was washed in 2×SSC and baked at 120°C for 30 minutes. Probe hybridisation to DNA was performed after pre-hybridisation of DIG Easy Hyb for 2 hours in a rotating 50 ml falcon tube. 1.5 µl of probe were added to 50 µl of ddH_2O and denatured for 5 minutes at 95°C. The hybridisation solution was prepared by dilution of probe in 3 ml of DIG Easy Hyb pre-warmed to 37°C and thorough mixing. The pre-hybridisation solution was removed and the hybridisation mix was transferred to the membrane and incubated over night.

After at least 16 hours, membrane was washed with low stringency buffer for 15 minutes. All steps were performed under gentle shaking at room temperature. The procedure was repeated twice with pre-heated high stringency buffer (0.5× SSC, 0.1% SDS, 58°C). The membrane was treated with washing buffer (0.1 M maleic acid, 0.15 M sodium chloride (adjusted with sodium hydroxide to pH 7.5), 0.3% Tween 20) for 2 minutes and blocking solution (0.1 M maleic acid, 0.15 M sodium chloride (adjusted with sodium hydroxide to pH 7.5), 1×blocking solution) for 1 hour.

The membrane was incubated with antibody solution (blocking solution, anti-Digoxigenin-AP, Fab fragments 1:1000) for 30 minutes and washed twice with washing buffer for 15 minutes. Equilibration in detection buffer (0.1 M Tris-HCl, 0.1 M NaCl, pH 9.5) for 3 minutes was followed by sealing the membrane into a plastic wrap. Chemiluminescent substrate was diluted 1:100 in detection buffer and distributed on the membrane drop wise. After 5 minutes of incubation, excess liquid was carefully squeezed off and the plastic wrap was carefully sealed around the membrane. Detection of chemiluminescence was performed by exposure of membrane to X-ray film for 15 to 30 minutes.

2.12. Microbiology methods

Bacteria culture

E. coli were grown over night on agar plates or in LB medium in an orbital shaker at 230 rpm and 37°C, excluding SW106, which had to be cultured at 42°C. Agar plates and LB medium were supplemented with the appropriate antibiotics: either 100 µg/ml ampicillin or 30 µg/ml kanamycin for bacteria with plasmid DNA. BAC selection was performed with 12.5 µg/ml chloramphenicol or 12.5 µg/ml chloramphenicol and 25 µg/ml kanamycin in double selection. Ampicilin concentrations was reduced to 50 µg/ml for double selection. For liquid culture, single colonies were picked using a sterile pipette tip.

Long term storage of bacteria

For long term storage of correct bacterial clones, 750 µl of bacterial culture in LB were combined with 250 µl sterile 99% glycerol and stored at -80°C.

Transformation of bacteria with electroporation

For transformation of electrocompetent *E. coli* (Emax), 2 ng of plasmid, 50-100 ng of BAC or 1.5 µl of ligation solution were combined with a 50 µl aliquot of cells. The mixture was transferred to a pre-cooled 2 mm electroporation cuvette, placed into the electroporator and pulsed for 5 ms at 2500 V. For successful DNA uptake, cells were incubated in 700 µl of LB medium at 37°C for 45 minutes before plating on agar plates containing antibiotics for selection. For blue-white screening agar plates were covered with X-Gal and IPTG prior to plating of bacteria.

Table 2.5.: Split conditions for different dish sizes

Culture dish	Medium [ml]	PBS [ml]	Accutase [ml]
96-well plate	0.15	0.25	0.02
48-well plate	0.25	0.5	0.05
24-well plate	0.5	1	0.15
12-well plate	1	1	0.25
6-well plate	2	3	0.5
T-25 flask	5	5	1
T-75 flask	15-20	10	4
T-150 flask	25-35	20	6
10 cm dish	10-15	10	4
15 cm dish	25-35	20	6

2.13. Tissue culture methods

2.13.1. Cultivation conditions and passaging

Cell culture was carried out in a humidified incubator at standard conditions of 37°C and 5% CO_2. Cells were handled in a sterile class II laminar flow hood with sterile material and pipette filter tips. Medium was changed every 2 days. Culture dish sizes, medium, PBS and detachment reagent volumes are listed in Table 2.5.

To avoid confluence greater than 90%, cells were regularly passaged. Old medium was removed and wells were washed with PBS. The cells were detached from the culture dish by addition of Accutase and incubation at 37°C for 3 to 5 minutes. After gentle tapping of the culture dish, cells were resuspended in fresh medium and singularised by pipetting up and down a few times. The required solution volume was transferred to a new dish containing pre-warmed medium and distributed evenly by gentle forward and backward movements. The dish was placed into the incubator for cultivation. If a defined number of cells had to be seeded, the cell concentration was determined with the improved Neubauer counting chamber.

2.13.2. Freezing and thawing of cells

For freezing of cells the desired cell number was detached and centrifuged at 320 g for 5 minutes. The pellet was resuspended in freezing medium containing 10% DMSO and 20% FCS and transferred to a 2 ml cryo vial. This was immediately stored in a freezing device transferred to -80°C. After 2 days the samples were moved to the gaseous phase of liquid nitrogen.

Thawing was conducted as quickly as possible, to minimise cell death caused by cytotoxicity of DMSO. Samples were pre-thawed in a water bath at 37°C and immediately transferred to 10 ml

of pre-warmed medium prepared in a 15 ml tube. Cells were spun down at 320 g for 5 minutes and resuspended in fresh medium. The solution was transferred to a new culture dish and left in the incubator without disturbing for at least 6 hours.

2.13.3. Isolation of porcine cells

Pigs were slaughtered by a butcher and tissue for cell isolation was placed in PBS. During transport to the laboratory, it was kept at 37°C. Prior to isolation, all necessary equipment and the tissue was thoroughly cleaned with 80% ethanol. The first 3 days of culture medium contained penicillin, streptomycin and amphotericin B. It was changed daily after careful washing with PBS. After this period antibiotic-free medium was used.

Isolation of pMSC from bone marrow

Porcine bone marrow MSCs were isolated from femur and tibia. The bone ends were sawed off and bone marrow was flushed with a pre-warmed heparin solution (1000 U heparin/ ml HBSS). The liquid was collected into a 100 mm petri dish and up to 20 ml were loaded onto 25 ml of lymphocyte separation medium. Separation of bone marrow residual cells was carried out via centrifugation for 20 minutes at 1000 g. To prevent gradient disturbance the centrifuge acceleration and brake were switched to soft mode. After spinning, mononuclear cells from the gradient interphase were washed in 20 ml HBSS and pelleted at 600 g for 10 minutes. For subsequent MSC culture, the pellet was resuspended in MSC medium (Advanced DMEM, 10% FBS, Glutamax 1×, non-essential amino acids 1×, FGF (5 ng/ml)) containing antibiotics, plated on one T-150 flask per bone and cultured.

Isolation of pMSC from adipose tissue

For adipose tissue MSC isolation, a 6 g piece of neck fat was weighed and cut to small pieces. It was placed in a 50 ml falcon tube containing 10 ml of a collagenase I solution (0.1% in PBS) and incubated at 37°C for 45 minutes. The sample was mixed gently from time to time. After complete digest the solution was filtered through a 100 µmstrainer into a new falcon tube. The tube was filled up with an equal volume of culture medium an spun for 10 minutes at 1,000 g. The cell pellet was resuspended in fresh medium, plated on two T-150 flasks and cultured.

Isolation of porcine kidney fibroblasts

Primary fibroblasts were isolated from pig kidney. The tissue was minced and digested with collagenase type II at 37°C for 30 minutes under gentle shaking. Cells were pelleted by centrifugation at 600 g for 10 minutes, washed HBSS and spun down again. The cell pellet was resuspended

in fresh culture medium (Dulbecco's modified Eagle medium, 10% FCS, 293 mg/l Glutamax 0.1 mM 2-mercaptoethanol, 1% nonessential amino acids, 1% sodium pyruvate)supplemented with antibiotics and plated on two collagen type 1 coated T-150 flasks.

2.13.4. Differentiation assays for pMSCs

Differentiation assays for porcine mesenchymal stem cells were carried out to demonstrate adipogenic, osteogenic and chondrogenic differentiation capacity.

Adipogenesis

Porcine MSCs were seeded at a density of 2×10^5 per well in a 6-well plate. Adipogenesis was induced in three out of six wells by cultivation in induction medium (pMSC medium with ITS+ ($1\times$), 1 μM dexamethasone, 50 μM 3-methyl-isobutylxanthine, 100 μM indomethacine). The remaining three samples – serving as controls – were cultured in normal growth medium. Medium was changed three times per week for 12 days. After this period, cells were washed twice with PBS and fixed by addition of 2 ml of 10% formalin solution. After 30 minutes of incubation, extensive washing with PBS and deionised water removed excess of formalin before cells were left for drying.

After fixation, lipids were stained with Oil Red O. Therefor, per well 1 ml of the Oil Red O working solution was incubated for 5 minutes. Wells were rinsed twice with 2 ml of 60% isopropanol and 3 times with tap water. Plates were covered with water and stored in the fridge until photos for documentation were taken.

Osteogenesis

To detect differentiation into osteoblasts, Von Kossa staining was performed to detect Ca^{2+} deposits on osteogenic cells. Porcine MSCs were seeded at a density of 30,000 cells per well into a 6-well plate and differentiation was induced after one day (pMSC medium, 10 mM dexamethasone, 10 mM beta-Glycerolphosphate, 50 μg/ml ascorbic acid-2-phosphate). Controls were continuously treated with normal growth medium. Medium was changed twice a week until fixation was performed after 19 days. Cells were washed with water to remove remaining PBS. Then 1 ml of a 3% $AgNO_3$ solution was added to each well and incubated for 10minutes at room temperature in the dark. For the second incubation step the plate was left for 15 minutes under UV light before washing twice with water. Excess of stain was removed and wells were washed 5 times with PBS. Photos were taken immediately after washing. Brown spots indicated Ca^{2+} deposits.

Chondrogenesis

5×10^5 pMSC from sub-confluent cultures were transferred to a 15 ml tube and pelleted by centrifugation at 3,400 g for 3 minutes. After washing with 10 ml of serum free medium, incomplete chondrogenic selection medium (pMSC medium without FGF) was carefully added to not disturb the pellet. Medium was changed three times a week for 19 days in total. Since pellets are not very firm during the first week, medium aspiration was performed very carefully. Growth factor (10 ng/ml TGF-beta) was always added to incomplete medium just before usage. For analysis, medium was removed and cells were washed twice with 5 ml PBS. The pellet was left to air dry after removal of PBS and could be frozen at -20°C until further processing. A papain digest was conducted for 6 hours at 60°C. The papain working solution (1 mg/ml) was prepared in chondrogenic dilution buffer (50 mM sodium phosphate, 2 mM EDTA, 2 mM N-acetyl-cystein, pH 6.5). Per tube 200 µl were added and vortexed briefly. To avoid evaporation during digest, lids were closed tightly. During all steps it was ensured that the pellet remained in solution.

For chondroitin quantitation, 50 µl of each sample and a chondroitin-6-sulphate standard ranging from 0.1 to 0.8 µg/ml were pipetted to a flat bottom 96-well plate in duplicates. For standard preparation a chondroitin stock solution (0.16 mg/ml in dilution buffer) was used. Then 200 µl the assay reagent (DMMB) were added to each well and absorption was measured at 595 nm.

In order to be able to standardise the chondroitin amount of each sample, it was set in relation to the contained DNA amount. For this purpose, DNA amounts were determined using Quanti-iT™PicoGreen dsDNA Assay Kit. Prior to sample processing, Pico green working solution was obtained by diluting the Pico green solution 1:200 in TE buffer. Furthermore, a λ DNA standard stock solution was diluted 1:50 and a dilution series ranging from 0 to 2 µg/ml was prepared. Sample dilutions (1:10) and standard samples were added to a black 96-well plate in triplicates and mixed with 100 µl of the PicoGreen working solution. After 5 minutes of incubation, fluorescence was measured at fluorescein settings of 485 nm/535 nm (0.1 s).

2.13.5. Transfection

Electroporation

For electroporation of cells, 1×10^6 cells were pelleted for 5 minutes at 320 g and resuspended in 800 µl of hypoosmolar electroporation buffer. After addition of DNA, the suspension was transferred to a 4 mm electroporation cuvette and incubated for 5 minutes at room temperature. Cells were pulsed at 1,200 V for 85 µsand incubated for 10 minutes. Then, 1 ml of medium was added to the cuvette and all liquid was transferred to an appropriate culture dish containing pre-warmed medium. The following day medium was changed to remove dead cells.

Lipofection

Porcine cells were split into a 6-well plate 24 hours before transfection, to reach 80 to 90% confluence the following day. The next day, the required DNA amount was mixed with 250 µl Opti-MEM and, in a second tube, the corresponding amount of Lipofectamine 2000 was added to 250 µl Opti-MEM, as well. Both solutions were incubated for 5 minutes. They were combined and incubated for 20 minutes. Meanwhile, cells were rinsed with PBS and 1 ml Opti-MEM was added to each well. The transfection mix was transferred drop-wise to each well. After 6 hours 2 ml of medium, was added. The following day, medium was exchanged.

Nanofection

Porcine cells were split into a 6-well plate 24 hours before transfection, to reach 80 to 90% confluence the following day. For each well, DNA was mixed with 100 µl diluent. In a second tube Nanofectin was added to 100 µl diluent at the required concentration. The nanofectin solution was transferred to the DNA, mixed and incubated for 20 minutes. Meanwhile, cells were rinsed with PBS and 2 ml culture medium were added to each well. The combined solution was transferred drop wise to the cells. After 2 to 4 hours, medium was changed.

Nucleofection

For nucleofection 5×10^5 cells were pelleted by centrifugation for 10 minutes at 90 g and resuspended in 100 µl nucleofection solution. After addition of DNA, the suspension was transferred to a nucleofection cuvette and pulsed using the program suggested by the manufacturer. A volume of 500 µl of medium were immediately added to the cuvette and then all liquid was transferred to a 6-well containing pre-warmed medium supplemented with 20% FCS. The following day medium was changed to remove dead cells.

2.13.6. Selection of transfected cells and picking clones

48 hours after transfection, cells were detached from the culture flask and replated in 15 cm dishes at the required density. Selection was carried out with G418 or blasticidin S at the determined optimal concentration. Medium was changed at least every two days until selection was completed and single cell colonies were visible on the plate. Picking of colonies was performed with small filter paper soaked in accutase after washing with PBS. These were placed on top of each colony for 2 minutes. Filters papers were transferred to 48-well plates with pre-heated culture medium supplemented with G418.

2.13.7. β-Galactosidase staining of eukaryotic cells

β-Galactosidase staining of cell transfected with lacZ constructs was performed in 6-well plates. After aspiration of medium cells were washed once with PBS and fixed with 2 ml of fixation solution (2% Formaldehyde 0.2% Glutaraldehyde in PBS) for 5 minutes. The fixation was removed through washing with PBS 3 to 5 times. Staining with complete staining solution (1 mg/ml X-Gal) at 37°C was carried out for 1 to 36 hours in the hybridisation oven. Excess of stain was washed away with PBS and photos were taken from cells covered with PBS.

2.13.8. Cell preparation for somatic cell nuclear transfer

The cell cycle of gene targeted clones was synchronised by serum starvation. Two days prior to SCNT, medium was changed to starvation medium lacking FGF-2 supplementation and containing only 0.5% FCS.

2.14. Fluorescence in situ hybridization

In order to validate BAC based targeting, but also for exclusion of random integration, fluorescence in situ hybridization (FISH) was conducted.

2.14.1. Probe production, validation and denaturation

A specific probe for the IL2Rg-neo BAC was produced by nick translation. For that purpose BAC maxiprep DNA was mixed according to Table 2.6 with a DNaseI/Polymerase mix and was incubated at 16°C. At defined time points reaction progress was quickly checked with agarose gel electrophoresis (1$\times$ TBE; 120 V). As soon as the gel showed a DNA smear concentrated around approximately 500 bp length, nick translation was stopped by quick freezing on dry ice and addition of EDTA.

Validation of IL2RG-bio probe sensitivity was performed with dot blot analysis. Therefore, 1 to 3 µl of probe were diluted 1:10 and 1:100 and were soaked on nitrocellulose membrane. After drying, the membrane was exposed to UV light for one minute and then incubated in AP1 buffer (0.1 M Tris, HCl pH7.5, 0,1 M NaCl, 2 mM $MgCl_2$, 0.05% Triton-X-100) for 1 minute. Subsequently, membrane was shaken in AP2 (AP1, 3% BSA) and then transferred to AP1-Streptavidin (6 ml AP1, 1 µl Streptavidin). Each step was performed under exclusion of light for 10 minutes. Washing was conducted twice with AP1 and 3 times with AP3 (0.1 M Tris HCl pH 9.5, 0.1 M NaCl, 50 mM $MgCl_2$) for 3 minutes per step. Staining with NBT/BCIP (20 µl NBT, 16.6 µl BCIP, 5 ml AP3) for 1 hour should result in a signal. If no dot is visible, the probe dilution was too high.

Table 2.6.: Nick translation

Component	Final concentration/amount
DNA	75 µg
10× NEB buffer	1×
dATP, dCTP, dGTP mix (1 mM)	50 µM
dTTP (1 mM)	37.3 µM
bio-dUTP (1 mM)	12.6 µM
β-mercaptoethanol (100 mM)	0.67 mM
DNse	10 U
Polymerase I	7.5 U
$MgCl_2$ (1 M)	13 mM
H_2O	add up to final volume

After sensitivity validation, clean probe material was obtained by sodium acetate/ethanol precipitation, which was performed with a mix of all necessary probes (1 and 2 µl IL2RG-bio, 3 µl Pg21-dig, 0.5 µl Cot1, 1 µl Salmon). This hybridization mix was resuspended in 5 µl of H_2O. Denaturation of probe mix was carried out by adding of 100% formamid, vortexing and 30 minutes of incubation at 37°C. Furthermore, addition of 5 µl of 40% dextran sulfate/2×SSC and 5 minutes incubation at 72°C lead to inhibition of renaturation. The hybridisation mix was ready to use after 30 minutes at 7°C and storage at -20°C.

2.14.2. Preparation of metaphase spreads and denaturation of chromosomes

For FISH analysis, target cells were in metaphase of mitosis. Therefore, HT1080 and ST007 were grown in a T-75 flask until 75% confluence and incubated in culture medium containing colcemid (0.8 µg/ml) for 3 to 5 hours. Cells from the supernatant and those still attached were collected and spun down for 5 minutes at 320 g. The pellet was slowly resuspended by drop-wise addition of 4 ml of hypotonic KCl/NaCitrate solution. After 15 minutes of incubation at 37°C, 0.1 volume of methanol:acetic acid (3:1, fixation solution) was added and additional 10 minutes of incubation at room temperature were performed. Centrifugation at 320 g for 5 minutes took place to spin down cells. The pellet was first dissolved in 1 ml of fixation solution pre-cooled at -20°C before adding further 7 ml. This washing was repeated four times. In between the fixation steps centrifugation was carried out at 700 g for 7 minutes. The supernatant was removed, except for half a milliliter. After final washing, the cell pellet was dissolved in 1 ml of fixation solution and incubated at -20°C for at least 10 minutes. Metaphase spreads were obtained by dropping five to eight drops of fixed cell nuclei onto ice-cold microscope slides from approximately 40 cm height.

Excess of liquid was soaked to tissue paper, before slides were quickly dried at 40°C on a slide warmer. Air drying was completed after 14 days at room temperature under exclusion of light.

For removal of free RNA, proteins and cytoplasm remains, object slides had to be treated with RNase and pepsin. Therefore, they were washed for 5 minutes in 2×SSC and treated with 200 µl of RNase working solution (200 µl 2×SSC, 2 µl RNase (10 mg/ml in 10 mMTris-HCl, pH 7.5)). This working solution was pipetted on the microscope slides and covered with a cover slip. RNA removal took place during 30 minutes in a humid chamber at 37°C. RNase was removed by washing 3 times with 2×SSC for 5 minutes. Pepsin digest was carried out for not longer than 1 minute at 37°C in a 10% pepsin working solution (in 100 µl 5 N HCl in 50 ml H_2O, preheated). Excess of pepsin was removed by washing with PBS for 5 minutes. After treatment with a rising ethanol series (70%, 90%, 100%) at -20°C for 3 minutes per concentration, object slides were left to air dry.

To obtain single strand chromosomes enabling probe hybridisation, metaphase spreads were denaturateted in 70% formamid/ 2×SSC (pH 7) for 1 minute 45 seconds at 72°C. Fixation of single strands was ensured by a rising ethanol series (70%, 90%, 100% at -20°C) for 5 minutes in each concentration. Object slides were ready to use for FISH after 1 hour of drying in the dark.

2.14.3. Probe hybridisation and antibody detection

For hybridization of probe to metaphase spreads, 10 µl of hybridisation mix was pipetted to the object slide and covered with a cover slip. After fixation of the cover slip with cement glue for 2 minutes at 72°C, hybridisation was carried out over night at 37°C. The next day, removal of cement glue and cover slips was followed by washing. Each step was carried out for 5 minutes. Firstly, 3 washing steps were conducted at 42°C with 2×SSC-Tween, then 3 steps with 1×SSC at 60°C and in the end again with 2×SSC-Tween at 42°C.

In order to block unspecific binding of antibody, object slides were treated each with 1 ml 1% BSA for 30 minutes at 37°C. Excess of BSA was washed off with 2×SSC-Tween for 5 minutes at 42°C. For specific antibody based detection of probe mixes, antibody solutions were spun down quickly and mixed for the detection of Biotin and Digoxigenin. Therefore, 200 µl of 1% BSA solution were mixed with 0.67 µl Cy3.5 and 1.33 µl Sheepantidig-fluorescein, transferred to the slide and covered with a cover slip. After incubation for 45 minutes at 37°C in a humid chamber, washing with 2×SSC at 42°C was repeated twice for 5 minutes.

Subsequently, DAPI staining of chromosomes was carried out with 0.5 µl DAPI in 10 ml 2×SSC-Tween. Of this working solution 1 ml was incubated on the slides for 2 minutes and washed twice with deionised water before drying in a dark chamber. Finally, antifade embedding with 35 µl antifade solution, covered with a 24×60 cover slip and incubation at 4°C completed the procedure.

3. Results

Genetic defects in Janus kinase 3 (JAK3) or the common gamma chain (IL2RG) cause severe combined immunodeficiency (SCID) in humans. The objective of this study was the generation of immunodeficient pigs for translational biomedical research by gene targeted inactivation of these two genes. The experimental approach and study results are presented in this section.

3.1. Overview of vector constructs

This section briefly presents important vector constructs used in this study. Details on molecular cloning of all vector constructs can be found in the appendix of this work.

Figure 3.1 shows a schematic overview of the CAGGS-Cherry-NLS (CCN) cassette. This encodes the red fluorescing protein mCherry controlled by the chicken β-actin promoter modified by a cytomegalo virus enhancer element (CAGGS promoter). This makes CAGGS a very strong promoter [179]. The simian virus 40 (SV40) nuclear localisation signal (NLS) drives active transport of the vector from the cytosol into the nucleus. The CCN cassette was introduced into the backbone of targeting constructs to enable visual screening of selected clones. Red cells indicate random integration of the complete vector, as with correct homologous recombination (HR) the backbone is lost.

Figure 3.2 depicts the construction of BAC targeting vectors using the IL2RG construct as an example. BAC-based constructs were generated by recombineering between a wildtype BAC and

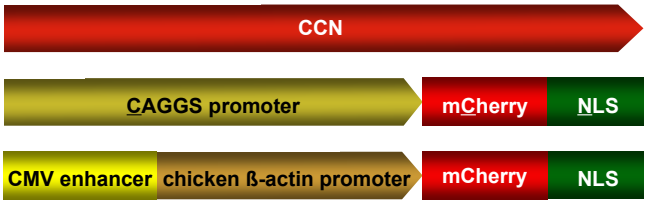

Figure 3.1.: The CAGGS-Cherry-NLS cassette
The CCN cassette enables visual exclusion of random integration events and drives active nuclear transport due to the nuclear localisation signal (NLS). The CAGGS promoter is a chicken β-actin promoter enhanced by a cytomegalo virus (CMV) element.

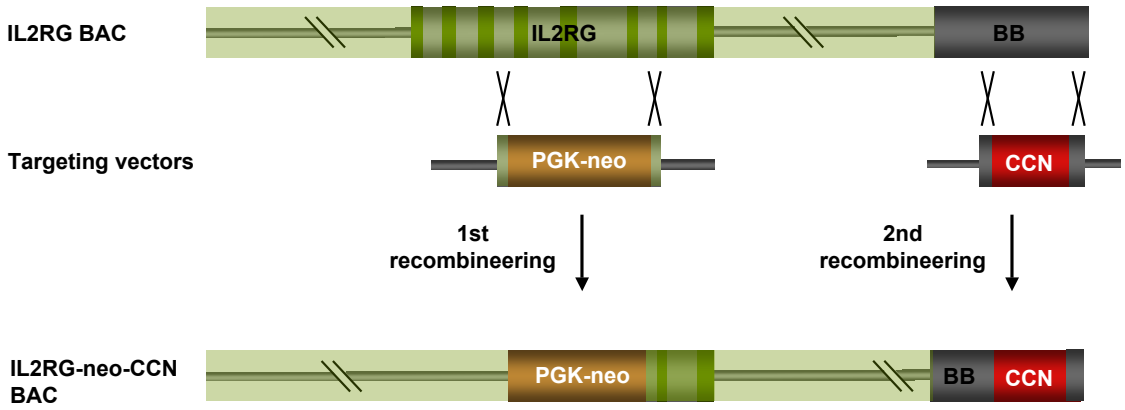

Figure 3.2.: Construction of the BAC gene targeting vector for IL2RG
The BAC targeting vectors were constructed by recombineering in two steps. A short targeting vector containing a PGK-neo positive selection cassette flanked by approximately 500 bp of 5' and 3' homology was used to replace parts of the IL2RG coding sequence. In a second recombineering step, partial replacement of the BAC backbone (BB) was performed with the CCN cassette also flanked with short homology regions.

a short targeting vector. The latter contained a PGK-neo selection cassette flanked by two approximately 500 bp homology arms. Homologous recombination was performed in *E. coli* strain SW106. The recombineering vector was designed in a way to disrupt the gene of interest. The IL2RG and the JAK3 BAC targeting constructs were further modified with the CCN described above. Therefore, a second recombineering step to introduce CCN into the backbone was followed.

Figure 3.3 summarises all BAC vectors used in this study. In the *IL2RG-neo-CCN* BAC exons 1-7 were deleted by the PGK-neo cassette. *JAK3-geo-CCN* BAC contained for positive selection a lacZ-neo fusion product (geo) instead of neo alone. This allowed also staining of transfected cells with β-Galactosidase. PGK-geo replaced exons 2-22 of the JAK3 gene in this vector. The RAG2-geo BAC was used for the assessment of BAC transfection efficiency only. Most of its only exon's sequence was deleted with PGK-geo.

Figure 3.4 shows the schematic picture of the JAK3 conventional vector. In this construct, exons 2-5 were replaced by PGK-neo. The CCN cassette in the plasmid backbone allowed visual screening and active nuclear transport.

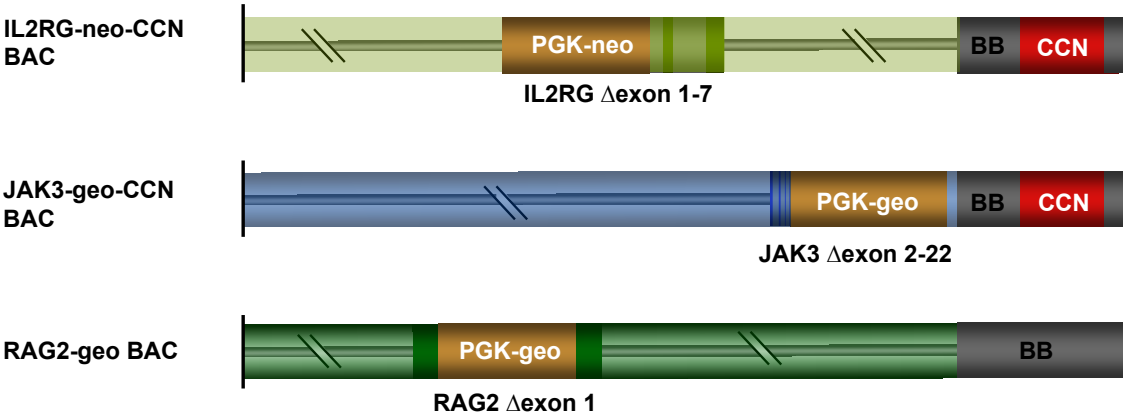

Figure 3.3.: BAC gene targeting vectors - schematic overview
The final BAC targeting constructs for IL2RG, JAK3 and RAG2 are shown. Parts of the coding sequnces were deleted and replaced either by PGK-neo selection or PGK-geo.

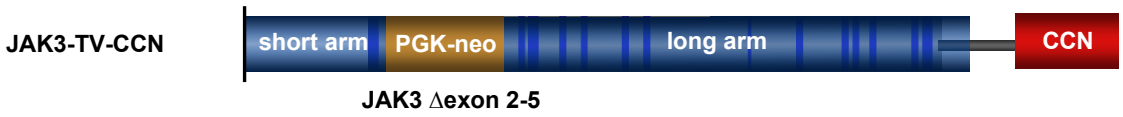

Figure 3.4.: JAK3 conventional gene targeting vector - schematic overview
The JAK3 conventional gene targeting vector contains a PGK-neo selection cassette flanked by a short 5' homology arm and a long 3' homology arm. The CCN cassette was inserted in the vector backbone and allowed active nuclear transport and visual screening.

3.2. Cells for gene targeting and SCNT

Cells used for the generation of large animal models by gene targeting and somatic cell nuclear transfer (SCNT) have to fulfill different parameters: suitable cells have high proliferation capacity in vitro, are efficiently transfectable and have the ability to produce healthy fertile pigs in SCNT. The characteristics of a suitable target cell are discussed in detail in Section 4.1.

Three different primary cell types have been tested and compared in this study: porcine kidney fibroblasts (pKDNF) and two of mesenchymal stem cell (pMSC) types. Cells were isolated from young pigs at the age of 2 to 5 months. The use of cells isolated from male individuals for SCNT made sex pre-determination of gene-targeted offspring possible. Male founder animals make sperm collection after sexual maturity possible and thus allow rapid expansion of the herd. In general low passage cells are preferable for gene targeting experiments and SCNT because genetic modification involves extended culture time.

3.2.1. Porcine mesenchymal stem cells

Porcine MSCs were isolated from two different sources in this study: bone marrow and adipose tissue. These two cell types were compared concerning their ability to trigger homologous recombination at the JAK3 or IL2RG loci and to produce healthy offspring by SCNT. After isolation, MSCs were characterised regarding differentiation capacity and transfection efficiency.

Isolation and characterisation

Defining criteria for human MSCs were are *in vitro* adherence to plastic, the expression profile of specific surface markers and *in vitro* differentiation into osteogenic, adipogenic and chondrogenic lineages [180]. MSCs have been isolated from different species and different tissue sources, such as bone marrow [181], fat, tendon, muscle, umbilical cord [182], peripheral blood, articular cartilage and synovial membrane [183].

In this study, porcine MSCs were isolated from bone marrow and adipose tissue Fibroblast-like cells adherent to plastic started to form colonies approximately 72 hours after isolation. Figure 3.5 shows a representative picture of bone marrow and fat derived pMSCs after first passage.

Human MSCs are defined by expression of surface markers CD105, CD73 and CD90, but do not show expression of CD45, CD34, CD14 or CD11b, CD79alpha or CD19 and HLA-DR surface molecules [180]. However, surface marker combinations unique to porcine mesenchymal stem cells have not yet been agreed on. Thus, multipotency of pMSCs was only determined by their capacity to differentiate into adipogenic, osteogenic and chondrogenic lineages. Representative results of typical differentiation assays are presented for bone marrow (BM) and adipose (AD)

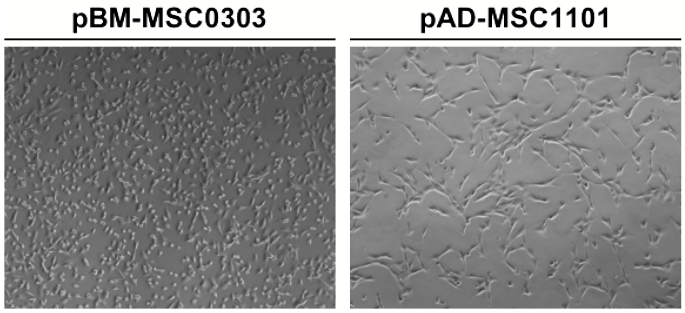

Figure 3.5.: pBM-MSCs and pAD-MSCs isolations
Mesenchymal stem cells isolated from bone marrow and adipose tissue have a fibroblast-like morphology. Cells from some preparations appear to be larger and more elongated than others. Passage 1. 5× magnification.

cell isolates pBM-MSC0712 and pAD-MSC1101. All differentiation experiments were carried out at passage 3.

Adipogenic differentiation Adipogenic differentiation of pMSCs was induced by culture in adipogenic induction medium for 12 days. Differentiation of pAD-MSCs to adipose cells by became visible as early as 3 days. Oil Red O staining confirmed lipid production by approximately 70% of cells in induction medium (Figure 3.6) . Controls cultured in pMSC maintenance medium showed some adipogenic differentiation on culture dish areas with high cell density (data not shown).
Bone marrow derived pMSCs showed lower adipogenic differentiation compared to pAD-MSCs. Lipid vesicle formation became visible 5 days after induction. Lipid staining demonstrated adipogenic differentiation for approximately 50% of cells. No spontaneous differentiation was observed when cells were cultured pMSC maintenance medium.

Osteogenic differentiation Osteogenic differentiation of pMSCs was performed by culture in osteogenic induction medium for 19 days and visualised by silver nitrate staining of calcium deposits on the cell surfaces.

Brown staining indicative of calcium deposition was visible for both cell types, but to varying extents (Figure 3.7). Porcine BM-MSC0712 showed darker staining and thus stronger calcium production. Some spontaneous differentiation was also observed in non-induced control cells. Although pAD-MSC1101 underwent osteogenesis, the amount of calcium produced seems to be lower as indicated by weaker staining, which was similar to bone marrow maintenance medium controls.

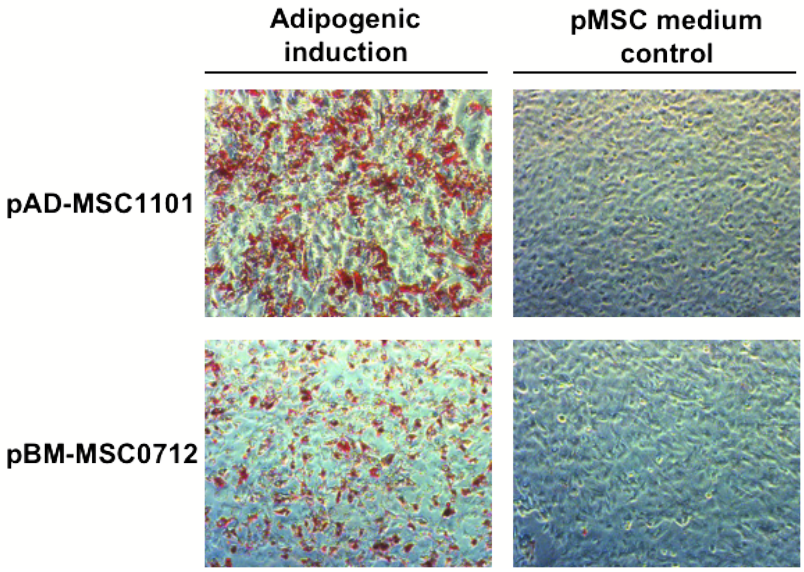

Figure 3.6.: Adipogenic differentiation of pMSCs
Oil Red O lipid vesicle staining was performed on cells cultured in pMSC culture and adipogenic induction medium after 12 days. Differentiation capacity for pBM-MSC0712 and pAD-MSC1101 was shown for approximately 50% and 70% of cells, respectively. 10 $\times$ magnification.

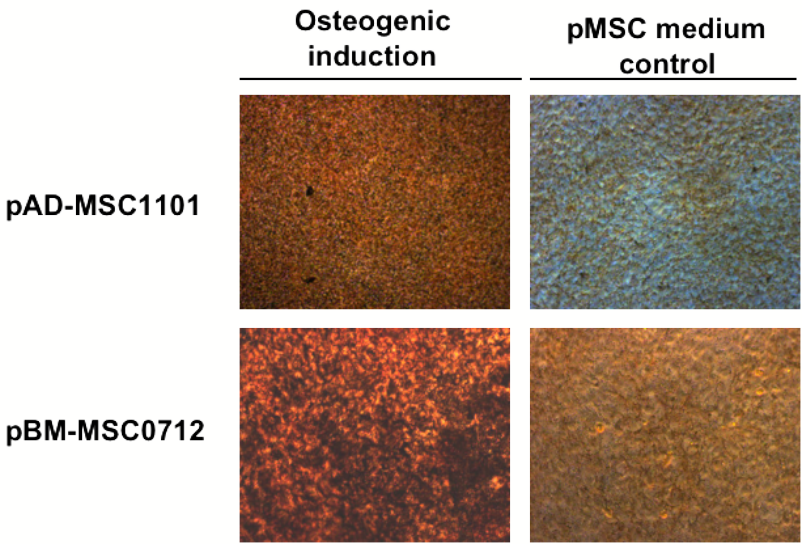

Figure 3.7.: Osteogenic differentiation of pMSC
Silver nitrate staining of calcium deposits of pMSCs was performed after 19 days of culture in osteogenic induction medium. Both bone marrow and fat pMSCs differentiate into calcium producing cells. However, pBM-MSC0712 undergo osteogenic differentiation to a higher extent. 10 $\times$ magnification.

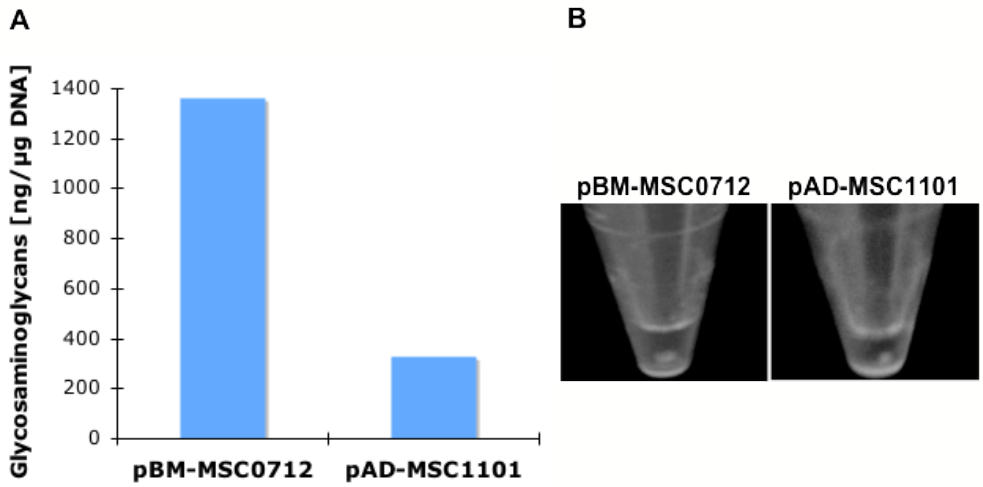

Figure 3.8.: Chondrogenic differentiation of pMSCs
3D cultures of pMSCs were assessed after 19 days of induction with TGF-β. Pellet formation of cells started 3 days after induction. A: Quantitation of glycosaminoglycans demonstrated higher differentiation potential of bone marrow derived MSCs (1360 ng/µg) compared to fat derived MSCs (330 ng/µg). B: This result was in line with the difference in pellet sizes observed.

Chondrogenic differentiation Chondrogenic differentiation of mesenchymal stem cells was performed in three dimensional cultures in medium supplemented with TGF-β. Cells were pelleted by centrifugation and cultured for 19 days. Loose pellets formed round compact cell aggregates as early as 3 days after induction. Quantification of Glycosaminoglycans normalised to DNA content provided a measure for chondrogenic differentiation.

Porcine AD-MSC1101 produced a much smaller pellet compared to BM-MSC0712 suggesting lower chondrogenic capacity (Figure 3.8 B). This was supported through quantification of glycosaminoglycans, which resulted in 1360 and 330 pg per µg DNA for pBM-MSCs and pAD-MSCs, respectively (Figure 3.8 A). Neither bone marrow nor adipose pMSC controls cultured in maintenance medium were able to differentiate and form pellets (data not shown).

Summary The data from differentiation assays proved that the isolated bone marrow and fat cells are multipotent mesenchymal stem cells. These cells showed varying differentiation potential, depending on their tissue source of origin.

Immortalisation of pMSCs

Gene targeting experiments involve transfection, selection and HR screening steps. Screening of clones, e.g. by fluorescence in situ hybridisation, requires sufficient cellular material, and thus,

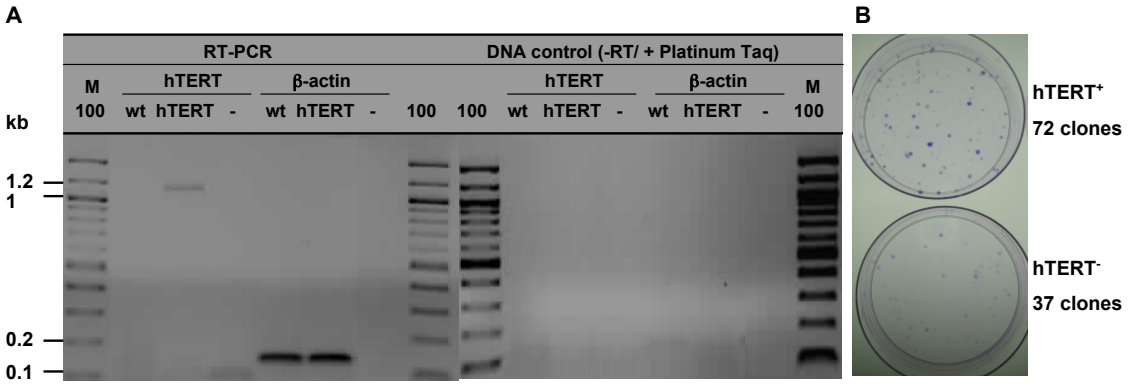

Figure 3.9.: Immortalisation of pMSC - hTERT expression and dilution assay
A: The RT-PCR gel shows that RNA was isolated (β actin RT-PCR) from samples free of genomic DNA (DNA control). The hTERT transfected cells do express hTERT (1.1 kb band). The capacity of hTERT$^+$ and hTERT$^-$ cells to form colonies was assessed. 100 cells seeded per 10 cm dish produced 72 and 37 colonies respectively. Hence, cells produced more and bigger colonies, if transfected with hTERT.

extended time in culture for proliferation. A cell sample of clones positive for gene targeting and frozen for SCNT may then be immortalised and expanded for analysis. If correct targeting could be confirmed, non-immortalised early passage cells of the clone could be used for SCNT.

The option to immortalise pMSCs was tested with expression of human telomerase reverse transcriptase (hTERT). pBM-MSC0712 were cotransfected with a hTERT vector and pmaxGFP at a 10:1 ratio of DNA amounts to be able to visually check transfection efficiency. Positive selection with blasticidin S was performed for 10 days and resulting colonies were pooled. hTERT transfected cells were cultured in parallel with control pBM-MSC0712 transfected with pmaxGFP only. Growth behaviour was compared for these cells in a dilution assay, in which 10, 50 and 100 cells were seeded. Crystal violet staining after 12 days showed that hTERT$^+$ cells produced more and bigger colonies than hTERT$^-$ controls (Figure 3.9B). Expression of hTERT was confirmed by RT-PCR as shown in Figure 3.9A. hTERT was expressed only in transfected cells, indicated by the 1.1 kb band in this sample. These results show that immortalisation of pMSCs can be conducted by expression of hTERT.

Genetic modification of pMSCs Different methods are available for the transfection of cells. The best method in regard of transfection efficiency and cell viability was determined using both plasmid and bacterial artificial chromosome (BAC) DNA encoding a visual marker gene. Efficiency was evaluated from the number of cells expressing the marker in randomly chosen optical fields. After transfection of cells assessment also included cell morphology and senescence.

Table 3.1.: Summary of pMSC plasmid transfection
Efficiency was determined 24 hours after transfection. The overall effect of transfection on cell viability was assessed based on cell death, maintenance of typical cell morphology and subsequent proliferation. Poor (*), medium (**) and good (***) viability, DNA/Nanofectin ratio (D/N), DNA/Lipofectamine ratio (D/L), not determined (n.d.).

Plasmid transfection	DNA [μg]	parameters	efficiency [%]	cell viability	fluorescence intensity
Electroporation	10	1200 V, 85 μs	40 to 70	***	low variation
Nucleofection	2	C-17	50	**	high variation
	2	U-23	90	*	high variation
BAC transfection	**DNA [μg]**	**parameters**	**efficiency [%]**	**cell viability**	**observations**
Nanofection	2-5	1:3.2 D/N ratio	n.d.	*	morphology changes
Lipofection	0.5-4	1:1-1:3 D/L ratio	0%- <10	*, **, ***	
	0.5	1:1 D/L ratio	<10	***	
Nucleofection	2, 4	C-17, U-23	n.d.	*	DNA purity critical
Electroporation	10	1200 V, 85 μs	n.d.	*	

Transfection using plasmid DNA Plasmid transfection of pBM-MSCs and pAD-MSCs was tested with nucleofection and electroporation. The experimental parameters and results are summarised in Table 3.1. Very high transfection efficiencies were obtained by nucleofection, which was carried out with pmaxGFP plasmid DNA. Fluorescence analysis could be performed microscopically as the vector encodes a cytomegalovirus promoter driven green fluorescent protein (GFP). Nucleofector program C-17 resulted in lower transfection efficiency (50%), but better cell viability than U-23 (90%) as shown in Figure 3.10. According to the manufacturer, nucleofection leads to fast and direct transport of DNA into the nucleus. This observation can be confirmed, since green fluorescence was detectable as early as 2 to 4 hours after nucleofection. However, nucleofected cells had a poor morphology with small size and round shape. They needed approximately 2 days in high serum medium (20% FCS) to recover.

Nucleofected cells varied markedly in fluorescence intensities with some intensive green cells indicating uptake of high plasmid copy numbers (Figure 3.10). Furthermore, rapid onset of gene expression provided by this method is not necessary in this study because drug selection for stable clones is not started until 48 hours after transfection. Thus, nucleofection was not considered to be a suitable method for gene targeting in pMSCs. Only experiments requiring high transfection efficiency and gene expression, e.g. immortalisation of MSCs (Section 3.2.1), were performed by nucleofection with program U-23.

Electroporation efficiency of pMSCs was standardly assessed for 10^6 cells with 10 μg pCAGGS-Cherry vector pulsed at 1200 V for 85 μs. Red fluorescence caused by CAGGS pro-

moter driven mCherry expression was assessed microscopically after 24 hours and ranged from 40% to 70% depending on the cell isolation. Figure 3.10 shows a representative picture of electroporation for pBM-MSC0712. Electroporation has been reported to generate single copy integrations and has been traditionally preferred for gene targeting [184]. In contrast to nucleofection, the intensity of fluorescence did not vary markedly between cells and cell morphology after transfection was not affected. Also one medium change after 24 hours was sufficient for the recovery of cells. In summary, electroporation provided a reasonable compromise between transfection efficiency and cell viability and was thus performed in gene targeting experiments.

Transfection using BAC DNA Transfection of somatic cells with BAC DNA showed to be very difficult. Due to the large construct size fewer copies are applied per μg DNA compared to smaller plasmids. Thus, the amount of DNA transfected often has to be increased to transfect higher cell numbers. However, this has to be carefully balanced with cell viability because large DNA amounts are cytotoxic.

Four different methods of pMSC transfection have been tested with *RAG2-geo BAC* in preliminary experiments: lipofection, nanofection, nucleofection and electroporation. This construct allows G418 selection and β-Galactosidase staining of cells after 3 to 5 days).

The experimental parameters and results are summarised in Table 3.1. Nanofection was not considered a suitable method because transfected cells showed reduced proliferation and morphology changes toward a big flat non-fibroblast cells compared to non-transfected controls (data not shown). This observation was independent of the DNA amount transfected.

DNA quality, concentrations and especially purity were found to be critical for nucleofection and electroporation. Low DNA concentration lead to an increase of the required solution volume, thereby causing dilution of the transfection buffer used. Massive cell death due to DNA impurity caused by the previous restriction digest, made phenol chloroform extraction and subsequent precipitation of DNA necessary. However, production of sufficient, intact BAC DNA was difficult, due to the large construct size. This resulted in low DNA yields from bacterial cultures, loss of material throughout the purification process and also partial degradation of BAC DNA. These problems impeded the production of transfected viable pMSC clones with electroporation or nucleofection of BAC DNA.

BAC transfection worked best with lipofection (data not shown). Precipitation of linearised BAC DNA was sufficient without prior phenol chloroform extraction for this method. Precipitation was sufficient to purify DNA from restriction enzyme and buffer as cells were not negatively affected regarding morphology or viability. Preliminary experiments were conducted with DNA amounts ranging from 0.5 to 4 μg of BAC DNA and with different DNA:Lipofectamine ratios. 0.5 and 1 μg of BAC DNA (1:1 ratio) showed best results regarding cell viability and transfection efficiency. The percentage of transfected cells was however, much lower compared to plasmid and ranged

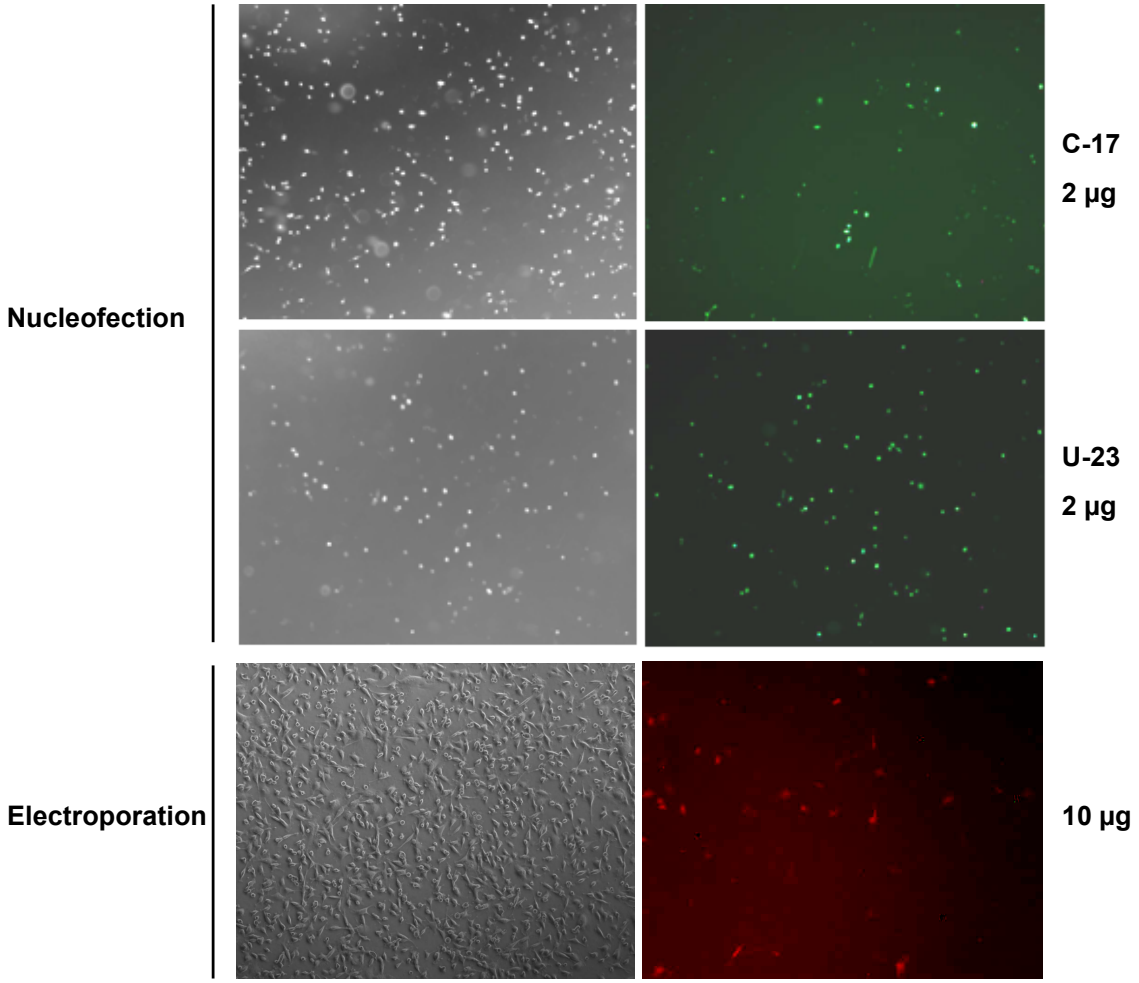

Figure 3.10.: Microscopy of pMSC plasmid transfection
Two nucleofection programs and electroporation were compared regarding transfection efficiency and cell viability was assessed 24 hours after transfection. BM-MSC1702 nucleofection (2 µg) of plasmid pmaxGFP resulted in 50% green cells for program C-17 and 90% for program U-23. Cell viability was higher for program C-17 than U-23. Electroporation of pBM-MSCs with 10 µg pCAGGS-Cherry showed good cell viability and transfection efficiency. 2.5 × magnification.

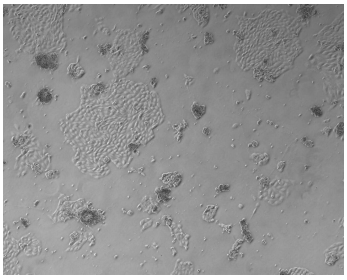

Figure 3.11.: pKDNF isolation
Porcine kidney cells represent a mixed population of cells after isolation. They have to be passaged to obtain a uniform fibroblast-like morphology. Passage 0. 5 $\times$ magnification.

from 5% to 10%. All other settings resulted in even lower numbers. Consequently, lipofection was used for subsequent BAC transfections with the determined parameters.

Summary of pMSC transfections Porcine MSCs were transfected in all following experiments with plasmid electroporation BAC DNA lipofection.

3.2.2. Porcine kidney fibroblasts

Porcine kidney fibroblasts (pKDNF) were also tested as an alternative cell type for gene targeting. After isolation, transfection conditions were established.

Porcine kidney fibroblasts were isolated from the interior of an adult kidney by mechanical and enzymatic dissociation. Cells were plated and colony formation became visible after 48 hours and a uniform fibroblast-like population could be cultured after first passage as non-fibroblast cells were lost. Figure 3.11 shows primary pKDNF 72 hours after isolation.

Genetic modification of pKDNF

Transfection using plasmid DNA Different methods of pKDNF transfection have been tested in regard to efficiency and cell viability. The experimental parameters and results obtained 24 hours after transfection are summarised in Table 3.2. Plasmid transfection of pKDNF was tested with electroporation, lipofection and nucleofection. pKDNF electroporation with 10 μg pmaxGFP (1200 V, 85 μs) resulted in poor transfection efficiency with approximately 20% cells showing green fluorescence. Cell viablity was not negatively affected. Transfection efficiency with lipofection was dependent on the applied DNA amount (1 to 6 μg) and the DNA:Lipofectamine ratios (1:1 up to 1:3). Although efficiencies of 50% were obtained, reduced cell proliferation and high rates of senescence made this method unsuitable.

Table 3.2.: Summary of pKDNF transfection with plasmid and BAC DNA
Transfection efficiency was observed 48 hours after transfection. The degree of cell viability was assessed depending on cell death and growth characteristics. Poor viability (*) up to good viability (***).

Plasmid transfection	DNA [μg]	parameters	efficiency [%]	cell viability	observation
Electroporation	10	1200 V, 85 μs	20	***	
Lipofection	1-6	1:1-1:3 D/L ratio	up to 50	*	senescence
Nucleofection	2, 4	U-13, U-23, U-12, T-16	up to 50	*, **	
	2-3	A-24	80-90	**	
BAC transfection	**DNA [μg]**	**parameters**	**efficiency [%]**	**cell viability**	**observations**
Lipofection	1-6	1:1-1:3 D/L ratio	0- <10	*, **, ***	
	1	1:2 D/L ratio	30	**	
Nucleofection	2, 4	A-24		*	DNA purity critical
Electroporation	10	1200 V, 85 μs		*	

Preliminary experiments for nucleofection were conducted with 2 μg plasmid pmaxGFP with nucleofector programs U-13, U-23, U-12, T-16 and A-24 to determine a suitable program (data not shown). A-24 performed best with transfection efficiency ranging from 50% (2 μg) to 70% (4 μg) and good cell viability 24 hours after nucleofection. Further optimisation of transfection conditions with different amounts of JAK3 targeting vector was conducted to mimic targeting conditions as closely as possible. The red mCherry protein expression cassette located on the vector backbone provided a convenient visual indicator allowing comparison of transient transfection efficiencies. Best results (80% to 90%) were produced with 2 and 3 μg plasmid DNA. As nucleofection resulted in very good efficiencies and pKDNF viablity was less affected than pMSC viability, this method was standardly used for transfection.

Transfection using BAC DNA BAC DNA nucleofection and electroporation of pKDNF was found to be just as difficult as for MSCs due to problems producing sufficiently pure BAC DNA. This made lipofection again the method of choice. The best efficiency (30%) was obtained after testing different DNA amounts (1 to 6 μg) and DNA:Lipofectamine ratios (1:1 up to 1:3) with 1 μg of BAC DNA and 1:2 ratio. Cell proliferation was reduced, but still acceptable after lipofection. This might be due to the transfer of fewer vector DNA copies per cell. Efficiencies were determined after 24 and 48 hours.

Summary of pKDNF transfections Subsequent experiments requiring pKDNF transfection were conducted with plasmid nucleofection and BAC lipofection.

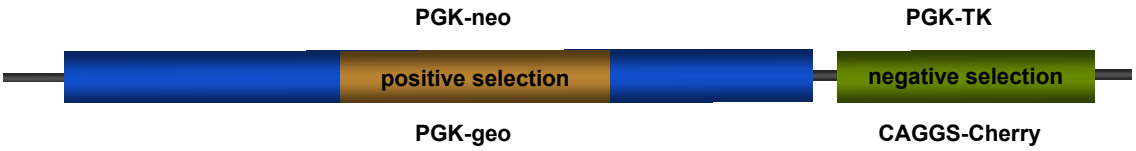

Figure 3.12.: Positive negative selection targeting vector
Schematic picture of the PNS vectors used in this study. PGK promoter driven neo or geo expression served for positive selection of transfected cells. PGK promoter driven thymidine kinase (TK) and CAGGS promoter driven mCherry expression were tested for negative selection.

3.3. Methods to select and enrich for targeted cell clones

The use of promoter-trap vectors to enrich cell bearing gene targeting events was not feasible in this study as will be discussed later (Section 3.6.1). Thus, a positive-negative selection strategy (PNS) was employed (Figure 3.12). A PGK promoter driven G418 *neo* or β*-geo* resistance gene was applied for positive selection in all targeting constructs. Negative markers are located outside the homology arms in the vector backbone. With homologous recombination (HR) the negative marker is lost, whereas it is retained upon random integration.Two approaches for the exclusion of random integration events were tested: negative selection with herpes simplex virus thymidine kinase and visual exclusion of random integration events by expression of a red fluorescence marker.

3.3.1. Positive selection of stably transfected cells

All cell isolations were characterised prior to gene targeting experiments to determine the optimal concentration of selection antibiotics. All targeting vectors carry a G418 resistance gene *neo*. Equal numbers of cells were seeded and cultured in pMSC medium containing 100 to 1000 µg/ml G418. Medium was changed regularly to remove dead cells. The minimum G418 concentration that induced killing of all cells within 10 days of selection was chosen as appropriate. Usually, it ranged from 100 to 800 µg/ml G418 depending on the cell isolate.

To test whether neo gene expression from BAC DNA is delayed, different selection induction time points were tested. G418 was therefore added either at day 2, 3, or 4. However, the number of stable cell clones after selection showed no differences. Therefore, selection was started at day 3 after BAC transfection in all subsequent experiments.

3.3.2. Negative selection with HSV-TK

A common HR enrichment approach involves negative selection of cells by expression of herpes simplex virus thymidine kinase (HSV-TK). This viral gene drives phosphorylation of ganciclovir

a 2'-deoxy-guanosine analogue, inhibiting DNA extension during DNA synthesis. Thus, HSV-TK expressing cells are not able to replicate DNA and die.

Fareed et al. (2002) have shown that human MSCs can be sensitised to ganciclovir with expression of HSV-TK [185]. To test whether TK negative selection can also be used for porcine MSCs, cells were transfected with the PGK-TK/PGK-neo vector. This plasmid was constructed to carry PGK promoter driven HSV-TK. The neo resistance gene was also expressed constitutively to enable positive selection of transfected cells. pAD-MSC1702 were electroporated with this construct and pmaxGFP at a 10:1 ratio and were cultured in medium supplemented with G418. Transfection was assessed by microscopy of green fluorescence after 24 h. Single colonies were obtained 10 days after the start of selection, pooled and subsequently cultured in MSC medium supplemented with 0.05 to 1 μg/ml ganciclovir (data not shown). Cell killing was concentration dependent and started two days after ganciclovir addition in PGK-TK positive cells. Within seven days all TK positive cells were dead, whereas pmaxGFP transfected negative controls were not affected. These results show that HSV-TK negative selection could be used for gene targeting enrichment in pMSC. However,

3.3.3. Visual exclusion of random integration events

Relatively easy screening for random integrations of gene targeting vector DNA can be performed by expression of a visual marker, such as red fluorescing mCherry protein or green GFP. The advantages of this approach over negative selection with TK are that cells with random integrations are not killed. They can be identified visually and excluded from SCNT if colonies from gene targeted cells are mixed with random integration cells. Furthermore, clones with vector integrations can be counted for HR efficiency evaluation.

A basic requirement for visual screening is a strong constitutive promoter driving marker expression. Fluorescence has to be visible with simple microscopy without the help of signal enhancement by camera. To test the practicality of different visual markers, pAD-MSC1702 were transfected with pPGK-GFP and pCAGGS-Cherry, respectively (data not shown). The transfections were performed under same conditions and with equal DNA amounts to result in similar transfection efficiencies. Strong red and only weak green fluorescence was visible after 48 hours. This result shows that CAGGS promoter based visual screening is better than with PGK. Thus, a CAGGS-Cherry expression cassette was cloned into the vector backbones of all gene targeting constructs for visual exclusion of random integration.

3.4. Gene targeting of IL2RG

Due to its function IL2RG is mainly expressed in lymphoid cells and tissues, but it has also been found in other cell types, e.g. adult lung fibroblasts [186]. As no data on MSCs or KDNFs expression are available and expression in these cell types is unlikely it was not possible to use a promoter trap approach. Thus, it was decided to apply positive negative selection (PNS) for gene targeting of IL2RG in these cell types. To increase the likelihood of homologous recombination between vector and chromosomal locus a BAC-based gene targeting vector with extensive homology was used.

3.4.1. Sequence homology of pig breeds

The porcine BAC library was derived from B cells of a Duroc breed, whereas target cells for gene targeting were isolated from German Landrace (Deutsche Landrasse, DL) or Landrace and Pietran hybrids (DL$\times$P). To determine whether the BAC and cells shared sufficient homology at the IL2RG locus, it was necessary to determine and compare the DNA sequence of both before generating the targeting vector. Thus, sequencing of 1 kb non-coding 5' and 3' flanking sequence of IL2RG was performed. Although sequence differences are most probable in non-coding regions 100% homology between the two breeds was determined. Thus, high genetic similarity was confirmed and BAC DNA could be used for targeting vector construction and gene targeting of IL2RG in DL and DL$\times$P breeds.

3.4.2. Construction of the IL2RG BAC targeting vector

The IL2RG BAC targeting vector *IL2RG-neo-CCN BAC* (197 kb) was constructed as shown in Figure 3.13. Exons 1 to 7 of porcine IL2RG were replaced with a PGK-neo positive selection cassette and the CCN cassette was placed in the vector backbone for visual exclusion of random integrations. The 5' and 3' homology arms had a length of 64 kb and 119 kb, respectively.

Introduction of the positive marker was performed by recombineering between a wildtype IL2RG BAC and a short recombineering vector by Schmidt (2008) [187]. As part of this study, the CCN cassette was constructed and recombineered to obtain the *IL2RG-neo-CCN BAC*. After homologous recombination between the wildtype allele and the targeting vector at the 5' and 3' sides of PGK-neo, exons 1 to 6 of IL2RG are deleted and the CCN cassette is lost (Figure 3.13).

3.4.3. Detection of gene targeting events

Transfection of pMSC and pKDNF with IL2RG-neo-CCN BAC was followed by selection with G418. Subsequent screening of clones for homologous recombination and random vector integration was based on visual screening, PCR analysis and fluorescence *in situ* hybridisation.

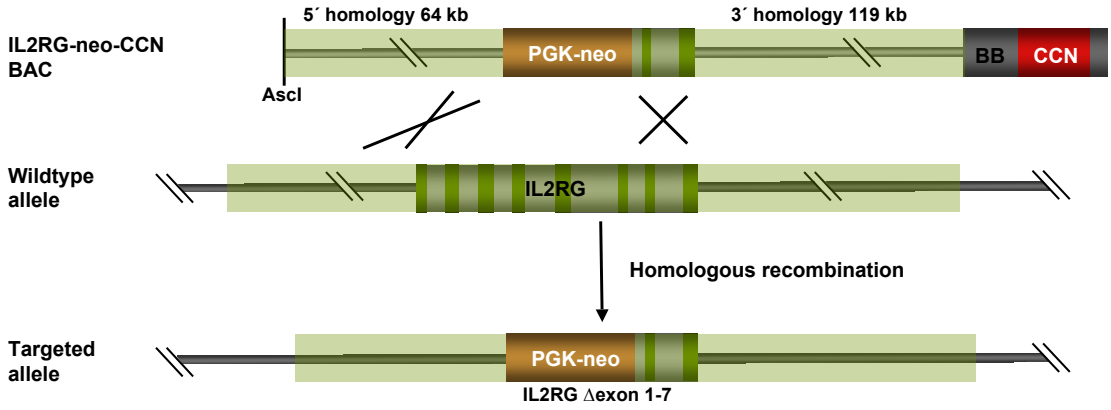

Figure 3.13.: IL2RG-neo-CCN BAC targeting
The IL2RG targeting BAC (197 kb) contains a PGK-neo positive selection cassette replacing exons 1-7. The marker is flanked by a 64 kb (5') and a 119 kb (3') homology arm. The CAGGS-Cherry-NLS (CCN) cassette in the vector backbone (BB, 14.5 kb) allows visual screening and active vector transport into the nucleus. Linearisation was performed at the AscI site prior to transfection. After homologous recombination between the wildtype allele and the targeting vector at the 5' and 3' sides of PGK-neo, exons 1 to 6 of IL2RG are deleted and the CCN cassette is lost.

Visual screening and PCR

Visual screening for red fluorescence of IL2RG-neo-CCN BAC transfected clones was performed to analyse random integration events, which caused expression of CAGGS-Cherry. With this method approximately 50% of clones could be excluded and analysis of non-fluorescing clones was performed by conventional PCR.

The cells used for targeting were male and thus hemizygous for the IL2RG gene. Consequently, IL2RG knock out by homologous recombination with the IL2RG-neo-CCN BAC can be detected by two PCRs. Figure 3.14 schematically depicts BAC targeting of IL2RG and the localisation of the PCR screening primers. Amplification of a 493 bp sequence of hypoxanthine-guanine phosphoribosyltransferase (HPRT) is performed (primers HPRT_F and HPRT_R). HPRT is also located on the X-chromosome and thus a suitable control to test if sufficient amounts of genomic DNA were present in the PCR reaction. IL2RG knock out is detected in a second PCR with primers IL2RG_HR_F and IL2RG_HR_R amplifying a 406 bp internal IL2RG sequence. This region is replaced by PGK-neo after homologous recombination with the BAC vector.

However, negative screening PCRs can indicate the lack of the target sequence within IL2RG or the lack of DNA. To increase reliability of negative PCR results, first round screenings were further analysed by repeated PCR in triplicate samples.

Definite IL2RG PCR negative clones were further tested for presence of the BAC backbone by amplification of a 399 bp fragment with primers BB_F and BB_R. This short sequence is only

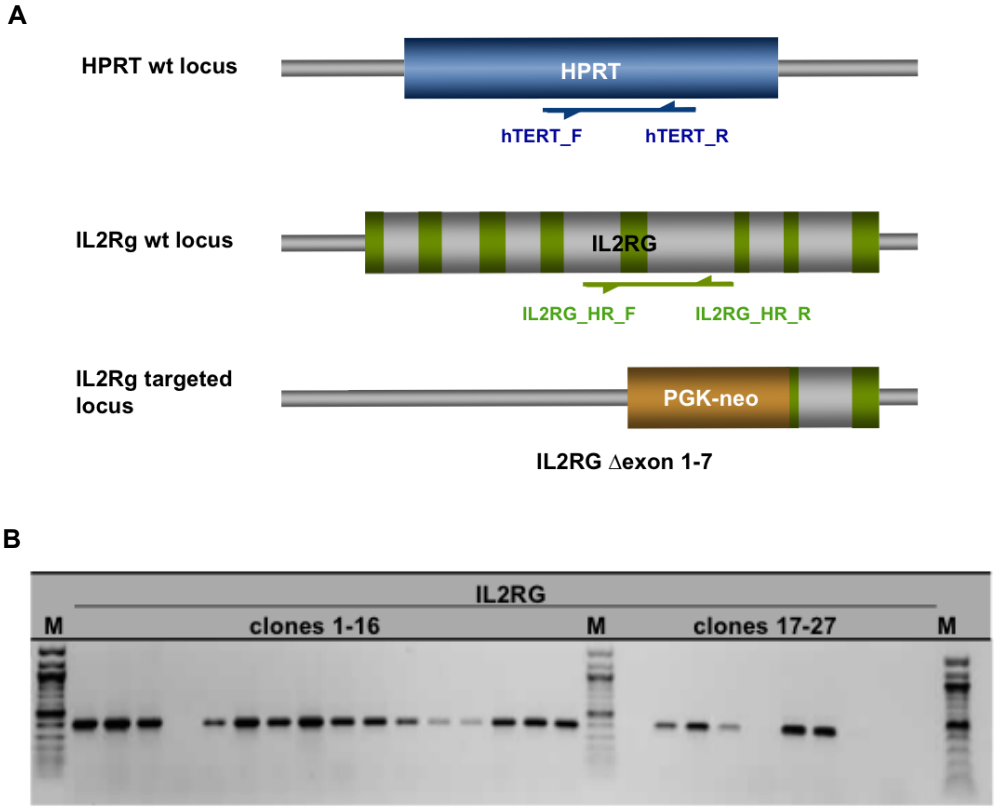

Figure 3.14.: PCR screening of IL2RG-neo-CCN BAC targeting
A: HPRT specific primers (blue half arrows) amplify a 493 bp fragment of this single copy gene in male cells and serve as control for DNA content. IL2RG_HR primers (green half arrows) produce a 406 bp PCR product (red line) from the wildtype locus on the X-chromosome. Correct gene targeting in male cells results in a deletion of most of IL2RG sequence including the two primer binding sides. Thus, no amplification takes place and the PCR is negative. B: First round IL2RG screening PCR. 27 clones were analysed for the presence of IL2RG. Those clones, which did not show a signal, were further analysed by HPRT PCR and repeated IL2RG PCR to see the lack of signal is caused by low DNA amounts in the sample.

amplified if random integration of the BAC takes place. However, it has to be taken into account that BAC backbone PCR negative clones are not necessarily free of random integration. BAC DNA breaks might lead to integration of BAC fragments not including the backbone sequence. This can cause lack of red fluorescence and negative backbone PCR results. Thus, this PCR approach is only a HR prescreening method to reduce the number of clones for subsequent screening steps.

Fluorescence *in situ* hybridisation

The BAC backbone PCR does not necessarily give information about all random integration events. If parts of the backbone are lost the PCR might be negative although random integration took place. Thus, a combination of PCR and fluorescence *in situ* hybridization (FISH) was designed according to Yang et al. (2003) to identify correctly targeted clones and those with additional random integration [188].

A Biotin-labelled FISH probe based on the whole BAC targeting vector enabled visual analysis of both targeting and random integration.

Probe testing was successfully carried out on human cell line HT1080 and porcine tumour cell line ST007. As standard protocols for metaphase spread preparation were available, these lines were suitable for this purpose. Figure 3.15 shows a representative picture of successful detection of the IL2RG locus on the X-chromosome of HT1080 cells. All chromosomes appear blue due to DAPI staining. For correct gene targeting in male cells one red signal on each sister chromatid of the X-chromosome is expected. Its centromere is stained with Pg21-dig probe in green. Additional signals on other chromosomes would show that integration of the BAC targeting vector in a random manner took place.

3.4.4. IL2RG gene targeting efficiencies

In total approximately 700 pBM-MSC, 300 pAD-MSC and 120 pKDNF clones were generated by transfection with IL2RG-neo-CCN BAC and selection with G418. Most clones were analysed visually and approximately 50% could be excluded because of red fluorescence indicating random vector integration. MSCs showed poor proliferation and early senescence, so that approximately 25% of generated clones could be used in subsequent analysis. Non-fluorescent clones were analysed by PCR, only if sufficient cells for DNA isolation were available. pBM-MSC and pKDNF clones that were PCR negative were analysed again with PCR in triplicates in order to confirm the first round screening. However, none of the clones continued proliferation to enable freezing and any further analysis. From approximately In total 3 clones were found to be PCR negative. pAD-MSC1702 clone 89 was IL2RG PCR negative, but still BAC backbone positive. This could be due to multiple vector introduction into the cells, or more probably, BAC DNA breakage and

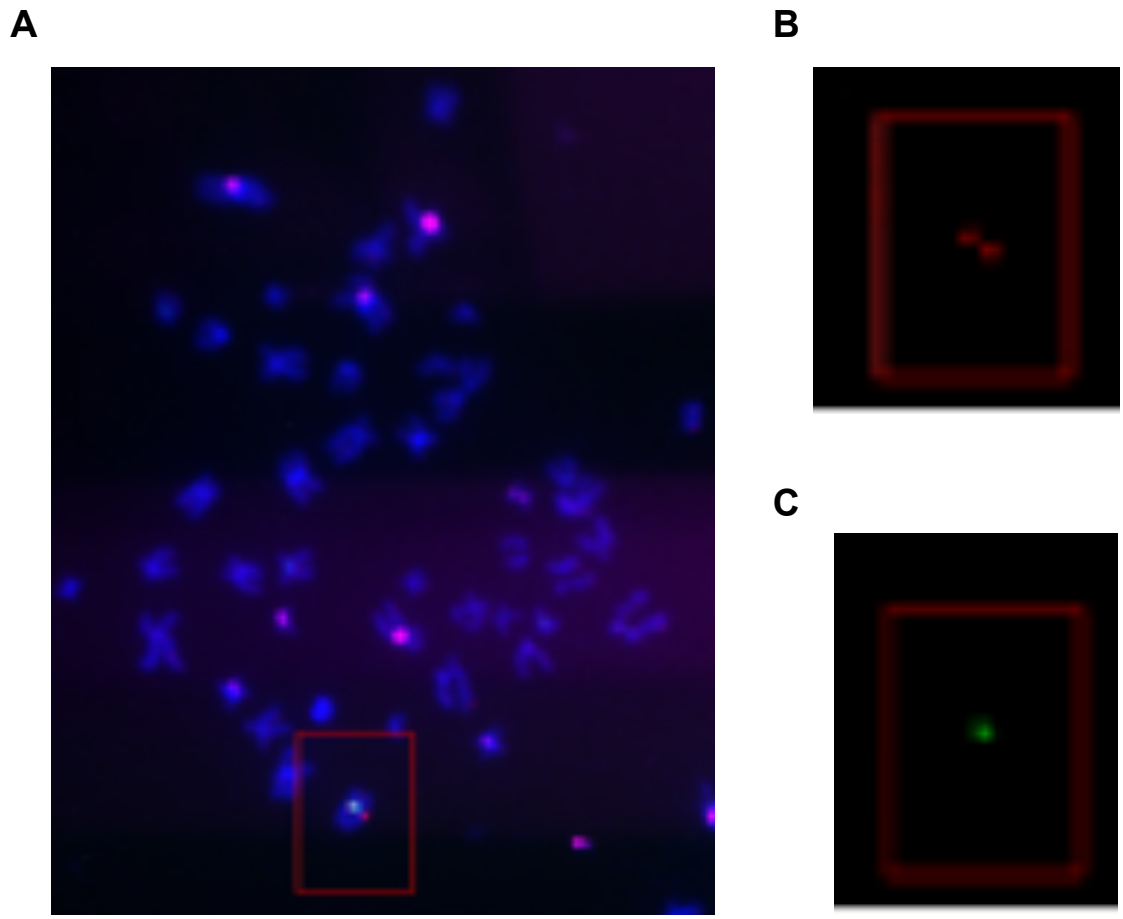

Figure 3.15.: Fluorescence in situ hybridisation
The biotin labelled IL2RG-neo-CCN BAC probe was tested on human cell line HT1080. Diploid, male HT1080 cells gave one correct X-chromosomal IL2RG locus signal on each sister chromatide (red). DNA is stained blue with DAPI and the X-chromosome centromer is stained green with Pg21-dig probe.

separate integration of the backbone. Clones pAD-MSC1101 18/6 and pBM-MSC1611 clone 15 were IL2RG negative in a first round screening.

Although there is some indication that BAC-based IL2RG targeting worked, its practical application for the generation of immunodeficient pigs is questionable.

3.5. BAC-based gene targeting of JAK3

Gene targeting of JAK3 was performed with two different approaches: BAC-based and conventional targeting. This made the construction of two vectors and the establishment of appropriate screening methods necessary.

3.5.1. Construction of the JAK3 BAC targeting vector

The JAK3 BAC targeting vector *JAK3-geo-CCN BAC* has a size of 198 kb (Figure 3.16). It was constructed to contain a PGK-geo selection cassette, which replaces exons 2-22 of the JAK3 gene. Introduction of the positive marker was performed by recombineering between a wildtype JAK3 BAC and a short recombineering vector. 5' and 3' homology arms have a length of 181 kb and 624 bp, respectively. The localisation of JAK3 at the 3' end of the BAC was not known at the beginning of this project. Otherwise it would have been constructed to have more homology on the 3' side. After homologous recombination between the wildtype allele and the BAC vector (Figure 3.16) at the 5' and 3' sides of PGK-geo, most of the JAK3 gene sequence is deleted and the CCN cassette is lost with HR.

3.5.2. Detection of gene targeting events by duplex qPCR

Homologous recombination screening for BAC targeted autosomal genes is not trivial. FISH analysis has to be preceded by qPCR on genomic DNA to quantify the gene copy number: two copies for no homologous recombination and one copy for single knock out. This distinction of one or two gene copies makes intensive optimisation of qPCR conditions essential. For this purpose, a duplex qPCR protocol with Taqman probes was established. Simultaneous quantification of reference gene HPRT and gene of interest JAK3 in a single tube should minimise inaccurate results.

A pre-requisite for duplex qPCR performance is amplification of target gene and reference gene at equal efficiency close to 100%. Duplex qPCR optimisation was carried out according to Tesson et al. (2002) in several steps. First, amplification efficiency was determined for separate HPRT and JAK3 qPCRs on different genomic DNA amounts. Quantification of 2-fold serial DNA dilutions ranging from 50 down to 3.125 ng DNA showed independence of amplification from

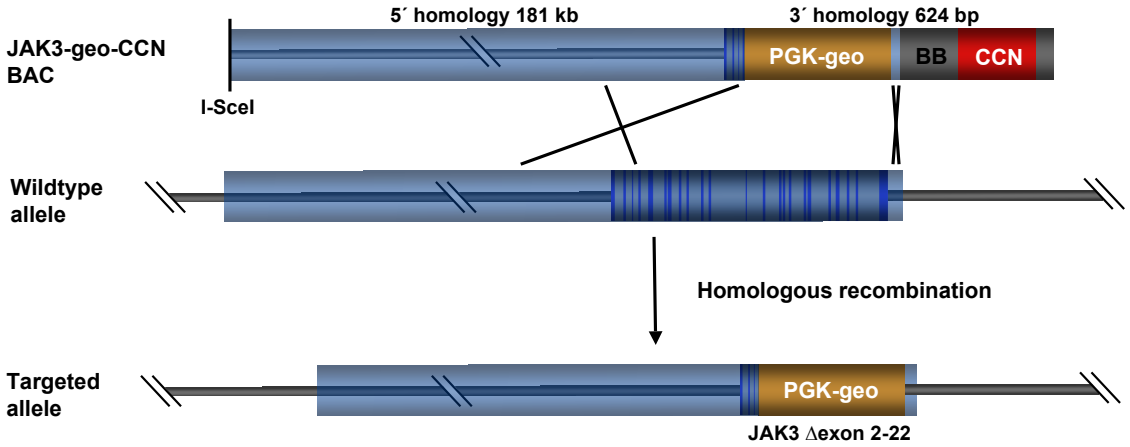

Figure 3.16.: JAK3 BAC-based targeting
The JAK3 targeting BAC contains a PGK-geo positive selection cassette replacing exons 2-22. The marker is flanked by a 5' (181 kb) homology and 3' (624 bp) homology arm. The CCN cassette allows visual screening and active vector transport into the nucleus. After homologous recombination between the wildtype allele and the BAC at the 5' and 3' sides of PGK-geo, most of the JAK3 gene sequence is deleted and CCN is lost.

DNA quantity in the range tested. PCR products were verified by agarose gel electrophoresis (data not shown).

Second, duplex PCR for both genes was performed. After optimisation of primer and probe concentrations, amplification of each product was independent of DNA quantity. Figure 3.17 shows the determined amplification cycle threshold (Ct) values in dependence of the inserted DNA amount. DNA quantity is expressed as $-log(ngDNA)$ in order to obtain a linear correlation. The resulting functions are almost parallel with slope values of -3.4475 (HPRT) and -3.352 (JAK3) and slope difference <0.1. This demonstrates equal efficiency for HPRT and JAK3 amplifications in the duplex qPCR reaction. As the correlation indices for the determined trend lines are >0.99 they represent the measured values accurately. They show that a 2-fold reduction in DNA amounts resulted in a Ct difference of one cycle.

qPCR optimisation for screening of JAK3 BAC-targeted clones was performed due to the BACs long homology arms. Conventional targeting vectors are normally designed to allow conventional PCR as a screening method. The complete JAK3 BAC sequence information was not available at the time of BAC vector construction. Later the JAK3 gene was found out to be localised on the very 3' end of the BAC. This feature makes conventional PCR screening spanning the short 3' homology arm applicable. A PCR positive control vector for JAK3 BAC-based targeting was cloned by Reindl (2010) [189].

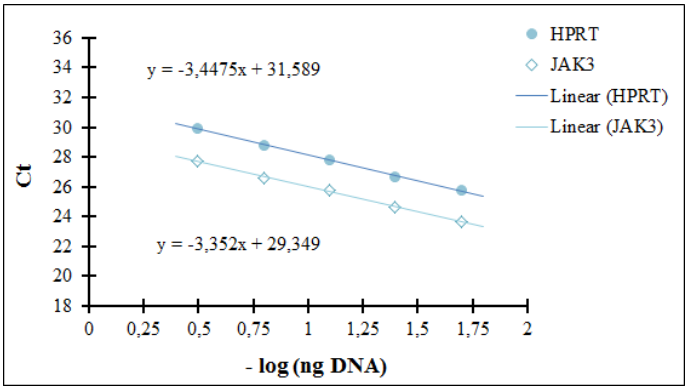

Figure 3.17.: Duplex qPCR with JAK3 and HPRT
Cycle threshold results for JAK3/HPRT duplex qPCR are depicted in dependence of $-log(ngDNA)$. Parallel trend lines indicate that fluorescence signals for both quantifications correlate equally with DNA amount.

3.5.3. JAK3 BAC-based gene targeting efficiencies

In total, approximately 800 pMSC and 100 pKDNF clones have been produced in roughly 35 transfection experiments with JAK3-geo-CCN BAC. Due to low transfection efficiency and the generation of only small numbers of clones per experiment (0 to 72), the number of transfections was very high. In general, reduced proliferation and early senescence were observed for the majority of clones. Most of them (>90%) were analysed only visually as they died before sufficient cellular material for PCR was available. As approximately 40% of clones expressed the red fluorescence marker, they could be excluded from further analysis. However, none of the clones analysed by PCR was positive for JAK3 gene targeting.

3.6. Conventional gene targeting of JAK3

To compare the effect of homology length on gene targeting efficiencies, a conventional vector design with a overall shorter sequence was tested as an alternative to BAC gene targeting. Both vectors were based on BAC DNA and contained the CCN cassette for visual exclusion. The gene targeting approach, including vector design and screening methods, that lead to successful JAK3 gene targeting is described in the following section.

3.6.1. Analysis of JAK3 expression

Janus kinase 3 expression is predominantly detected in lymphoid and myeloid lineages of hematopoietic tissues. However, it was also found in other tissues such as brain, spinal cord,

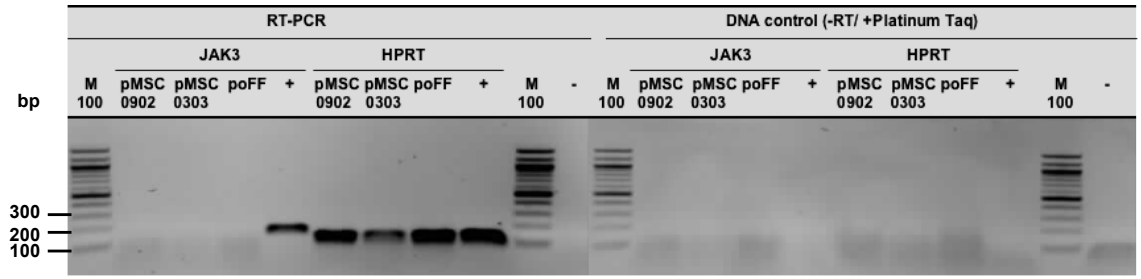

Figure 3.18.: JAK3 expression analysis
In negative (-) and DNA controls no product was detected. RNA presence was confirmed by RT-PCR of HPRT. JAK3 is not expressed in pMSC0903, pMSC0303 or porcine fetal fibroblasts (poFFs). Spleen RNA served as positive control (+) for JAK expression. 100 bp DNA marker (M 100).

heart, liver, lung and also in epithelial cancer cells including primary breast cancer cell lines [62, 186, 190–194].

To test whether a promoter-trap approach could be applied, RT-PCR expression analysis of JAK3 in pBM-MSCs was performed prior to construction of the targeting vector. Figure 3.18 depicts the RT-PCR agarose gel analysis. RNA presence in the reaction samples was proven by RT-PCR of the housekeeping gene HPRT and spleen RNA served as RT-PCR positive control for JAK3 expression. Primers JAK3_Ex2/3_F and Ex3/4_R were designed across exon-intron boundaries to produce a 176 bp product and exclude amplification of DNA. All DNA control samples were negative. The RT-PCR showed that JAK3 was not expressed in pBM-MSC isolations 0902, 0303 or porcine fetal fibroblasts (poFFs). Based on this experiment a promoter-trap approach was excluded and a positive selection vector had to be constructed.

3.6.2. Vector construction

Figure 3.19 shows a schematic overview of the final JAK3 targeting vector *JAK3-TV-CCN* and homologous recombination at the JAK3 wildtype locus. The vector was constructed to a final length of 22,126 bp with a 3,268 bp short homology arm 5' of a PGK-neo selection cassette, which replaces exons 2-5. The 3' long homology arm had a length of 10,544 bp. Visual screening and active transport across the nuclear envelope were possible, because of the CCN cassette located in the vector backbone. The vector was linearised at the MluI restriction site. Figure 3.19 shows homologous recombination during JAK3 conventional gene targeting.

Preliminary transfection tests showed that the JAK3 targeting vector with the CCN cassette in forward and reverse resulted in similar numbers of G418 resistant clones (data not shown). This indicated that the orientation of the CMV enhancer in the CAGGS promoter does not cause

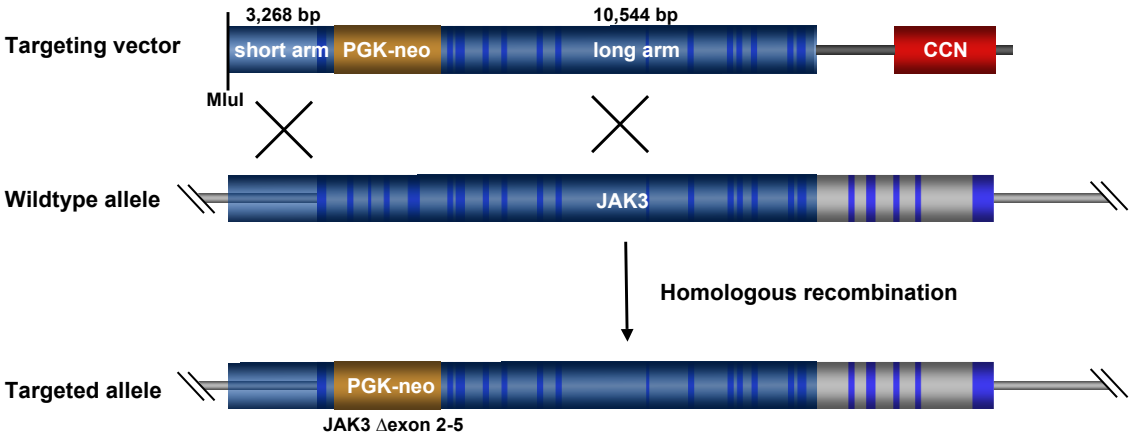

Figure 3.19.: JAK3 conventional gene targeting
The conventional targeting vector contains a PGK-neo positive selection cassette replacing exons 2-5. The marker is flanked by a 5' short (5,268 bp) homology and 3' long /10,544 bp) homology arm. The CCN cassette allows visual screening and active vector transport into the nucleus. Linearisation was performed at the MluI site prior to transfection. After homologous recombination between the wildtype allele and the targeting vector at the 5' and 3' sides of PGK-neo, exons 2 to 5 of JAK3 are deleted and CCN is lost.

orientation dependent effects on neo expression. For all future experiments the forward oriented cassette was used.

3.6.3. Detection of gene targeting events

Transfection of pMSCs and pKDNFs with JAK3-TV-CCN was followed by selection with G418. Subsequent screening of clones for homologous recombination and random vector integration was based on visual screening, PCR and Southern blot analysis.

Visual screening

CCN is integrated into genome and expressed upon random vector integration, which is occurring far more often than HR. Red fluorescence of cells was observed by microscopy. Figure 3.20 shows a red pKDNF clone with strong fluorescence, which probably took up multiple copies of the vector. Depending on the cell isolation used, 48 to 80% of stably JAK3 targeting vector transfected clones were expressing Cherry and did not have to be picked or further analysed. Some of the clones further cultured and screened by PCR established red fluorescence a bit later. Others appeared to be white throughout several passages, although they were Cherry PCR positive (see Section 3.6.3).

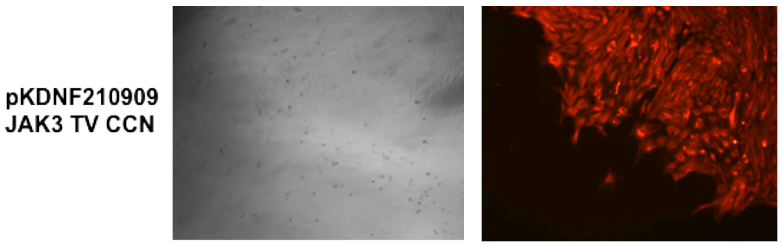

Figure 3.20.: Visual screening for random vector integration
A pKDNF2109 clone obtained after transfection with JAK3-TV-CCN shows strong expression of mCherry. This enables exclusion of this clone from furthre consuming screening procedures. Under normal light the pKDNF clones appear to be very flat and difficult to see. 5 $\times$ magnification.

Gene targeting PCR

JAK3 conventional targeting makes PCR screening for HR events applicable. Due to the short 5' homology arm (3.3 kb), PCR spanning this sequence can be performed to confirm correct localisation of the vector in the genome. DNA does not have to be purified with columns, but can be obtained from relatively small cell numbers treated with igepal buffer. This method is less time consuming and clones negative for targeting PCR can be excluded at a very early stage without extended time in culture.

Figure 3.21 summarises all PCRs with constructs, primers and product lengths. Screening primers were designed to amplify product only from correctly targeted clones. The reverse primer binds within the PGK promoter sequence (JAK3_targscreen_R2), the forward primer (JAK3_targscreen_F2) in the wildtype allele sequence upstream of the short arm. A PCR control vector was constructed as a positive control for PCR. It contains the forward primer binding site, short arm and the PGK promoter. It was shortened by excision of 376 bp of short arm sequence to distinguish positive targeting events from the control fragment size and avoid possible contamination of clone samples. An endogenous control PCR was performed to test if each sample contained sufficient DNA for amplification. This was conducted with the same forward targeting screening primer and a reverse primer (JAK3_endo_R) binding the wildtype allele at a 3.7 kb distance.

Figure 3.21 shows a representative PCR screening agarose gel picture for two pBM-MSC clones. Negative controls do not produce a signal and JAK3 positive control PCR shows the expected band. Both samples 14 and 15 contain enough genomic DNA as amplification of the endogenous control fragment was successful. Clone 14 is negative for gene targeting, whereas clone 15 is positive. Despite intensive optimisation (see below), unspecific amplification products remained. The pattern showed a band at approximately 2.2 kb for targeting and for the

endogenous control PCR. As both PCR set ups have the forward primer in common, it must be responsible for unspecific binding.
To confirm that the observed 3.4 kb band represents a targeting event, sequencing of the isolated DNA band was performed. This proved correct gene targeting with the junction between the genomic locus and the targeting vector short arm.

PCR optimisation is critical before any targeting experiment can be performed to make sure correct events are detected. Optimisation was conducted in several steps (data not shown). 16 primer pairs were tested in regards of specificity. The suitable conditions, including choice of DNA polymerase and annealing temperature were determined for the best pair (data not shown). To mimic the later screening conditions, control vector was mixed with genomic DNA at a 1:1 ratio. Furthermore, amplification on low DNA copy numbers was performed under addition of igepal buffer to the PCR reaction mix. Despite the fact that PCR optimisation was successful and that down to two copies of PCR control vector could be detected, HR screening PCRs of selected single cell clones showed unspecific bands.

Nested and Cherry PCR

As the screening PCRs from single cell clones showed additional bands, nested PCR was performed on the purified 3.4 kb JAK3 targeting band. Primers JAK3_nest_F and JAK3_nest_R generated a 3.3 kb PCR product as they were designed to bind within the 3.4 kb targeting band. The forward primer is located just 5' of the short homology arm. BstXI restriction digest of the nested PCR band produced a characteristic band pattern of 1.4 kb, 1 kb and 0.9 kb for correct gene targeting.

Positive clones were also screened by a short (325 bp) Cherry specific PCR in order to exclude clones with correct JAK3 targeting and additional random integration. A representative gel picture for nested and cherry PCR and a BstXI digest is shown in Figure 3.22.

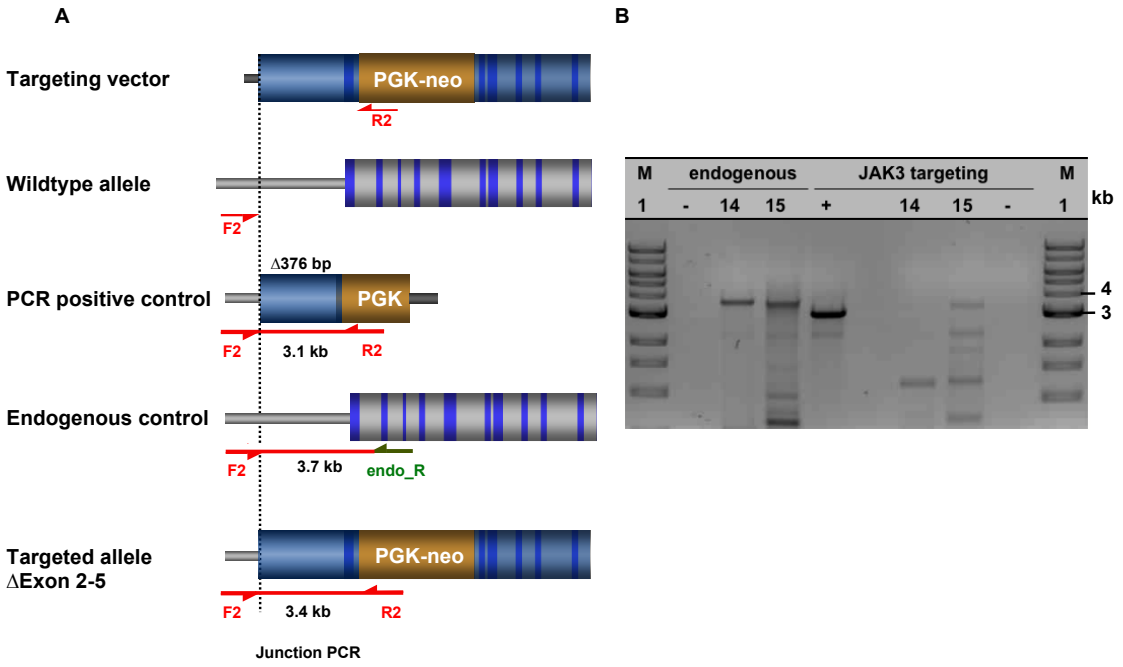

Figure 3.21.: Gene targeting PCR - basic principle and example
A: The JAK3 screening primers (F2 and R2) were designed to not amplify DNA from the wildtype allele or the randomly integrated targeting vector. They bind 5' of the short arm and in the PGK promoter to amplify a 3.4 kb product only after correct gene targeting. The endogenous control PCR sample (3.7 kb) serves as a control for sufficient genomic DNA. The forward primer is identical to that from the screening PCR to mimic conditions more closely. The reverse primer is located in the region deleted after gene targeting occurred (primer enod_R). JAK3 PCR control vector proves the PCR success. B: DNA samples of clones 14 and 15 contain sufficient DNA to amplify the 3.7 kb endogenous control product. PCR control vector amplification shows that PCR for homologous recombination screening worked. Clone 15 is positive for JAK3 targeting, whereas clone 14 is negative. Positive control (+, 3.1 kb), negative (water) control (−), 1 kb DNA marker (M1).

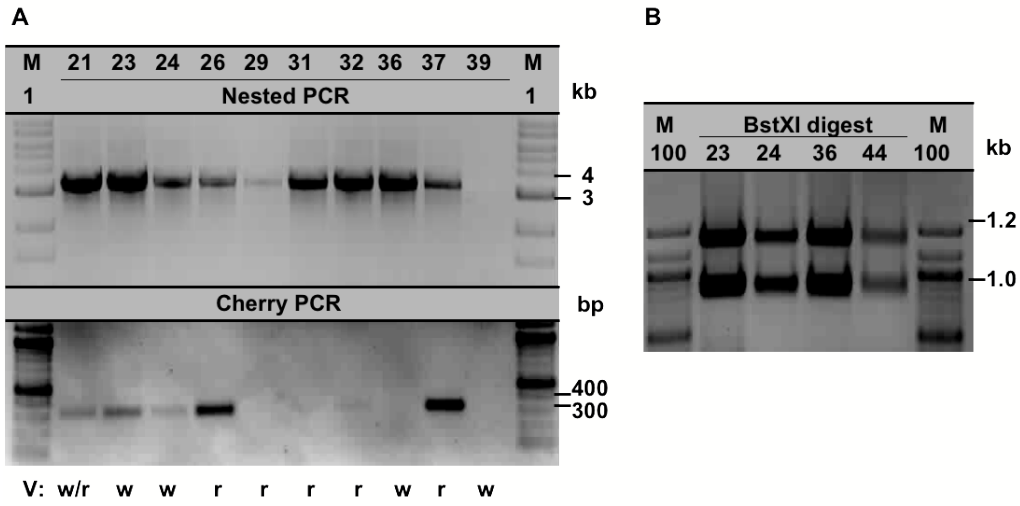

Figure 3.22.: Visual analysis, nested/ cherry PCR and BstXI restriction digest of transfected clones
A: 7/ 9 nested PCR (3.3 kb) positive clones are cherry positive (325 bp). Visual screening results (V) are indicated as red (r) and white (w). B: The nested PCR band was digested with BstXI to check if a characteristic band pattern demonstrates its correctness. The expected bands were 1.4 kb, 0.8 kb and 100 bp. 100 bp DNA marker (M100), 1 kb DNA marker (M1).

JAK3 conventional gene targeting efficiencies

The possibility to generate JAK3 gene targeted clones was first tested by analysis of small pools, containing up to 5 clones. Single cell clones were generated after confirmation of successful proof-of-principle for the use in SCNT.

Conventional JAK3 gene targeting was performed with different cell types and cell isolations. The results are summarised in Table 3.3. In pMSCs, the total gene targeting efficiencies determined by PCR ranged from 9% (pBM-MSC1101) to 16% (pAD-MSC1101). JAK3 gene targeting was also successful for pKDNF2109 with 6%. The frequency of clones not carrying random integration of the vector in addition to correct gene targeting ranged between 4% and 6%.

Table 3.3.: JAK3 conventional gene targeting efficiencies
Gene targeting of porcine JAK3 was successful for kidney fibroblasts, bone marrow and fat derived MSCs. Results from PCR analysis in single cell clones showed different efficiencies depending on cell isolation and cell type. not determined (nd), homologous recombination (HR), random integration (RI).

	pBM-MSC 0712	pAD-MSC 1101	pBM-MSC 1101	pKDNF 2109
HR	6%	4%	nd	4%
HR + RI	5%	12%	nd	2%
Total	11%	16%	9%	6%

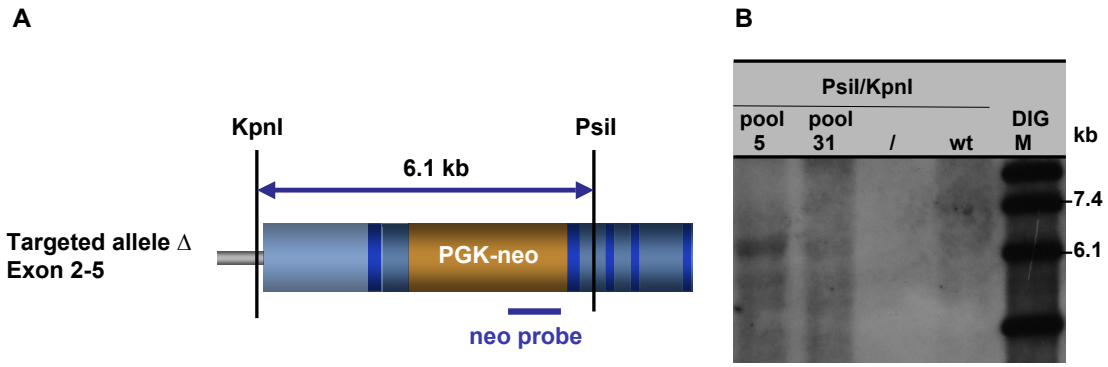

Figure 3.23.: Southern Blot screening of SCNT clones
Detection of a 6.1 kb genomic DNA fragment from JAK3 gene targeted pools 9 and 31. DNA was digested with KpnI/PsiI and resulted in a 6.1 kb DNA fragment, which could be detected with neo specific probe.

3.6.4. Southern blot of gene targeted clones

Southern blotting was performed to confirm correct gene targeting for clones analysed by PCR before performing SCNT. Genomic DNA was amplified with whole genome amplification kit (REPLI-g) and digested with KpnI/PsiI. DNA fragments were separated by gel electrophoresis, blotted on a membrane and detected by a DIG-labelled neo specific probe.

Figure 3.23 shows the schematic overview of the Southern blot and the results for pBM-MSC0902 pool 9 and pBM-MSC0303 pool 31. The expected 6.3 kb band confirming correct homologous recombination 5' of PGK-neo. Additional smaller bands probably result from whole genome amplification that could also generate smaller DNA products. Targeted cells were obtained by positive selection in 48 well plates. Exclusion of contamination with other cells cannot be guaranteed although only one colony per well was visible. Consequently, cells are termed pools and not clones in the following text.

3.7. Production of gene targeted pigs

SCNT with JAK3 gene targeted pBM-MSC and pAD-MSC clones was performed at the Institute of Molecular Animal Breeding and Biotechnology (Prof. Dr. Eckhard Wolf, LMU Munich) by Mayuko Kurome and Valeri Zakhartschenko. In embryo transfer (ET) 97 to 195 reconstructed embryos were transferred by Barbara Kessler (Institute of Molecular Animal Breeding and Biotechnology, LMU Munich) to recipient sows. Table 3.4 summarises all SCNT and ET results.

The first piglets were born on 13.02.2011 after 114 days of gestation. In this experiment clone pools from pMSC isolations pBM-MSC0303 (pool 31) and pBM-MSC0902 (pool 9) were used for

Table 3.4.: SCNT of JAK3 gene targeted clones
In total 3 SCNT and ET experiments have been performed. Details on transferred cells, embryos and piglets born are listed. No pregnancy (n.p.), clones from other projects (*)

ET date	clone	embryos	gestation	piglets
22.10.2010	pBM-MSC0303 pool 31	97	114	3 live born: #19, #20, #21 2 stillborn: #42A, #42B
	pBM-MSC0902 pool 9	195	114	1 stillborn: #43
27.05.2011	pAD-MSC1101 23, 44	98	n.p.	
	pAD-MSC1101 23, 44	117	n.p.	

the two sows (sows 42 and 43) separately. Sow 43 had one stillborn piglet (piglet #43), whereas 42 gave birth to three living piglets (piglets #19, 20 and 21) and two stillborn piglets (piglets #42A, 42B). All animals looked normal and piglets seemed healthy with a birth weights between 1.3 and 1.5 kg. Only piglet #43 had a increased tongue. Liveborn piglets had to be sacrificed after 21, 23 and 38 days, after they had repeated umbilical hernia. Despite surgery, piglets could not be saved. Umbilical hernia had occurred before, when pBM-MSC0303 had been used as nuclear donors. Epigenetic reasons probably lead to these problems so that they were not used as nuclear donors again.

The general applicability of pAD-MSCs as nuclear donors for SCNT was tested as no practical experience was available in our group. Single cell pAD-MSC1101 clones were used. From the one sow used, in total 9 out of 10 piglets were liveborn. Piglets had a birth weight between 1.2 and 1.3 kg and remained healthy.

From the last embryo transfer round with JAK3 gene targeted pAD-MSC1101 clones, no early pregnancy was detected. In total four recipient sows were prepared f

3.7.1. Analysis of transgenic piglets

Analysis of transgenic piglets born on 13.02.2011 was performed to confirm JAK3 gene targeting and to exclude additional random integration. It had to be tested whether piglets were derived from one single clone as cell pools were used for nuclear transfer. Piglet analysis was conducted with PCR, Southern Blot and partial sequencing.

3.7.2. PCR

Figure 3.24 shows the targeting PCR analysis of the JAK3 gene targeted piglets. All samples show the expected 3.4 kb band for correct JAK3 gene targeting and are PCR positive for endogenous PCR control. Additional unspecific bands observed earlier on single cell clones are again visible for both PCRs. Nested and Cherry PCR analysis for further confirmation of results was

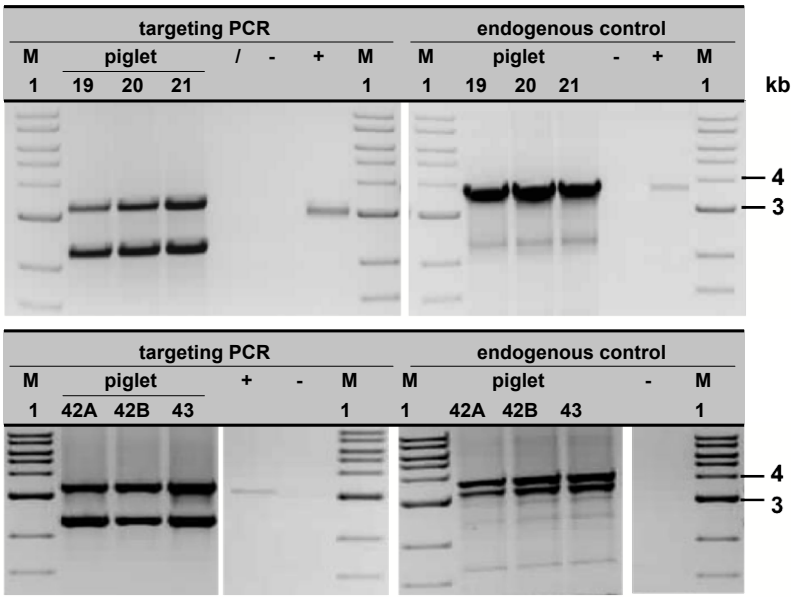

Figure 3.24.: PCR screen of JAK3 gene targeted piglets
All piglets show the correct band for gene targeting of JAK3. 1 kb DNA marker (M1), positive (+), negative (H2O).

performed. Piglets are Cherry negative, whereas nested PCRs produced the expected 3.3 kb band (data not shown). The targeting PCR band was sequenced and the junction between the wildtype locus and the vector short arm could be confirmed.

3.7.3. Southern blot screening

Southern blot analysis was performed for further investigations of transgenic piglets. Genomic DNA was digested with different restriction enzyme combinations. DNA fragments were separated by gel electrophoresis, blotted on a membrane and detected with a DIG-labeled neo probe.

The probe binding site, restriction digests and resulting fragment sizes are shown in Figure 3.25 A. Digest of genomic DNA and hybridisation with neo specific probe was performed to prove correct homologous recombination in the long arm region 3' of the selection cassette. AseI digestion of genomic DNA should produce a single 12 kb band from the long arm side. Correct length cannot be determined directly as no DIG-labeled DNA marker for Southern blot detection of fragments bigger than 8.6 kb is available. Thus a AseI/NsiI double digest should further shorten the 12 kb band to obtain a defined size of 5.9 kb. With this approach a targeting vector internal fragment is detected, but the correct localisation of the vector in the endogenous locus cannot be proven. Piglets #19, 20, 21, 42A and 42B all showed the expected band pattern for neo hybridisation. This indicates that pBM-MSC0303 pool 9 is probably not a mixture of different cell clones, but one single clone. The AseI digest of DNA from piglet 43 produced a signal of incorrect size indicating that no correct targeting was performed in the donor cell. Alternatively, pool 31 was a mixture of correctly targeted cells and random integrants. Piglet 43 then might be derived from a random integration clone.

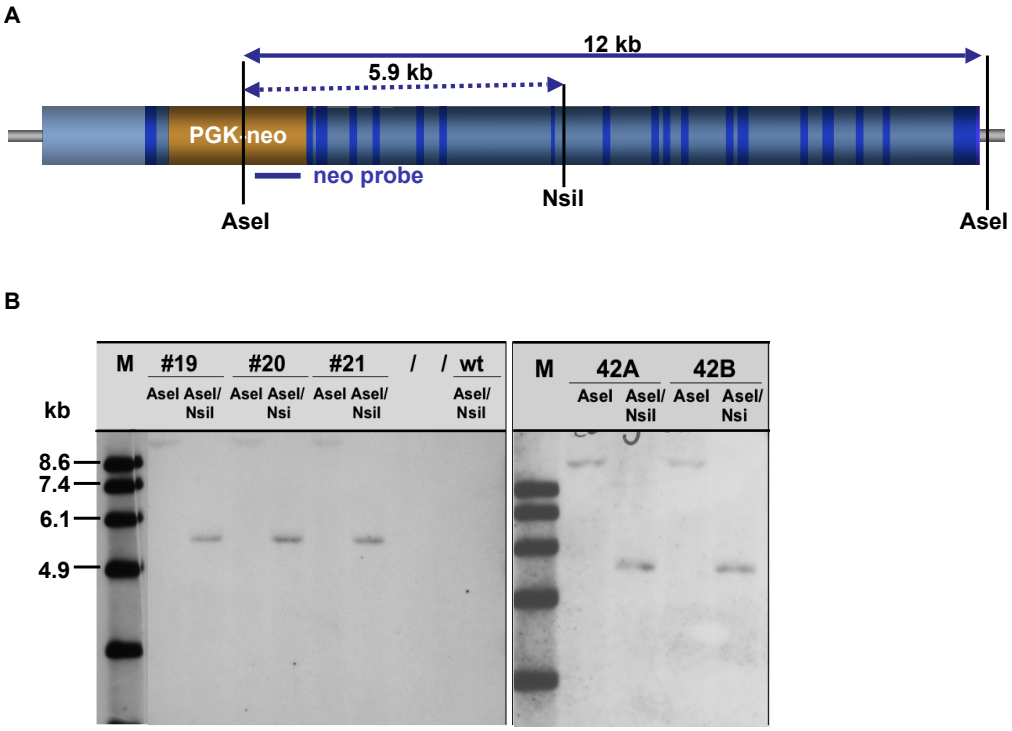

Figure 3.25.: Neo Southern blot of the piglets 19, 20, 21, 42A, 42B
A: To prove correct HR on the vector 3' side a AseI (12 kb) and a AseI/NsiI (5.9 kb) digest were performed. B: Piglets 19, 20 21, 42A and 42B show the expected 12 kb and 5.9 kb signals expected for the long arm digest AseI and AseI/NsiI. No additional signals indicate that no additional random integration of the vector has happened. Wildtype control DNA (wt) does not have a neo signal.

4. Discussion

It is essential to study human cells under *in vivo* conditions in biomedical research fields, such as regenerative medicine or cancer research. Thus far, immunodeficient mice were intensively used for this purpose [1]. However, the major drawbacks in their application are their small size and the physiological differences in comparison to humans [12, 14]. As pigs resemble humans more closely in these aspects, they are considered to be a more predictive recipient for human cell transplantation.

Mutations in the genes encoding janus kinase 3 (JAK3) and interleukin-2 receptor gamma chain (IL2RG) cause severe combined immunodeficiency (SCID) in humans and mice [37, 50, 195, 196]. The resulting defect is caused by impaired signaling of the immunomodulatory cytokines IL-2, IL-4, IL-7, IL-9, IL-15 and IL-21. These require functional signal transduction via IL2RG and JAK3 to perform their task in humoral and cellular immunity [92]. In SCID patients, loss of function mutations in one of the two genes affect or even eliminate the organism's immune defense against foreign antigens [197].

It was the objective of this study to generate immunodeficient pigs by knock out of IL2RG or JAK3. Gene knock outs in pigs can be achieved by gene targeting, an approach based on homologous recombination (HR) between a targeting vector and a target locus. The modified cell is subsequently used in somatic cell nuclear transfer (SCNT) to produce an animal carrying the introduced modification [136].

The experimental design was crucial for the success of the project. It involved the choice of suitable target cells and the construction of efficient targeting vectors to accomplish gene targeting and to produce healthy offspring by SCNT.

4.1. Target genes

The choice of IL2RG and JAK3 as candidate genes for the generation of immunodeficient pigs was based on the experience with human patients and knowledge from mouse models. IL2RG deficient mice exhibit a high degree of impairment regarding immune rejection against transplanted cells. However, only the combination of this knock out with an additional inactivation of recombination activating genes 1 or 2 (RAG1, RAG2) caused defects in T, B and NK cell function [1]. This disparity is due to species-specific differences in cytokine function between mouse and

human [92]. As the pig is more similar to humans in many aspects, it is possible that targeting IL2RG or JAK3 might be sufficient to obtain the expected phenotype. However, this assumption can only be confirmed or disproved after successful knock out has been performed.

Gene targeting of IL2RG or JAK3 causes the identical phenotype as both genes are involved in the same signaling pathway [49]. The IL2RG deficient founder and all other male individuals will immediately exhibit the defective phenotype due to the X-chromosomal recessive mode of inheritance [37]. This would possibly further reduce viability of SCNT derived male founder animals as will be discussed in detail in Section 4.5. High standards for immunodeficient animal housing and care including a designated pathogen-free (DPF) facility would have to be available from the first generation on. In contrast to this, a knock out of autosomal JAK3 would not lead to a phenotype in the founder or other heterozygous individuals. This approach was preferred as generation of immunodeficient male and female pigs could be performed by breeding on demand. However, at the beginning of this project, knock out strategies for both target genes were tested to examine which approach can be performed successfully.

4.2. Choice of cells

For successful generation of gene targeted pigs, the availability of cells, which are susceptive to modification by homologous recombination (HR) and to reprogramming by SCNT, is essential.

4.2.1. Prerequisites for somatic cell nuclear transfer

Somatic cells are restricted in their ability to differentiate and are not capable of generating a complete organism [198]. For successful SCNT the donor nucleus has to be set back in its developmental status to totipotency if it is to participate in the development of a viable animal. The general feasibility of reprogramming of a somatic cell nucleus to a totipotent state was proven in different mammalian cloning experiments [149, 199, 200]. The first study to demonstrate that epigenetic modifications accumulated in an adult differentiated nucleus can be successfully remodeled resulted in the generation of *Dolly* [147].

However, in the majority of experiments, reprogramming of somatic cells was often incomplete and resulted in abnormalities of nuclear transplant embryos. These observations motivated the search for the reasons for reduced reprogramming capacity. Early experiments indicated that cloning efficiency by SCNT is inversely correlated with the differentiation state of the donor nucleus [201, 202]. For example, Hiiragi and Solter (2005) tested mouse blastomeres from different developmental stages. They demonstrated that a cell's potency to be reprogrammed decreases with progression of development. Interestingly, this effect could be observed even at these very early development stages [203].

As embryonic stem (ES) cells from pigs are not available, somatic cell types have to be applied for cloning experiments. Thus far, pig SCNT has been performed mainly with fetal fibroblasts. However, more differentiated cells including granulosa-derived cells and salivary gland derived progenitors were also successful [200, 204–207]. A cell type used more recently for cloning of pigs were primary kidney fibroblasts (pKDNF) [208].

As multipotent adult stem cells are not terminally differentiated, they might be more efficient nuclear donors than the cell types used thus far. A study supporting this theory was performed by Kumar *et al.* (2007). They demonstrated that SCNT embryos derived from porcine mesenchymal stem cells (pMSCs) showed improved blastocyst formation rates, higher cell numbers and a lower apoptosis incidence compared to embryos from fetal fibroblasts. Furthermore, the expression pattern of pluripotency genes and other reprogramming related genes resembled in vivo derived embryos more closely [209]. Faast *et al.* (2006) reported blastocyst formation rates to be even twice as high for pMSCs compared to ear fibroblast from the same animal [210]. However, studies on pig cloning with pMSCs only evaluated embryos, but not the birth of viable animals. Hence, the question if porcine MSCs are suitable the generation of gene targeted pigs by SCNT remains open.

4.2.2. Prerequisites for gene targeting

Apart from the requirement for nucleus reprogramming, cellular characteristics necessary for the introduction of genetic modifications have to be considered. Gene targeting experiments involve a long process of transfection, selection and screening. For the target cell to complete this entire process, Clark *et al.* (2000) proposed a requirement of 45 population doublings [156]. This is a major barrier for many differentiated cell types, which are often not capable of long term proliferation. It is further essential for gene targeting that the target cell can be efficiently transfected and selected without negative impact on proliferative capacity.

Bosch *et al.* (2006) show that porcine mesenchymal stem cells fulfill the prerequisites for successful gene targeting. They demonstrated extended proliferation, genetic modification and single cell cloning [181]. However, also primary porcine kidney fibroblasts were of interest for this study as Klymiuk *et al.* (2011) have shown that these cells can be used for BAC-based gene targeting [208].

Thus, pMSCs and pKDNF were chosen as targets for this study. With this approach both a multipotent adult stem cell and a differentiated representative were available and could be compared regarding their performance in gene targeting and SCNT.

4.2.3. Isolation and characterisation of pMSC

To examine if MSCs isolated from different tissues, exhibit differences in their ability to trigger HR and to generate viable animals, MSCs from bone marrow (BM) and adipose (AD) tissue were compared. Both cell types pBM-MSC and pAD-MSC were easy to isolate by standard methods and showed high proliferation capacity. Standard characterisation of human MSCs is carried out on the basis of adherence to plastic, surface marker profile expression and differentiation into adipogenic, chondrogenic and osteogenic lineages. As a unique surface marker profile for the identification of pig MSCs has not been agreed on, differentiation assays present the standard means of characterisation. These assays showed that pBM-MSCs were highly capable of undergoing osteogenesis and chondrogenesis. Adipogenesis was also possible, but to a lesser extent. Porcine AD-MSCs showed the opposite profile. Fat production was visible for a majority of cells, whereas bone and cartilage differentiation were more limited.

Taken together, it was possible to confirm that isolated cells from both tissues were truly multipotent pMSCs. The differentiation profiles are in line with other studies. Bosch *et al.* (2006) reported a similar behaviour for porcine bone marrow MSCs. They showed adipogenic differentiation in approximately 1% to 15% of cells cultured in induction medium, but no differentiation in normal culture medium. Osteogenic and chondrogenic capacities were high, as seen in this study. However, the quantitative comparison to other studies is not possible, as different induction media compositions were used.

Although MSCs show long-term proliferation, strategies to further prolong their life-span could be tested. Alternatively, these approaches might be also interesting for the application on pKDNF. Special culture conditions can have a positive effect on cell growth. For example, McFarland and Holliday (1999) showed that culture of primary human fetal foreskin and lung cells supplemented with L-carnosine increases maximum population doublings for 10 divisions [157]. Other factors, for instance the oxygen tension during cell culture can be optimised. Culture under hypoxic (2%) instead of normoxic (20%) conditions has been intensively studied. It enhanced proliferation of pig fetal fibroblasts and MSCs from different species [181, 158, 211, 212]. Reduction of oxidative stress and DNA damage are assumed to be the major reason for this effect.

4.2.4. Immortalisation of pMSC

Genetic modification, selection and single cell cloning can be detrimental for cell proliferation. Thus, extensive analysis of clones for molecular characterisation, e.g. by fluorescence *in situ* hybridisation, is often impossible. In this study, immortalisation of porcine MSCs transfected with a human telomerase reverse transcriptase gene (hTERT) was confirmed. Wei *et al.* (2008) have also shown prolonged life span in hTERT expressing MSCs from chinese Guizhou minipig. They further demonstrated that this approach reduced apoptosis without induction of changes in

morphology, surface marker expression, differentiation capacity or karyotype [213]. Immortalisation of MSCs has also been successfully conducted for different species including human and different tissue sources, such as pig fetal pancreas [214, 215].

Taken together, hTERT expression based immortalisation can be performed to produce sufficient cells for analysis from a single cell clone. As immortalised cells do not support embryonic development after day 40, they could not be used for cloning [216]. Hence, only a portion of cells would be used for hTERT transfection and subsequent analysis.

4.3. Design of gene targeting experiments

Successful gene targeting experiments require suitable vector design, selection and screening for targeting events.

4.3.1. Construction of the targeting vectors

The use of isogenic DNA was reported to be essential for homologous recombination in inbred species, such as the mouse [217, 166]. However, non-isogenic DNA has been successfully used for gene targeting in pigs [153, 218]. Also in this study construction of targeting vectors from isogenic DNA was not necessary to drive HR between vector and target locus. All vector constructs were derived from porcine BAC DNA from a Duroc breed, but German Landrace (DL) and DL-Pietran hybrids were used as cell donors. Sequencing of IL2RG non-coding flanking regions proved identity between the two pig breeds at this locus. Thus, very high homology between the whole vectors and the target loci can be assumed, which is sufficient to drive HR.

As JAK3 is not expressed in porcine MSCs, the use of a promoter trap construct was not feasible for HR enrichment. Hence, the basic principle of HR enrichment in this study was based on a positive negative selection (PNS) vector design. The PGK-neo selection marker cassette contained in the 22 kb JAK3 conventional targeting vector and 198 kb IL2RG targeting BAC allowed positive selection with G418. Only the JAK3 BAC vector (199 kb) was modified with geo, a lacZ-neo fusion gene allowing β-Galactosidase staining of transfected cells. The targeting vectors were in parts generated by recombineering, which Testa *et al.* (2003) have shown to be suitable for the construction of large gene targeting vectors [219].

The IL2RG BAC-based vector carried 64 kb and 119 kb 5' and 3' homology arms. The JAK3 conventional targeting vector had only a 3.3 kb short and a 10.5 kb long homology arm. With this design, both constructs fulfilled the targeting vector requirements stated by Thomas, Deng and Capecchi (1992) [166, 165]. They demonstrated in a large scale experimental setup that HR efficiency positively correlates with the length of homology present on the vector. They tested constructs with different homology extents and found that HR frequency increases exponentially

in homology size range of 2 kb and 10 kb. Saturation was reached at approximately 14 kb, so that the conventional vector was designed to this length. They further stated that a minimum homology arm length of 1 kb is necessary for successful HR. Only the JAK3 BAC targeting vector did not fulfill this criterion. Of its 199 kb total size, only 624 bp presented the 3' homology arm. However, in other gene targeting studies, also less than 1 kb have been shown to be sufficient for HR [220].

To assess transfection efficiency and to visually identify random integration events, the mCherry gene placed under the control of the strong chicken β-actin (CAGGS) promoter [179]. It was introduced together with a SV40 virus derived nuclear localisation signal (NLS) into all vector backbones and termed CAGGS-Cherry-NLS (CCN) cassette. Its function in HR enrichment and efficiency is discussed in Sections 4.3.2 and 4.4.2.

4.3.2. Enrichment, selection and clone picking

Some groups have reported the birth of non-modified offspring from selected single cell clones and pools [148, 153]. This observation underlines the need for optimisation of selection conditions in gene targeting experiments. The most important parameters include G418 concentration, the selection induction time point and duration.

Appropriate selection pressure had to be tested separately for each cell isolation. The kill curve analysis to determine the suitable G418 concentration ensured sufficient but not over intensive selection. Here, G418 concentration was chosen to kill the cells within 10 to 12 days. Selectable marker expression from BAC DNA has been reported to be delayed in comparison to plasmid [221]. However, in this study no differences could be observed in experiments comparing different selection starting points. Probably too few stable clones were produced to obtain statistically relevant results.

Marques and Thomson (2006) have reported the loss of targeted cells during selection and attributed this observation to a selective growth disadvantage of targeted clones at silent loci [222]. To minimise the risk of selection being initiated too early and killing of resistant clones, selection was always induced 48 hours after transfection for conventional gene targeting. This time point was late enough to allow neo expression and the establishment of G418 resistance as red fluorescence could be detected as early as 24 hours after transfection. Selection was continued throughout the whole experiment until SCNT to exclude growth of non-resistant cells. In this study, regular medium changes and splitting of colonies ensured a proper concentration and contact of all cells to selection medium. This way reduction of G418 concentration caused by fast growing resistant clones could be avoided.

For further enrichment of gene targeted clones, visual screening and negative selection of random vector integrations were tested. Jin *et al.* (2003) have used a PNS approach with HSV-TK in

pig fetal fibroblasts and reported a 10-fold increase in targeting efficiency [223]. However, double drug selection under standard culture conditions restricted proliferation of resistant clones. Only a serum concentration increase to 15% reduced senescence. In contrast, with visual screening cellular stress can be reduced, as additional agents in the culture medium are not required. The Cherry-based approach was preferred in this study although negative selection would have been also applicable for pig MSCs. With visual screening, ganciclovir concentration-dependent effects, such as survival of negative clones and cell isolation specific concentrations do not have to be examined. Cherry expression also allows the estimation of transfection efficiency and the possibility to determine both HR efficiency and random integration (RI) in the statistics. This will be further discussed in Section 4.4. For effective visual screening high marker expression levels are important. The CAGGS promoter was strong enough to provide good visibility of red fluorescent clones. This is due to the fact that it is a strong promoter enforced by a CMV enhancer element [179].

4.3.3. Homologous recombination screening

Visual screening for random integration reduced the number of clones, which had to be expanded and further analysed, by 48% to 80%. This enrichment strategy is very time and cost effective and will thus be of interest also for other gene targeting projects. Vazquez-Manrique *et al.* (2010) published a similar approach with eGFP as a visual marker in *C.elegans* [224]. However, this is the first reported use of visual exclusion of RI for gene targeting in large animals.

Some non-fluorescing clones were identified as PCR positive for Cherry after passaging. Parts of the CAGGS-Cherry cassette might have got lost after transfection due to shearing of DNA so that gene expression could not be observed although RI occurred. Thomas and Capecchi (1990) have reported loss or damage of the HSV-TK negative selection marker in 99% of selected colonies [225]. Zijlstra *et al.* (1989) have made this observation only in 50% of clones [226]. With 48% to 80% of clearly red clones, Cherry-based screening proved to be more suitable for enrichment.

After visual analysis of clones generated by BAC transfection, cells should be further analysed. According to Yang and Seed (2003) a combination of PCR and fluorescence *in situ* hybridisation (FISH) provides reliable identification of BAC-targeted clones [188]. Hence, (q)PCR and FISH conditions were optimised. Duplex qPCR optimisation for JAK3 BAC targeting was performed according to Tesson *et al.* (2002) [227]. Gomez-Rodriguez *et al.* (2008) argue that FISH analysis can produce false positive results, but thus far no alternative approach except qPCR has been established [228].

Conventional JAK3 targeting screening by PCR did not produce specific results despite intensive optimisation. This made the application of additional nested PCR necessary. The two main

factors that hindered specific PCR amplification were thereby repetitive sequences and low GC content. At the onset of this study the porcine JAK3 sequence was not annotated. The human gene contains a non-transcribed JAK3 exon in front of the porcine exon 1 homologue. Homology comparison revealed a similar "exon 0" in the pig gene located 6.4 kb in front of exon 1. The intronic region in between contains highly repetitive sequence patterns from retrotransposons. These were mainly short and long interspersed elements (SINE and LINE), which are spread throughout the genome [229]. The forward PCR screening primer is located in the middle of a 1.5 kb LINE and thus the extra PCR bands probably resulted from unspecific binding within this LINE or other homologous LINEs. The low GC content of 38% in this LINE element further restricted an increase of the annealing temperature during PCR. Thus more stringent conditions for more specific amplification could not be applied.

For continuing this study, two possible strategies have to be assessed. The PGK-neo cassette could be moved further downstream so that the screening primers could be set in a less repetitive region. Alternatively, the JAK3-TV-CCN short homology arm could be shortened to not carry the repetitive sequence and allow the design of a specific primer. However, this size reduction could affect homologous recombination efficiency [166].

Southern blot analysis of JAK3 gene targeted clones offers the opportunity to accurately examine the targeted locus. This can be done without PCR amplification steps prone to produce unspecific signals. Other groups have also reported PCR results sometimes to be false positive. For example, Ramsoondar *et al.* (2011) showed that 3 out of 10 PCR positive clones were not targeted when analysed with Southern blot [204]. To overcome these problems, Southern blot conditions were optimised thereby allowing accurate analysis of the JAK3 locus.

4.4. Gene targeting efficiencies

4.4.1. BAC-based gene targeting

Thus far, no studies on BAC-based gene targeting in MSCs have been published. Gene targeting experiments conducted in mouse embryonic stem (ES) cells proved to be efficient with HR rates ranging between 6% and 28% [219, 188, 230, 231]. In contrast, gene targeting with BAC vectors was not successful in this study.

The main impediments thereby seemed to be difficulties with transfection. Plasmid transfection of pMSC demonstrated that efficient vector delivery was feasible in general. However, transfectability was much lower with BAC DNA although different methods were tested and key parameters were optimised. Lipofection produced best results, but still below 10%. Phelps *et al.* (2007) have reported low DNA:Lipofectamine ratios to produce highest efficiencies for BAC transfection [232]. This result was confirmed in the IL2RG and JAK3 BAC experiments. As also

observed in this study, Montigny *et al.* (2003) have shown a strong dependence between DNA purity and transfection efficiency [221]. Porcine MSCs might be especially sensitive in this regard and due to this reason stop proliferation. Low transfection efficiency did not turn out to be the main problem, but rather this effect of BAC transfection pMSC growth.

Many clones went into senescence before they could be expanded or analysed by PCR. Hence, the generation of sufficient clones for statistical analysis of HR frequencies was not possible. However, it was demonstrated that IL2RG-neo-CCN BAC can trigger HR at the target locus in pMSCs. PCR screening identified that 0.7% (2/300) fat and 0.1% (1/700) bone marrow MSC clones generated by IL2RG BAC transfection were targeted. However, none was applicable for SCNT as cell preservation was not possible. In general, clone numbers, which died before PCR analysis could not be assessed. It is possible that positive clones have died without being analysed as the three identified clones also went into senescence shortly after picking.

Klymiuk *et al.* (2011) reported similar efficiency for a BAC-based vector in porcine kidney fibroblast. Homologous recombination at the CFTR locus was carried out with a frequency of 1.57% (7/446) [208]. In contrast to pMSCs in this study, at least 6 targeted cell clones continued proliferation and could be used for SCNT. It was confirmed in this study that pKDNF can be efficiently transfected with IL2RG and JAK3 BAC targeting vectors and that they can be used for single cell cloning. Kidney fibroblasts seemed to be less sensitive to transfection with big DNA constructs than MSCs and could be manipulated by nucleofection without negative effects on cell proliferation. Considering the differences between the two cell types, there is a strong indication that BAC targeting might not be feasible for the application in pMSCs. In total, 120 pKDNF have been analysed for IL2RG BAC targeting in this study, but none of the clones was targeted. If similar efficiencies are assumed for IL2RG BAC targeting in pMSC (0.1% to 0.7%) and pKDNF, the number of clones analysed by PCR was too small to identify a positive event.

In contrast to IL2RG, JAK3 BAC targeting was not possible in porcine MSCs or KDNF in this study, although approximately 800 and 100 cell clones were generated, respectively. Assuming that proliferation of MSCs was affected equally by JAK3 and IL2RG BAC transfection, it can be stated that IL2RG gene targeting was more efficient than for JAK3. The reason might be the disadvantage of the short 3' homology arm of only 624 bp in JAK3-geo-CCN BAC. In contrast, for homologous recombination in mouse ES cells 472 bp of homology were sufficient to form crossover junctions [220]. Theoretically, gene targeting efficiency of IL2RG could be expected to be lower than for JAK3. This is due to the fact that only one gene copy is present and thus the probability of contact between vector and chromosomal locus is reduced. In mouse ES cells BAC-based targeting of the X-chromosomal HPRT gene was possible with 33% and 57% of colonies being correctly modified [233]. However, HR is very efficient in mES cells and chemical enrichment is available for HPRT targeting. This might be the reason why positive clones could

be identified. Hence, it is not possible to compare efficiency numbers to the experiments on JAK3 and IL2RG BAC targeting.

Taken together BAC-based targeting in our study was possible for IL2RG in pMSCs, but it is not recommended. Low transfection efficiency and frequent senescence of transfected clones hindered the application of BAC targeted pBM-MSCs in SCNT. Strategies to improve cell viability after transfection, e.g. the increase of serum concentration for picked clones as performed by Marques *et al.* (2006), might enhance viability of BAC transfected pMSCs [222].

4.4.2. Conventional gene targeting

Big differences in HR efficiency were observed for BAC-based and conventional targeting of JAK3. Porcine KDNF and bone marrow and fat tissue pMSCs were compared in this study regarding HR frequency at the JAK3 gene locus. Initial proof of principle tests performed on small pools of clones were successful. They were followed by single cell clone generation and HR analysis.

Visual screening preceded targeting PCRs to exclude clones with random integration. Some clones –PCR positive for JAK3 targeting– revealed in subsequent analysis to carry additional RI as a Cherry fragment could be amplified by PCR. Thus, it was possible that targeted clones were discarded during visual pre-screening. Consequently, the reported HR efficiencies in this work describe the minimum number and are possibly higher.

The generation of clones with HR and additional RI makes the distinction of two efficiency types necessary: HR_{only} stands for those clones, which could be used for SCNT, as they did not carry RI. HR_{total} includes all targeted clones regardless of additional events. Thus, it provides better information about the cell's intrinsic capability to drive HR. A negative selection approach with HSV-TK would have killed HR and RI positive clones, so that HR_{total} could not be assessed.

JAK3 gene targeting worked in pBM-MSC, pAD-MSC and pKDNF and was dependent on the used cell type. HR_{total} ranged from 6% to 16%, thus indicating a difference of the cell types intrinsic capability to drive HR. Porcine KDNF produced 6% targeted clones. Pig BM-MSCs were targeted with similar efficiencies of 9% and 11% depending on the cell isolation. HR_{total} was 16% and thus highest for pAD-MSC1101. Comparison of this value to pBM-MSC1101 allows exclusion of genetic background effects, as these cells were isolated from the same animal. With 9% HR_{total}, pBM-MSC1101 were much less efficient than the corresponding MSC isolation from adipose tissue.

In contrast to these numbers, HR_{only} values were similar for all cell isolations and ranged from 4% (pKDNF2109, pAD-MSC1101) to 6% (pBM-MSC0712). Here it becomes clear that pAD-MSC1101 were practically not better than the other cell types, due to the high rate of additional RI events. Maybe the high portion of clones with HR and RI is caused by good transfection

efficiency and introduction of much higher plasmid copy numbers compared to the other cell types. Approaches to reduce the copy number per cell ratio might improve rates in favour of HR_{only}. If this shift cannot be achieved, pBM-MSCs and pKDNF can be considered to be equally applicable for gene targeting.

Large data sets on factors influencing gene targeting efficiency are available for mouse ES cells. Some studies proved that HR efficiency depends on the gene locus to be targeted and thus confirm our study result. Differences in HR frequency were demonstrated to be very variable even in cells from the same isolation. Sedivy *et al.* (1999) have summarised 23 gene targeting experiments in human somatic cells and found HR rates between 0.1 and 37% depending on the target locus [234].

Active transport of the targeting vector from the cytosol into the nucleus across the stable nuclear membrane is promoted by the NLS in the CCN cassette. This feature might have caused the good efficiencies observed for conventional JAK3 gene targeting in this study. After transfection, the accessibility of the vector in the nucleus is essential to trigger HR. This is hindered by the nuclear membrane, which is stable during S phase and breaks down subsequently, during G2 phase of the cell cycle. HR efficiency has been demonstrated by different groups to be highest in S phase, i.e. at a time point when the nuclear membrane is stable [235–238]. Hence, the NLS can allow vector access to the nucleus when the cell's HR machinery is most active. A study confirming a positive effect of the NLS on gene targeting efficiencies was performed by Mir *et al.* (2004). They tested a combined approach involving cell cycle synchronisation in S phase and a NLS. They found that the percentage of HR positive clones increased from 4.4% to 32.7% when the NLS was encoded on the targeting vector [167]. As this result is very promising, cell cycle synchronisation of pMSCs and pKDNF for JAK3 gene targeting should be tested in future experiments in this study.

4.5. Somatic cell nuclear transfer

4.5.1. Pregnancy and birth

Generation of cloned pigs from somatic cell nuclear transfer of pBM-MSCs and pAD-MSCs was successful in this study. Early pregnancies with targeted cells were established in 50% of recipient sows (2 out of 4) and went to term. This number is in range with frequencies determined in other studies, in which results varied strongly. For example 10.7% and 75% have been reported by Lai *et al.* (2002) and Rogers *et al.* (2008), respectively [239, 240].

The rates of transferred embryos derived from pBM-MSC0303 and pBM-MSC0902 developing to living animals were 3.1% and 0.5%, respectively. These numbers are in line with the majority of cloning experiments on adult or fetal somatic cells. Wilmut *et al.* (2002) have summarised

this overall rate to be only 0% to 4% [159]. Compared to these results, single cell clones from pAD-MSC1101 produced higher rates, as 6.8% of reconstructed embryos developed to viable animals. They were also better than pre-adipocytes, for which Tomii *et al.* (2009) reported a 4.2% rate [241]. A possible reason for this observation might be that AD-MSCs are less differentiated than pre-adipocytes and possibly reprogrammed more efficiently. Oh *et al.* (2011) also used AD-MSCs for successful cloning of dogs and 2.4% of reconstructed embryos developed to healthy animals [242]. This rate is lower compared to pAD-MSCs but direct comparison of these results is hindered by the fact that species-specific differences might exist.

In this study, litter sizes from pBM-MSC derived embryos with 1 to 5 piglets were smaller than from a normal porcine pregnancy as has been reported in other pig cloning studies from targeted and non-targeted cells [153, 239, 206, 218]. The mean litter normally has a size of 10 piglets [122]. In this regard pAD-MSC1101 again showed good results as 9 out of 10 piglets from one litter were live born and survived. In contrast, gene targeted pBM-MSC0303 and pBM-MSC0902 generated 3/5 and 0/1 live born piglets, but non survived longer than 38 days.

In summary, SCNT with pMSC was successful, but high differences were observed for bone marrow and adipose tissue cells. BM-MSCs performed similar to somatic cells used in previous studies regarding embryo development and birth. AD-MSC1101 derived embryos were clearly better in terms of high development rates, litter sizes and overall survival of animals. The possible reasons for these results are discussed in Section 4.5.2.

In this study the number of SCNT experiments was too low to obtain sufficient data for statistical evaluation of cloning efficiencies. Repeated conduction of pAD-MSC1101 SCNT with gene targeted embryos will give valuable information about the performance of these cells. It will also be necessary to test other adipose tissue MSC isolations in order to evaluate if pAD-MSC are good nuclear donors in general or if the high efficiencies in this study are a feature of the pAD-MSC1101 cell isolation in particular.

4.5.2. Physical appearance of piglets

There is a strong indication that incomplete reprogramming in transferred nuclei is the cause of low SCNT efficiency as in the majority of cloning experiments abnormalities were reported: these included embryonic arrest, high abortion rates, defective placentas, neonatal abnormalities, shorter life span, obesity, respiratory problems and large offspring syndrome [243–246]. The epigenetic alterations, which are not completely reset in some cloned animals, include shortened telomeres in cloned embryos, aberrant DNA methylation or imprinting, incomplete reprogramming of the donor cell nucleus, and asynchrony of oocyte and donor nuclei cell cycles.

The claim that telomeres are irreversibly shortened in cloned animals is still not clarified. In theory telomeres are expected to be longer in normal SCNT embryos compared to the somatic

cell they were derived from because of high level expression of telomerase in normal embryos. This was confirmed in some studies on cloned sheep and goats, in which telomeres were compared to age-matched controls [147, 247, 248]. However, no significant differences in telomere length were reported in other studies on calves and pigs [249–251].

Many defects in cloned animals are similar to human diseases related to imprinting defects. Imprinted genes are expressed in a monoallelic pattern depending on the parent of origin and are regulated by DNA methylation. During normal embryo development the present imprinted methylation pattern is erased before the new parental pattern is established [252–254]. Abnormal methylation of five imprinted genes was reported in 96% of SCNT-derived pre-implatation mouse embryos. Reprogramming defects in imprinted genes were also observed in organs of cloned pigs [255]. As these genes are regulators of fetal growth and as cloned pigs were significantly smaller than controls, Jiang *et al.* (2007) assumed a correlation.

In this study, piglets born generally looked healthy. One still born piglet (#43) derived from pBM-MSC0902 showed an enlarged tongue. Less problems occurred with pBM-MSC0303 derived piglets #19, 20 and 21 as their phenotype was normal, but these piglets died because of repeated umbilical hernia. This has been observed in one other experiment using the same cell isolate in this group. In humans, an enlarged tongue and abdominal wall defects are clinical finding associated with Beckwith-Wiedeman syndrome (BWS). This is a disease caused by incorrect imprinting on growth regulatory genes, e.g. H19-IGF2, on chromosome 11p15.5 [256]. Due to the similarities between BWS patients and the piglets born after pBM-MSC SCNT, an imprinting defect corresponding to BWS can be assumed. Consequently, a repeat of SCNT with these cells is not recommended.

In contrast to piglets derived from bone marrow, animals produced from pAD-MSC1101 SCNT did not exhibit any phenotypic defects and survived. Dean *et al.* (2001, 2003) showed that *in vitro* culture alone already negatively affects DNA methylation. They report loss of imprinting, biallelic expression and abnormal development [257, 258]. Allegrucci *et al.* (2007) confirmed that accumulation of epigenetic changes occurs during culture in human ES cells [259]. As all MSC isolations –regardless of tissue source– were cultured under equal conditions, culture-induced specific effects on bone marrow MSCs can be excluded. However, it is possible that these cells are more sensitive to epigenetic changes during culture than pAD-MSC1101.

Several groups reported that the donor cell genome is not fully demethylated after SCNT [260–263]. As a consequence methylation of DNA remains higher than in normal embryos. Bonk *et al.* (2007) compared *in vivo* produced, parthenogenetic, *in vitro* fertilized and SCNT pig blastocyst and observed significant differences in DNA methylation at 12 genomic loci [264]. However, microarray studies revealed that the majority of genes is reprogrammed as only 5% of several thousand genes were not correctly transcribed in early nuclear transfer embryos [265–267]. Smith *et al.* (2005) even found abnormal gene expression in only 1% of genes [268]. Incomplete ex-

pression of gene products critical in early development, e.g. Oct-4, may be especially detrimental [202]. However, defects in genes essential for embryonic development probably cause embryo loss at early stages before death. Impaired expression of other genes, which are not imprinting related, might have also caused health problems in the JAK3 gene targeted piglets in this study. As this was not examined, this question remains open.

Taken together there is a strong indication that pAD-MSC1101 are suitable nuclear donors as birth and survival rates were high and as no phenotypic abnormalities could be observed. Thus, future gene targeting experiments should be preferably in this cell isolation for the production of JAK3 heterozygous knock out animals.

4.5.3. Possible improvement strategies for SCNT

A broad variety of alternative or supportive approaches to increase the cloning efficiency by SCNT is under investigation by other groups. Some approaches are based on improving reprogramming of the donor nucleus, e.g. by treatment with chemicals, which influence the chromatin structure. Acetylation of histones is an epigenetic modification causing chromatin structure relaxation and may thus enhance accessibility of DNA to remodeling factors. Inhibitors of histone deacetylase, such as trichostatin A, scriptaid or valproic acid have shown to positively influence the development of cloned pigs [269–272]. The incubation with egg cell extracts is an alternative to improve cloning efficiency. For example, SCNT donor cells for SCNT in *Xenopus laevis* oocyte extracts improved blastocyst formation rates in pigs [273]. Rathbone *et al.* (2010) also observed an increase of live birth rates with this approach in sheep [274]. Other groups have demonstrated the positive effect of growth factors on the developmental potential of porcine SCNT preimplantation embryos, e.g. by vascular endothelial growth factor (VEGF) [275, 276]. Huang *et al.* (2011) reported vitamin C treatment to induce a more than 2-fold enhancement in pig blastocyst formation and to increase pregnancy rates [277]. As this approach is very promising and was also shown to be successful for pigs in particular, it should be tested for future experiments.

4.5.4. Analysis of homologous recombination

Homologous recombination in gene targeted pigs was analysed for the transgenic piglets #19, 20, 21, 42A, 42B and 43. All piglets were targeting and nested PCR positive. Sequencing of the targeting DNA band further confirmed the junction between the genomic locus and the vector short arm. Southern blot analysis of JAK3 targeted pBM-MSC clones subsequently used for SCNT confirmed correct gene targeting 5' of the PGK-neo cassette. Gene targeted piglets further analysed for HR at the 3' long homology arm showed a signal approximately at the expected size. As no additional bands from neo probe hybridisation were visible, RI of the vector is not probable.

In summary, there is strong evidence that the piglets born were truly JAK3 gene targeted. To complete the line of arguments further analysis of the piglets should be performed. Homologous recombination on the 5' HR arm should be demonstrated also on piglet DNA. Furthermore, the size of the 3' HR signal should be determined with help of a suitable DIG labeled marker.

4.6. Alternative approaches to this study

The experimental design for the generation of immunodeficient pigs was discussed at the beginning of this section. It had to be chosen carefully and was performed within the boundaries set by state of the art methods available. Since the onset of this work, alternative techniques have been established, optimised and demonstrated to allow efficient gene targeting.

Viral vector delivery

Gene targeting experiments based on viral delivery of the targeting vector have been successfully performed. The most commonly used system uses non-pathogenic recombinant adeno-associated viruses (rAAV). Russel and Hirata (1998) showed that these single stranded DNA viruses are capable of inducing HR in human fibroblasts at frequencies 10 times higher than RI of the vector [278]. It is assumed that HR efficiency is that high because of direct translocation of the vector into the nucleus by the viral system similar to the NLS sequence used in this study. The major drawback is that the small packaging size of rAAV restricted to approximately 4.5 kb. It could be expected that gene targeting efficiencies especially for silent genes are consequently reduced. However, a positive selection vector with only 1.5 kb and 1.3 kb flanking homologies was still able to trigger HR at the CFTR locus, which is not expressed in fetal fibroblasts [240].

The application of rAAV vectors could be present a possible alternative approach for this study on pMSC, as the human MSCs have already been successfully modified. The COL1A locus was corrected in cells from *osteogenesis imperfecta* patients with efficiencies ranging from 60% to 82% in positive selected clones [279]. Furthermore, viral vector delivery was already used for the generation of different gene targeted pigs, e.g. also including a model for human breast cancer [280, 240, 281]. Thus, this might be an alternative approach to induce gene targeting in porcine JAK3 or IL2RG maybe with greater efficiencies than obtained in this study.

Gene targeting with endonucleases

The use of conventional vectors has been the standard method for the generation of gene targeted livestock for years, due to the lack of more efficient and easier alternatives. More and more evidence on the high efficiency of gene targeting with endonucleases, e.g. Zinc finger nucleases (ZFN), is available today. These molecules can be transferred to the cell as DNA or RNA and

induce genome alterations by induction of specific DNA double strand breaks (DSB). This causes a loss or gain of several bases at the DSB position, as a repair mechanism based on non homologous end joining is triggered. Alternatively, specific alterations can be performed by a cotransfer of ZFNs and a small targeting vector, which is used as a repair template in HR.

Thus far, ZFN-based gene targeting has been performed efficiently in various species including mouse, rat, rabbit and zebrafish [282, 283, 171, 173, 284]. This approach was also applied for gene targeting at the IL2RG locus in human and rat cells [285, 283]. X-SCID rats were thereby produced with efficiencies above 20% after ZFN mRNA injection into the pronucleus of fertilized oocytes. This shows that low gene targeting efficiencies can be circumvented with this technique. Thus far, ZFNs have been applied for pig gene targeting only in one recent study. Hausschild *et al.* (2011) used ZFNs for a biallelic knock out of the GGTA1 gene [172].

The major disadvantage of ZFN mediated gene targeting is the frequent induction of DSBs at off-target sites due to lack of specificity. Thus, intensive pre-testing of specificity is essential to avoid cytotoxicity and enable subsequent generation of viable animals.

More recently, an alternative approach less cytotoxic but as efficient has been published [286]. Transcription activator-like effector (TALE) proteins from *Xanthomonas genus* plant pathogens contain sequence specific DNA binding residues connected to a translocation domain, nuclear localisation signal and a transcriptional activation domain. The DNA binding domain can be easily engineered to recognise specific base patterns. Connection of TALE proteins with a nuclease (TALEN) triggers DSB induction and induces the same repair machinery as ZFNs. In the study by Mussolino *et al.* (2011), human IL2RG specific TALENs disrupted the gene at 14% and CCR5 at 17% frequency *in vitro*. IL2RG targeting was less efficient compared to a corresponding ZFN approach (37%). However, CCR5 TALENs were highly specific, in contrast to a ZFN, which caused disruption in CCR5 and the highly homologous CCR2 locus at similar rates [286]. Given their performance in these early studies, TALENs will probably play a major role in future projects involving generation of gene targeted animals including pigs. Gene targeting of JAK3 with TALENS might be better than ZFNs, as sequence homology to other janus kinase family members might decrease ZFN specificity. In general, with the ongoing optimisation of endonuclease-based gene targeting, this approach could be used for the disruption of porcine JAK3 or IL2RG.

4.6.1. Induced pluripotent stem cells

The major barrier to highly efficient production of gene targeted pigs is the lack of cells that show high homologous recombination rates and cloning efficiency. Mouse embryonic stem cells show these characteristics, which make gene targeting efficient. Despite immense effort, the derivation of porcine embryonic stem cells has not produced positive results, yet. Some groups

have claimed successful isolation of porcine ES-like cells, but these are not commonly accepted to be true ES cells, thus far.

The application of induced pluripotent stem cells (iPS cells), which have been derived from a differentiated cell, may present a major improvement for gene targeting in pigs. The first report on the production of iPS cells from the mouse was published by Takahashi and Yamanaka (2006) [287]. They showed the successful reprogramming of fibroblasts by retroviral transduction of four transcription factors: OCT3/4, C-MYC, KLF4 and SOX2. These cells resembled ES cells very closely and were shown to be capable of teratoma formation and of contribution to chimeric mice upon blastocyst injection. Since this early study, iPS cells have been generated from various species including human, sheep, rat and monkey [288–291]. Since this early study different approaches for the introduction of the transcription factors have been tested. For example, pluripotency induction with retroviral vector or episomal vectors [292, 293]. In contrast, Wu *et al.* (2009) used a drug inducible system for the expression of the reprogramming factors [294].

Pig iPS cells might circumvent the need for ES cell generation or help to establish culture conditions for these cells. Different groups have stated the production of pig iPS cells. For example, Esteban *et al.* (2009) have reported the derivation of Tibetan miniature pig iPS cells and Montserrat *et al.* (2011) lately reprogrammed pig ear fibroblast [295, 296]. Wu *et al.* (2011) have demonstrated gene correction of fumarylacetoacetate hydrolase and application of iPS cells for the generation of healthy mice [297]. The establishment of IL2RG or JAK3 gene targeted pigs might also become possible if contribution to chimera development or the application in SCNT can be confirmed for the pig iPS cells published thus far.

4.7. Outlook and Applications

Studies aiming at generation of gene targeted large animals present long term projects because of the experimental set up and long gestation times. The following section gives an overview of future steps necessary for the progress of this study and briefly lists possible applications of immunodeficient pigs in biomedical research.

The successful generation of JAK3 gene targeted pigs was reported in this study. Future steps will include the repetition of gene targeting experiments with the JAK3 conventional vector. Due to high HR and cloning efficiency for pAD-MSC1101, these particular cells and other fat MSC isolations should be tested further. A transfection protocol modification might influence the transfer of vector copy numbers in favour of single HR events and reduce the number of additional RIs. In future experiments, gene targeted clones can be rapidly generated. Detection of Cherry by PCR can precede the gene targeting screening PCR. Approximately 95% of clones not exhibiting red fluorescence can be excluded if 5% of HR_{only} efficiency is assumed. The few remaining clones could be analysed by targeting PCR and Southern blot. As DL pigs can reach

a weight of 150 to 180 kg after 12 months, generation of immunodeficient minipigs should also be considered. Minipigs have a maximum weight of 30 to 60 kg and are thus more similar to humans in this aspect [122]. They could be also generated with JAK3 vector applied in this study.

Phenotype analysis was not possible in the animals developed thus far as immunodeficiency will be established only in homozygous knock out pigs. Targeted and SCNT-derived founder animals have to reach sexual maturity to be used for generation of a herd for breeding. The F1 generation born after insemination would still be heterozygous and only crossing would produce JAK3$^{-/-}$ in the F2. These animals will have to be born under sterile conditions in a DPF facility. A first indication about a SCID phenotype in human patients is immune cell blood count and comparison to normal values. To analyse the JAK3 deficient animals, this and other tests will have to be performed. These can involve the analysis of T, B and NK cells for their activation of the JAK-STAT signaling pathway and downstream molecules by γ_C cytokine treatment. After phenotype confirmation, practical application by transplantation of different cell types, e.g. haematopoietic cells, liver cells and MSCs, will give information about the capacity of JAK3$^{-/-}$ deficient pigs for immune rejection.

In their application, immunodeficient pigs will be useful for basic and application-oriented studies in various biomedical research fields. They can provide in vivo conditions similar to the human body. Thereby, the transplanted cell type determines the application field: Tumour cell engraftment will give insight in processes during carcinogenesis or metastasis formation and also allow for the testing of therapeutic approaches. These can include cell-based approaches, such as anti-cancer primed cells. The Introduction of a human immune system in the pig by transfer of HSCs can elucidate hematopoiesis, but also serve as a system for the study of infectious diseases, such as HIV or Dengue. In regenerative medicine, e.g. bone and cartilage cell transfer to sites of defect, e.g. the knee joint, will provide a strong basis for the testing of human stem cell based therapeutic approaches.

In general, the immunodeficient pig will not replace the mouse as a valuable research tool, but it will rather present an advancement for human cell-based studies. Especially, in biomedical research areas, in which mice did not adequately represent human biology, immunodeficient pigs will bridge the gap between bench and bedside.

5. Bibliography

1. L. D. Shultz, F. Ishikawa, and D. L. Greiner, Humanized mice in translational biomedical research., *Nat Rev Immunol*, vol. 7, no. 2, pp. 118–130, 2007 Feb.

2. L. D. Shultz, B. L. Lyons, L. M. Burzenski, B. Gott, X. Chen, S. Chaleff, M. Kotb, S. D. Gillies, M. King, J. Mangada, D. L. Greiner, and R. Handgretinger, Human lymphoid and myeloid cell development in nod/ltsz-scid il2r gamma null mice engrafted with mobilized human hemopoietic stem cells., *J Immunol*, vol. 174, no. 10, pp. 6477–6489, 2005 May 15.

3. F. Ishikawa, M. Yasukawa, B. Lyons, S. Yoshida, T. Miyamoto, G. Yoshimoto, T. Watanabe, K. Akashi, L. D. Shultz, and M. Harada, Development of functional human blood and immune systems in nod/scid/il2 receptor gamma chain(null) mice., *Blood*, vol. 106, no. 5, pp. 1565–1573, 2005 Sep 1.

4. J. McCune, H. Kaneshima, J. Krowka, R. Namikawa, H. Outzen, B. Peault, L. Rabin, C. C. Shih, E. Yee, and M. Lieberman, The scid-hu mouse: a small animal model for hiv infection and pathogenesis., *Annu Rev Immunol*, vol. 9, pp. 399–429, 1991.

5. D. E. Mosier, Human immunodeficiency virus infection of human cells transplanted to severe combined immunodeficient mice., *Adv Immunol*, vol. 63, pp. 79–125, 1996.

6. D. A. Bente, M. W. Melkus, J. V. Garcia, and R. Rico-Hesse, Dengue fever in humanized nod/scid mice., *J Virol*, vol. 79, no. 21, pp. 13797–13799, 2005 Nov.

7. T. Nomura, H. Nakajima, T. Hongyo, E. Taniguchi, K. Fukuda, L. Y. Li, M. Kurooka, K. Sutoh, P. M. Hande, T. Kawaguchi, M. Ueda, and H. Takatera, Induction of cancer, actinic keratosis, and specific p53 mutations by uvb light in human skin maintained in severe combined immunodeficient mice., *Cancer Res*, vol. 57, no. 11, pp. 2081–2084, 1997 Jun 1.

8. D. J. Flavell, S. L. Warnes, C. J. Bryson, S. A. Field, A. L. Noss, G. Packham, and S. U. Flavell, The anti-cd20 antibody rituximab augments the immunospecific therapeutic effectiveness of an anti-cd19 immunotoxin directed against human b-cell lymphoma., *Br J Haematol*, vol. 134, no. 2, pp. 157–170, 2006 Jul.

9. S. K. Singh, C. Hawkins, I. D. Clarke, J. A. Squire, J. Bayani, T. Hide, R. M. Henkelman, M. D. Cusimano, and P. B. Dirks, Identification of human brain tumour initiating cells., *Nature*, vol. 432, no. 7015, pp. 396–401, 2004 Nov 18.

10. C. S. Mitsiades, N. S. Mitsiades, R. T. Bronson, D. Chauhan, N. Munshi, S. P. Treon, C. A. Maxwell, L. Pilarski, T. Hideshima, R. M. Hoffman, and K. C. Anderson, Fluorescence imaging of multiple myeloma cells in a clinically relevant scid/nod in vivo model: biologic and clinical implications., *Cancer Res*, vol. 63, no. 20, pp. 6689–6696, 2003 Oct 15.

11. R. L. Sah and A. Ratcliffe, Translational models for musculoskeletal tissue engineering and regenerative medicine., *Tissue Eng Part B Rev*, vol. 16, no. 1, pp. 1–3, 2010 Feb.

12. G. F. Muschler, V. P. Raut, T. E. Patterson, J. C. Wenke, and J. O. Hollinger, The design and use of animal models for translational research in bone tissue engineering and regenerative medicine., *Tissue Eng Part B Rev*, vol. 16, no. 1, pp. 123–145, 2010 Feb.

13. P. Vavken and M. M. Murray, Translational studies in anterior cruciate ligament repair., *Tissue Eng Part B Rev*, vol. 16, no. 1, pp. 5–11, 2010 Feb.

14. C. R. Chu, M. Szczodry, and S. Bruno, Animal models for cartilage regeneration and repair., *Tissue Eng Part B Rev*, vol. 16, no. 1, pp. 105–115, 2010 Feb.

15. E. Glanzmann and P. Riniker, [essential lymphocytophthisis; new clinical aspect of infant pathology]., *Ann Paediatr*, vol. 175, no. 1-2, pp. 1–32, 1950 Jul-Aug.

16. M. Noguchi, H. Yi, H. M. Rosenblatt, A. H. Filipovich, S. Adelstein, W. S. Modi, O. W. McBride, and W. J. Leonard, Interleukin-2 receptor gamma chain mutation results in x-linked severe combined immunodeficiency in humans., *Cell*, vol. 73, no. 1, pp. 147–157, 1993 Apr 9.

17. S. M. Russell, N. Tayebi, H. Nakajima, M. C. Riedy, J. L. Roberts, M. J. Aman, T. S. Migone, M. Noguchi, M. L. Markert, R. H. Buckley, J. J. O'Shea, and W. J. Leonard, Mutation of jak3 in a patient with scid: essential role of jak3 in lymphoid development., *Science*, vol. 270, no. 5237, pp. 797–800, 1995 Nov 3.

18. A. Puel, S. F. Ziegler, R. H. Buckley, and W. J. Leonard, Defective il7r expression in t(-)b(+)nk(+) severe combined immunodeficiency., *Nat Genet*, vol. 20, no. 4, pp. 394–397, 1998 Dec.

19. K. Schwarz, G. H. Gauss, L. Ludwig, U. Pannicke, Z. Li, D. Lindner, W. Friedrich, R. A. Seger, T. E. Hansen-Hagge, S. Desiderio, M. R. Lieber, and C. R. Bartram, Rag mutations in human b cell-negative scid., *Science*, vol. 274, no. 5284, pp. 97–99, 1996 Oct 4.

20. D. Moshous, I. Callebaut, R. de Chasseval, B. Corneo, M. Cavazzana-Calvo, F. Le Deist, I. Tezcan, O. Sanal, Y. Bertrand, N. Philippe, A. Fischer, and J. P. de Villartay, Artemis, a novel dna double-strand break repair/v(d)j recombination protein, is mutated in human severe combined immune deficiency., *Cell*, vol. 105, no. 2, pp. 177–186, 2001 Apr 20.

21. C. Kung, J. T. Pingel, M. Heikinheimo, T. Klemola, K. Varkila, L. I. Yoo, K. Vuopala, M. Poyhonen, M. Uhari, M. Rogers, S. H. Speck, T. Chatila, and M. L. Thomas, Mutations in the tyrosine phosphatase cd45 gene in a child with severe combined immunodeficiency disease., *Nat Med*, vol. 6, no. 3, pp. 343–345, 2000 Mar.

22. H. K. Dadi, A. J. Simon, and C. M. Roifman, Effect of cd3delta deficiency on maturation of alpha/beta and gamma/delta t-cell lineages in severe combined immunodeficiency., *N Engl J Med*, vol. 349, no. 19, pp. 1821–1828, 2003 Nov 6.

23. G. de Saint Basile, F. Geissmann, E. Flori, B. Uring-Lambert, C. Soudais, M. Cavazzana-Calvo, A. Durandy, N. Jabado, A. Fischer, and F. Le Deist, Severe combined immunodeficiency caused by deficiency in either the delta or the epsilon subunit of cd3., *J Clin Invest*, vol. 114, no. 10, pp. 1512–1517, 2004 Nov.

24. C. Soudais, J. P. de Villartay, F. Le Deist, A. Fischer, and B. Lisowska-Grospierre, Independent mutations of the human cd3-epsilon gene resulting in a t cell receptor/cd3 complex immunodeficiency., *Nat Genet*, vol. 3, no. 1, pp. 77–81, 1993 Jan.

25. A. Arnaiz-Villena, M. Timon, C. Rodriguez-Gallego, P. Iglesias-Casarrubios, A. Pacheco, and J. R. Regueiro, T lymphocyte signalling defects and immunodeficiency due to the lack of cd3 gamma., *Immunodeficiency*, vol. 4, no. 1-4, pp. 121–129, 1993.

26. F. Cossu, Genetics of scid., *Ital J Pediatr*, vol. 36, p. 76, 2010.

27. R. H. Buckley, R. I. Schiff, S. E. Schiff, M. L. Markert, L. W. Williams, T. O. Harville, J. L. Roberts, and J. M. Puck, Human severe combined immunodeficiency: genetic, phenotypic, and functional diversity in one hundred eight infants., *J Pediatr*, vol. 130, no. 3, pp. 378–387, 1997 Mar.

28. R. A. Gatti, H. J. Meuwissen, H. D. Allen, R. Hong, and R. A. Good, Immunological reconstitution of sex-linked lymphopenic immunological deficiency., *Lancet*, vol. 2, no. 7583, pp. 1366–1369, 1968 Dec 28.

29. R. H. Buckley, Molecular defects in human severe combined immunodeficiency and approaches to immune reconstitution., *Annu Rev Immunol*, vol. 22, pp. 625–655, 2004.

30. M. D. Railey, Y. Lokhnygina, and R. H. Buckley, Long-term clinical outcome of patients with severe combined immunodeficiency who received related donor bone marrow transplants without pretransplant chemotherapy or post-transplant gvhd prophylaxis., *J Pediatr*, vol. 155, no. 6, pp. 834–840, 2009 Dec.

31. B. Neven, S. Leroy, H. Decaluwe, F. Le Deist, C. Picard, D. Moshous, N. Mahlaoui, M. Debre, J.-L. Casanova, L. Dal Cortivo, Y. Madec, S. Hacein-Bey-Abina, G. de Saint Basile, J.-P. de Villartay, S. Blanche, M. Cavazzana-Calvo, and A. Fischer, Long-term outcome after hematopoietic stem cell transplantation of a single-center cohort of 90 patients with severe combined immunodeficiency., *Blood*, vol. 113, no. 17, pp. 4114–4124, 2009 Apr 23.

32. A. Fischer, S. Hacein-Bey, F. Le Deist, C. Soudais, J. P. Di Santo, G. de Saint Basile, and M. Cavazzana-Calvo, Gene therapy of severe combined immunodeficiencies., *Immunol Rev*, vol. 178, pp. 13–20, 2000 Dec.

33. M. Cavazzana-Calvo, S. Hacein-Bey, G. de Saint Basile, F. Gross, E. Yvon, P. Nusbaum, F. Selz, C. Hue, S. Certain, J. L. Casanova, P. Bousso, F. L. Deist, and A. Fischer, Gene therapy of human severe combined immunodeficiency (scid)-x1 disease., *Science*, vol. 288, no. 5466, pp. 669–672, 2000 Apr 28.

34. S. Hacein-Bey-Abina, C. von Kalle, M. Schmidt, F. Le Deist, N. Wulffraat, E. McIntyre, I. Radford, J.-L. Villeval, C. C. Fraser, M. Cavazzana-Calvo, and A. Fischer, A serious adverse event after successful gene therapy for x-linked severe combined immunodeficiency., *N Engl J Med*, vol. 348, no. 3, pp. 255–256, 2003 Jan 16.

35. R. H. Buckley, The multiple causes of human scid., *J Clin Invest*, vol. 114, no. 10, pp. 1409–1411, 2004 Nov.

36. M. Noguchi, H. Yi, H. M. Rosenblatt, A. H. Filipovich, S. Adelstein, W. S. Modi, O. W. McBride, and W. J. Leonard, Interleukin-2 receptor gamma chain mutation results in x-linked severe combined immunodeficiency in humans. cell 73: 147-157. 1993., *J Immunol*, vol. 181, no. 9, pp. 5817–5827, 2008 Nov 1.

37. J. M. Puck, S. M. Deschenes, J. C. Porter, A. S. Dutra, C. J. Brown, H. F. Willard, and P. S. Henthorn, The interleukin-2 receptor gamma chain maps to xq13.1 and is mutated in x-linked severe combined immunodeficiency, scidx1., *Hum Mol Genet*, vol. 2, no. 8, pp. 1099–1104, 1993 Aug.

38. N. A. Cacalano and J. A. Johnston, Interleukin-2 signaling and inherited immunodeficiency., *Am J Hum Genet*, vol. 65, no. 2, pp. 287–293, 1999 Aug.

39. M. Noguchi, S. Adelstein, X. Cao, and W. J. Leonard, Characterization of the human interleukin-2 receptor gamma chain gene., *J Biol Chem*, vol. 268, no. 18, pp. 13601–13608, 1993 Jun 25.

40. T. Takeshita, H. Asao, J. Suzuki, and K. Sugamura, An associated molecule, p64, with high-affinity interleukin 2 receptor., *Int Immunol*, vol. 2, no. 5, pp. 477–480, 1990.

41. T. Takeshita, H. Asao, K. Ohtani, N. Ishii, S. Kumaki, N. Tanaka, H. Munakata, M. Nakamura, and K. Sugamura, Cloning of the gamma chain of the human il-2 receptor., *Science*, vol. 257, no. 5068, pp. 379–382, 1992 Jul 17.

42. M. Kondo, T. Takeshita, N. Ishii, M. Nakamura, S. Watanabe, K. Arai, and K. Sugamura, Sharing of the interleukin-2 (il-2) receptor gamma chain between receptors for il-2 and il-4., *Science*, vol. 262, no. 5141, pp. 1874–1877, 1993 Dec 17.

43. A. Kawahara, Y. Minami, and T. Taniguchi, Evidence for a critical role for the cytoplasmic region of the interleukin 2 (il-2) receptor gamma chain in il-2, il-4, and il-7 signalling., *Mol Cell Biol*, vol. 14, no. 8, pp. 5433–5440, 1994 Aug.

44. S. M. Russell, A. D. Keegan, N. Harada, Y. Nakamura, M. Noguchi, P. Leland, M. C. Friedmann, A. Miyajima, R. K. Puri, and W. E. Paul, Interleukin-2 receptor gamma chain: a functional component of the interleukin-4 receptor., *Science*, vol. 262, no. 5141, pp. 1880–1883, 1993 Dec 17.

45. M. Noguchi, Y. Nakamura, S. M. Russell, S. F. Ziegler, M. Tsang, X. Cao, and W. J. Leonard, Interleukin-2 receptor gamma chain: a functional component of the interleukin-7 receptor., *Science*, vol. 262, no. 5141, pp. 1877–1880, 1993 Dec 17.

46. Y. Kimura, T. Takeshita, M. Kondo, N. Ishii, M. Nakamura, J. Van Snick, and K. Sugamura, Sharing of the il-2 receptor gamma chain with the functional il-9 receptor complex., *Int Immunol*, vol. 7, no. 1, pp. 115–120, 1995 Jan.

47. J. G. Giri, M. Ahdieh, J. Eisenman, K. Shanebeck, K. Grabstein, S. Kumaki, A. Namen, L. S. Park, D. Cosman, and D. Anderson, Utilization of the beta and gamma chains of the il-2 receptor by the novel cytokine il-15., *EMBO J*, vol. 13, no. 12, pp. 2822–2830, 1994 Jun 15.

48. H. Asao, C. Okuyama, S. Kumaki, N. Ishii, S. Tsuchiya, D. Foster, and K. Sugamura, Cutting edge: the common gamma-chain is an indispensable subunit of the il-21 receptor complex., *J Immunol*, vol. 167, no. 1, pp. 1–5, 2001 Jul 1.

49. J. J. O'Shea, M. Pesu, D. C. Borie, and P. S. Changelian, A new modality for immunosuppression: targeting the jak/stat pathway., *Nat Rev Drug Discov*, vol. 3, no. 7, pp. 555–564, 2004 Jul.

50. P. Macchi, A. Villa, S. Giliani, M. G. Sacco, A. Frattini, F. Porta, A. G. Ugazio, J. A. Johnston, F. Candotti, and J. J. O'Shea, Mutations of jak-3 gene in patients with autosomal severe combined immune deficiency (scid)., *Nature*, vol. 377, no. 6544, pp. 65–68, 1995 Sep 7.

51. P. Mella, R. F. Schumacher, T. Cranston, G. de Saint Basile, G. Savoldi, and L. D. Notarangelo, Eleven novel jak3 mutations in patients with severe combined immunodeficiency-including the first patients with mutations in the kinase domain., *Hum Mutat*, vol. 18, no. 4, pp. 355–356, 2001 Oct.

52. L. D. Notarangelo, P. Mella, A. Jones, G. de Saint Basile, G. Savoldi, T. Cranston, M. Vihinen, and R. F. Schumacher, Mutations in severe combined immune deficiency (scid) due to jak3 deficiency., *Hum Mutat*, vol. 18, no. 4, pp. 255–263, 2001 Oct.

53. F. Candotti, S. A. Oakes, J. A. Johnston, S. Giliani, R. F. Schumacher, P. Mella, M. Fiorini, A. G. Ugazio, R. Badolato, L. D. Notarangelo, F. Bozzi, P. Macchi, D. Strina, P. Vezzoni, R. M. Blaese, J. J. O'Shea, and A. Villa, Structural and functional basis for jak3-deficient severe combined immunodeficiency., *Blood*, vol. 90, no. 10, pp. 3996–4003, 1997 Nov 15.

54. J. L. Roberts, A. Lengi, S. M. Brown, M. Chen, Y.-J. Zhou, J. J. O'Shea, and R. H. Buckley, Janus kinase 3 (jak3) deficiency: clinical, immunologic, and molecular analyses of 10 patients and outcomes of stem cell transplantation., *Blood*, vol. 103, no. 6, pp. 2009–2018, 2004 Mar 15.

55. I. Firmbach-Kraft, M. Byers, T. Shows, R. Dalla-Favera, and J. J. Krolewski, tyk2, prototype of a novel class of non-receptor tyrosine kinase genes., *Oncogene*, vol. 5, no. 9, pp. 1329–1336, 1990 Sep.

56. J. J. Krolewski, R. Lee, R. Eddy, T. B. Shows, and R. Dalla-Favera, Identification and chromosomal mapping of new human tyrosine kinase genes., *Oncogene*, vol. 5, no. 3, pp. 277–282, 1990 Mar.

57. A. F. Wilks, Cloning members of protein-tyrosine kinase family using polymerase chain reaction., *Methods Enzymol*, vol. 200, pp. 533–546, 1991.

58. A. G. Harpur, A. C. Andres, A. Ziemiecki, R. R. Aston, and A. F. Wilks, Jak2, a third member of the jak family of protein tyrosine kinases., *Oncogene*, vol. 7, no. 7, pp. 1347–1353, 1992 Jul.

59. K. Yamaoka, P. Saharinen, M. Pesu, V. E. T. r. Holt, O. Silvennoinen, and J. J. O'Shea, The janus kinases (jaks)., *Genome Biol*, vol. 5, no. 12, p. 253, 2004.

60. M. Kawamura, D. W. McVicar, J. A. Johnston, T. B. Blake, Y. Q. Chen, B. K. Lal, A. R. Lloyd, D. J. Kelvin, J. E. Staples, and J. R. Ortaldo, Molecular cloning of l-jak, a janus family protein-tyrosine kinase expressed in natural killer cells and activated leukocytes., *Proc Natl Acad Sci U S A*, vol. 91, no. 14, pp. 6374–6378, 1994 Jul 5.

61. T. Musso, J. A. Johnston, D. Linnekin, L. Varesio, T. K. Rowe, J. J. O'Shea, and D. W. McVicar, Regulation of jak3 expression in human monocytes: phosphorylation in response to interleukins 2, 4, and 7., *J Exp Med*, vol. 181, no. 4, pp. 1425–1431, 1995 Apr 1.

62. C. B. Gurniak and L. J. Berg, Murine jak3 is preferentially expressed in hematopoietic tissues and lymphocyte precursor cells., *Blood*, vol. 87, no. 8, pp. 3151–3160, 1996 Apr 15.

63. M. C. Riedy, A. S. Dutra, T. B. Blake, W. Modi, B. K. Lal, J. Davis, A. Bosse, J. J. O'Shea, and J. A. Johnston, Genomic sequence, organization, and chromosomal localization of human jak3., *Genomics*, vol. 37, no. 1, pp. 57–61, 1996 Oct 1.

64. R. F. Schumacher, P. Mella, R. Badolato, M. Fiorini, G. Savoldi, S. Giliani, A. Villa, F. Candotti, A. Tampalini, J. J. O'Shea, and L. D. Notarangelo, Complete genomic organization of the human jak3 gene and mutation analysis in severe combined immunodeficiency by single-strand conformation polymorphism., *Hum Genet*, vol. 106, no. 1, pp. 73–79, 2000 Jan.

65. C. Janeway, *Immunobiology: the immune system in health and disease*. New York: Garland Science, 6th ed ed., 2005.

66. C. Dubey and M. Croft, Accessory molecule regulation of naive cd4 t cell activation., *Immunol Res*, vol. 15, no. 2, pp. 114–125, 1996.

67. S. Hugues, Dynamics of dendritic cell-t cell interactions: a role in t cell outcome., *Semin Immunopathol*, vol. 32, no. 3, pp. 227–238, 2010 Sep.

68. P. Pierre, S. J. Turley, E. Gatti, M. Hull, J. Meltzer, A. Mirza, K. Inaba, R. M. Steinman, and I. Mellman, Developmental regulation of mhc class ii transport in mouse dendritic cells., *Nature*, vol. 388, no. 6644, pp. 787–792, 1997 Aug 21.

69. M. Cella, A. Engering, V. Pinet, J. Pieters, and A. Lanzavecchia, Inflammatory stimuli induce accumulation of mhc class ii complexes on dendritic cells., *Nature*, vol. 388, no. 6644, pp. 782–787, 1997 Aug 21.

70. L. L. Lanier, S. O'Fallon, C. Somoza, J. H. Phillips, P. S. Linsley, K. Okumura, D. Ito, and M. Azuma, Cd80 (b7) and cd86 (b70) provide similar costimulatory signals for t cell proliferation, cytokine production, and generation of ctl., *J Immunol*, vol. 154, no. 1, pp. 97–105, 1995 Jan 1.

71. M. McHeyzer-Williams, S. Okitsu, N. Wang, and L. McHeyzer-Williams, Molecular programming of b cell memory., *Nat Rev Immunol*, vol. 12, no. 1, pp. 24–34, 2012 Jan.

72. http://www.blobs.org/science/article.php?article=12, 2011.

73. S. Gillis, M. M. Ferm, W. Ou, and K. A. Smith, T cell growth factor: parameters of production and a quantitative microassay for activity., *J Immunol*, vol. 120, no. 6, pp. 2027–2032, 1978 Jun.

74. P. E. Baker, S. Gillis, M. M. Ferm, and K. A. Smith, The effect of t cell growth factor on the generation of cytolytic t cells., *J Immunol*, vol. 121, no. 6, pp. 2168–2173, 1978 Dec.

75. H. Schorle, T. Holtschke, T. Hunig, A. Schimpl, and I. Horak, Development and function of t cells in mice rendered interleukin-2 deficient by gene targeting., *Nature*, vol. 352, no. 6336, pp. 621–624, 1991 Aug 15.

76. T. R. Malek, A. Yu, V. Vincek, P. Scibelli, and L. Kong, Cd4 regulatory t cells prevent lethal autoimmunity in il-2rbeta-deficient mice. implications for the nonredundant function of il-2., *Immunity*, vol. 17, no. 2, pp. 167–178, 2002 Aug.

77. W. Liao, D. E. Schones, J. Oh, Y. Cui, K. Cui, T.-Y. Roh, K. Zhao, and W. J. Leonard, Priming for t helper type 2 differentiation by interleukin 2-mediated induction of interleukin 4 receptor alpha-chain expression., *Nat Immunol*, vol. 9, no. 11, pp. 1288–1296, 2008 Nov.

78. J. Cote-Sierra, G. Foucras, L. Guo, L. Chiodetti, H. A. Young, J. Hu-Li, J. Zhu, and W. E. Paul, Interleukin 2 plays a central role in th2 differentiation., *Proc Natl Acad Sci U S A*, vol. 101, no. 11, pp. 3880–3885, 2004 Mar 16.

79. B. Sadlack, H. Merz, H. Schorle, A. Schimpl, A. C. Feller, and I. Horak, Ulcerative colitis-like disease in mice with a disrupted interleukin-2 gene., *Cell*, vol. 75, no. 2, pp. 253–261, 1993 Oct 22.

80. J. J. Peschon, P. J. Morrissey, K. H. Grabstein, F. J. Ramsdell, E. Maraskovsky, B. C. Gliniak, L. S. Park, S. F. Ziegler, D. E. Williams, C. B. Ware, J. D. Meyer, and B. L. Davison, Early lymphocyte expansion is severely impaired in interleukin 7 receptor-deficient mice., *J Exp Med*, vol. 180, no. 5, pp. 1955–1960, 1994 Nov 1.

81. S. Chappaz, L. Flueck, A. G. Farr, A. G. Rolink, and D. Finke, Increased tslp availability restores t- and b-cell compartments in adult il-7 deficient mice., *Blood*, vol. 110, no. 12, pp. 3862–3870, 2007 Dec 1.

82. H. Gascan, J. F. Gauchat, M. G. Roncarolo, H. Yssel, H. Spits, and J. E. de Vries, Human b cell clones can be induced to proliferate and to switch to ige and igg4 synthesis by interleukin 4 and a signal provided by activated cd4+ t cell clones., *J Exp Med*, vol. 173, no. 3, pp. 747–750, 1991 Mar 1.

83. R. Kuhn, K. Rajewsky, and W. Muller, Generation and analysis of interleukin-4 deficient mice., *Science*, vol. 254, no. 5032, pp. 707–710, 1991 Nov 1.

84. N. Noben-Trauth, L. D. Shultz, F. Brombacher, J. F. J. Urban, H. Gu, and W. E. Paul, An interleukin 4 (il-4)-independent pathway for cd4+ t cell il-4 production is revealed in il-4 receptor-deficient mice., *Proc Natl Acad Sci U S A*, vol. 94, no. 20, pp. 10838–10843, 1997 Sep 30.

85. K. Ozaki, R. Spolski, C. G. Feng, C.-F. Qi, J. Cheng, A. Sher, H. C. r. Morse, C. Liu, P. L. Schwartzberg, and W. J. Leonard, A critical role for il-21 in regulating immunoglobulin production., *Science*, vol. 298, no. 5598, pp. 1630–1634, 2002 Nov 22.

86. A. L. Wurster, V. L. Rodgers, A. R. Satoskar, M. J. Whitters, D. A. Young, M. Collins, and M. J. Grusby, Interleukin 21 is a t helper (th) cell 2 cytokine that specifically inhibits the differentiation of naive th cells into interferon gamma-producing th1 cells., *J Exp Med*, vol. 196, no. 7, pp. 969–977, 2002 Oct 7.

87. M. Strengell, T. Sareneva, D. Foster, I. Julkunen, and S. Matikainen, Il-21 up-regulates the expression of genes associated with innate immunity and th1 response., *J Immunol*, vol. 169, no. 7, pp. 3600–3605, 2002 Oct 1.

88. T. A. Waldmann, S. Dubois, and Y. Tagaya, Contrasting roles of il-2 and il-15 in the life and death of lymphocytes: implications for immunotherapy., *Immunity*, vol. 14, no. 2, pp. 105–110, 2001 Feb.

89. H. Suzuki, G. S. Duncan, H. Takimoto, and T. W. Mak, Abnormal development of intestinal intraepithelial lymphocytes and peripheral natural killer cells in mice lacking the il-2 receptor beta chain., *J Exp Med*, vol. 185, no. 3, pp. 499–505, 1997 Feb 3.

90. J. P. Lodolce, D. L. Boone, S. Chai, R. E. Swain, T. Dassopoulos, S. Trettin, and A. Ma, Il-15 receptor maintains lymphoid homeostasis by supporting lymphocyte homing and proliferation., *Immunity*, vol. 9, no. 5, pp. 669–676, 1998 Nov.

91. M. K. Kennedy, M. Glaccum, S. N. Brown, E. A. Butz, J. L. Viney, M. Embers, N. Matsuki, K. Charrier, L. Sedger, C. R. Willis, K. Brasel, P. J. Morrissey, K. Stocking, J. C. Schuh, S. Joyce, and J. J. Peschon, Reversible defects in natural killer and memory cd8 t cell lineages in interleukin 15-deficient mice., *J Exp Med*, vol. 191, no. 5, pp. 771–780, 2000 Mar 6.

92. Y. Rochman, R. Spolski, and W. J. Leonard, New insights into the regulation of t cells by gamma(c) family cytokines., *Nat Rev Immunol*, vol. 9, no. 7, pp. 480–490, 2009 Jul.

93. K. Teshigawara, H. M. Wang, K. Kato, and K. A. Smith, Interleukin 2 high-affinity receptor expression requires two distinct binding proteins., *J Exp Med*, vol. 165, no. 1, pp. 223–238, 1987 Jan 1.

94. X. Wang, M. Rickert, and K. C. Garcia, Structure of the quaternary complex of interleukin-2 with its alpha, beta, and gammac receptors., *Science*, vol. 310, no. 5751, pp. 1159–1163, 2005 Nov 18.

95. H. M. Wang and K. A. Smith, The interleukin 2 receptor. functional consequences of its bimolecular structure., *J Exp Med*, vol. 166, no. 4, pp. 1055–1069, 1987 Oct 1.

96. Y. Nakamura, S. M. Russell, S. A. Mess, M. Friedmann, M. Erdos, C. Francois, Y. Jacques, S. Adelstein, and W. J. Leonard, Heterodimerization of the il-2 receptor beta- and gamma-chain cytoplasmic domains is required for signalling., *Nature*, vol. 369, no. 6478, pp. 330–333, 1994 May 26.

97. M. C. Friedmann, T. S. Migone, S. M. Russell, and W. J. Leonard, Different interleukin 2 receptor beta-chain tyrosines couple to at least two signaling pathways and synergistically mediate interleukin 2-induced proliferation., *Proc Natl Acad Sci U S A*, vol. 93, no. 5, pp. 2077–2082, 1996 Mar 5.

98. K. Nelms, A. D. Keegan, J. Zamorano, J. J. Ryan, and W. E. Paul, The il-4 receptor: signaling mechanisms and biologic functions., *Annu Rev Immunol*, vol. 17, pp. 701–738, 1999.

99. R. Hofmeister, A. R. Khaled, N. Benbernou, E. Rajnavolgyi, K. Muegge, and S. K. Durum, Interleukin-7: physiological roles and mechanisms of action., *Cytokine Growth Factor Rev*, vol. 10, no. 1, pp. 41–60, 1999 Mar.

100. K. Imada and W. J. Leonard, The jak-stat pathway., *Mol Immunol*, vol. 37, no. 1-2, pp. 1–11, 2000 Jan-Feb.

101. W. J. Leonard, Role of jak kinases and stats in cytokine signal transduction., *Int J Hematol*, vol. 73, no. 3, pp. 271–277, 2001 Apr.

102. D. C. van Gent, J. H. Hoeijmakers, and R. Kanaar, Chromosomal stability and the dna double-stranded break connection., *Nat Rev Genet*, vol. 2, no. 3, pp. 196–206, 2001 Mar.

103. B. Corneo, D. Moshous, T. Gungor, N. Wulffraat, P. Philippet, F. L. Le Deist, A. Fischer, and J. P. de Villartay, Identical mutations in rag1 or rag2 genes leading to defective v(d)j recombinase activity can cause either t-b-severe combined immune deficiency or omenn syndrome., *Blood*, vol. 97, no. 9, pp. 2772–2776, 2001 May 1.

104. D. G. Schatz and Y. Ji, Recombination centres and the orchestration of v(d)j recombination., *Nat Rev Immunol*, vol. 11, no. 4, pp. 251–263, 2011 Apr.

105. D. G. Schatz, M. A. Oettinger, and D. Baltimore, The v(d)j recombination activating gene, rag-1., *Cell*, vol. 59, no. 6, pp. 1035–1048, 1989 Dec 22.

106. M. A. Oettinger, B. Stanger, D. G. Schatz, T. Glaser, K. Call, D. Housman, and D. Baltimore, The recombination activating genes, rag 1 and rag 2, are on chromosome 11p in humans and chromosome 2p in mice., *Immunogenetics*, vol. 35, no. 2, pp. 97–101, 1992.

107. M. A. Oettinger, D. G. Schatz, C. Gorka, and D. Baltimore, Rag-1 and rag-2, adjacent genes that synergistically activate v(d)j recombination., *Science*, vol. 248, no. 4962, pp. 1517–1523, 1990 Jun 22.

108. G. C. Bosma, R. P. Custer, and M. J. Bosma, A severe combined immunodeficiency mutation in the mouse., *Nature*, vol. 301, no. 5900, pp. 527–530, 1983 Feb 10.

109. D. E. Mosier, R. J. Gulizia, S. M. Baird, and D. B. Wilson, Transfer of a functional human immune system to mice with severe combined immunodeficiency., *Nature*, vol. 335, no. 6187, pp. 256–259, 1988 Sep 15.

110. J. M. McCune, R. Namikawa, H. Kaneshima, L. D. Shultz, M. Lieberman, and I. L. Weissman, The scid-hu mouse: murine model for the analysis of human hematolymphoid differentiation and function., *Science*, vol. 241, no. 4873, pp. 1632–1639, 1988 Sep 23.

111. T. Lapidot, F. Pflumio, M. Doedens, B. Murdoch, D. E. Williams, and J. E. Dick, Cytokine stimulation of multilineage hematopoiesis from immature human cells engrafted in scid mice., *Science*, vol. 255, no. 5048, pp. 1137–1141, 1992 Feb 28.

112. R. M. Hesselton, D. L. Greiner, J. P. Mordes, T. V. Rajan, J. L. Sullivan, and L. D. Shultz, High levels of human peripheral blood mononuclear cell engraftment and enhanced susceptibility to human immunodeficiency virus type 1 infection in nod/ltsz-scid/scid mice., *J Infect Dis*, vol. 172, no. 4, pp. 974–982, 1995 Oct.

113. K. A. Biedermann, J. R. Sun, A. J. Giaccia, L. M. Tosto, and J. M. Brown, scid mutation in mice confers hypersensitivity to ionizing radiation and a deficiency in dna double-strand break repair., *Proc Natl Acad Sci U S A*, vol. 88, no. 4, pp. 1394–1397, 1991 Feb 15.

114. L. D. Shultz, P. A. Lang, S. W. Christianson, B. Gott, B. Lyons, S. Umeda, E. Leiter, R. Hesselton, E. J. Wagar, J. H. Leif, O. Kollet, T. Lapidot, and D. L. Greiner, Nod/ltsz-rag1null mice: an immunodeficient and radioresistant model for engraftment of human hematolymphoid cells, hiv infection, and adoptive transfer of nod mouse diabetogenic t cells., *J Immunol*, vol. 164, no. 5, pp. 2496–2507, 2000 Mar 1.

115. L. D. Shultz, S. Banuelos, B. Lyons, R. Samuels, L. Burzenski, B. Gott, P. Lang, J. Leif, M. Appel, A. Rossini, and D. L. Greiner, Nod/ltsz-rag1nullpfpnull mice: a new model system with increased levels of human peripheral leukocyte and hematopoietic stem-cell engraftment., *Transplantation*, vol. 76, no. 7, pp. 1036–1042, 2003 Oct 15.

116. S. W. Christianson, D. L. Greiner, R. A. Hesselton, J. H. Leif, E. J. Wagar, I. B. Schweitzer, T. V. Rajan, B. Gott, D. C. Roopenian, and L. D. Shultz, Enhanced human cd4+ t cell engraftment in beta2-microglobulin-deficient nod-scid mice., *J Immunol*, vol. 158, no. 8, pp. 3578–3586, 1997 Apr 15.

117. M. Ito, H. Hiramatsu, K. Kobayashi, K. Suzue, M. Kawahata, K. Hioki, Y. Ueyama, Y. Koyanagi, K. Sugamura, K. Tsuji, T. Heike, and T. Nakahata, Nod/scid/gamma(c)(null) mouse: an excellent recipient mouse model for engraftment of human cells., *Blood*, vol. 100, no. 9, pp. 3175–3182, 2002 Nov 1.

118. E. Traggiai, L. Chicha, L. Mazzucchelli, L. Bronz, J.-C. Piffaretti, A. Lanzavecchia, and M. G. Manz, Development of a human adaptive immune system in cord blood cell-transplanted mice., *Science*, vol. 304, no. 5667, pp. 104–107, 2004 Apr 2.

119. T. Yahata, K. Ando, T. Sato, H. Miyatake, Y. Nakamura, Y. Muguruma, S. Kato, and T. Hotta, A highly sensitive strategy for scid-repopulating cell assay by direct injection of primitive human hematopoietic cells into nod/scid mice bone marrow., *Blood*, vol. 101, no. 8, pp. 2905–2913, 2003 Apr 15.

120. B. Aigner, S. Renner, B. Kessler, N. Klymiuk, M. Kurome, A. Wunsch, and E. Wolf, Transgenic pigs as models for translational biomedical research., *J Mol Med (Berl)*, vol. 88, no. 7, pp. 653–664, 2010 Jul.

121. N. Verma, A. W. Rettenmeier, and S. Schmitz-Spanke, Recent advances in the use of sus scrofa (pig) as a model system for proteomic studies., *Proteomics*, vol. 11, no. 4, pp. 776–793, 2011 Feb.

122. K. N. J Weiss, J Maeß, *Haus- und Versuchstierpflege*. Stuttgart: Enke Verlag, 2nd ed., 2008.

123. D. L. Butler, S. A. Goldstein, R. E. Guldberg, X. E. Guo, R. Kamm, C. T. Laurencin, L. V. McIntire, V. C. Mow, R. M. Nerem, R. L. Sah, L. J. Soslowsky, R. L. Spilker, and R. T. Tranquillo, The impact of biomechanics in tissue engineering and regenerative medicine., *Tissue Eng Part B Rev*, vol. 15, no. 4, pp. 477–484, 2009 Dec.

124. J. R. Turk and M. H. Laughlin, Physical activity and atherosclerosis: which animal model?, *Can J Appl Physiol*, vol. 29, no. 5, pp. 657–683, 2004 Oct.

125. J. F. Granada, G. L. Kaluza, R. L. Wilensky, B. C. Biedermann, R. S. Schwartz, and E. Falk, Porcine models of coronary atherosclerosis and vulnerable plaque for imaging and interventional research., *EuroIntervention*, vol. 5, no. 1, pp. 140–148, 2009 May.

126. C. J. Phelps, C. Koike, T. D. Vaught, J. Boone, K. D. Wells, S.-H. Chen, S. Ball, S. M. Specht, I. A. Polejaeva, J. A. Monahan, P. M. Jobst, S. B. Sharma, A. E. Lamborn, A. S. Garst, M. Moore, A. J. Demetris, W. A. Rudert, R. Bottino, S. Bertera, M. Trucco, T. E. Starzl, Y. Dai, and D. L. Ayares, Production of alpha 1,3-galactosyltransferase-deficient pigs., *Science*, vol. 299, no. 5605, pp. 411–414, 2003 Jan 17.

127. C. Denning, P. Dickinson, S. Burl, D. Wylie, J. Fletcher, and A. J. Clark, Gene targeting in primary fetal fibroblasts from sheep and pig., *Cloning Stem Cells*, vol. 3, no. 4, pp. 221–231, 2001.

128. R. Jaenisch and B. Mintz, Simian virus 40 dna sequences in dna of healthy adult mice derived from preimplantation blastocysts injected with viral dna., *Proc Natl Acad Sci U S A*, vol. 71, no. 4, pp. 1250–1254, 1974 Apr.

129. M. Lavitrano, A. Camaioni, V. M. Fazio, S. Dolci, M. G. Farace, and C. Spadafora, Sperm cells as vectors for introducing foreign dna into eggs: genetic transformation of mice., *Cell*, vol. 57, no. 5, pp. 717–723, 1989 Jun 2.

130. E. F. Wagner, T. A. Stewart, and B. Mintz, The human beta-globin gene and a functional viral thymidine kinase gene in developing mice., *Proc Natl Acad Sci U S A*, vol. 78, no. 8, pp. 5016–5020, 1981 Aug.

131. R. E. Hammer, V. G. Pursel, C. E. J. Rexroad, R. J. Wall, D. J. Bolt, K. M. Ebert, R. D. Palmiter, and R. L. Brinster, Production of transgenic rabbits, sheep and pigs by microinjection., *Nature*, vol. 315, no. 6021, pp. 680–683, 1985 Jun 20-26.

132. A. Hofmann, B. Kessler, S. Ewerling, M. Weppert, B. Vogg, H. Ludwig, M. Stojkovic, M. Boelhauve, G. Brem, E. Wolf, and A. Pfeifer, Efficient transgenesis in farm animals by lentiviral vectors., *EMBO Rep*, vol. 4, no. 11, pp. 1054–1060, 2003 Nov.

133. A. J. Clark, P. Bissinger, D. W. Bullock, S. Damak, R. Wallace, C. B. Whitelaw, and F. Yull, Chromosomal position effects and the modulation of transgene expression., *Reprod Fertil Dev*, vol. 6, no. 5, pp. 589–598, 1994.

134. O. Smithies, R. G. Gregg, S. S. Boggs, M. A. Koralewski, and R. S. Kucherlapati, Insertion of dna sequences into the human chromosomal beta-globin locus by homologous recombination., *Nature*, vol. 317, no. 6034, pp. 230–234, 1985 Sep 19-25.

135. J. A. Piedrahita, S. H. Zhang, J. R. Hagaman, P. M. Oliver, and N. Maeda, Generation of mice carrying a mutant apolipoprotein e gene inactivated by gene targeting in embryonic stem cells., *Proc Natl Acad Sci U S A*, vol. 89, no. 10, pp. 4471–4475, 1992 May 15.

136. C. Denning and H. Priddle, New frontiers in gene targeting and cloning: success, application and challenges in domestic animals and human embryonic stem cells., *Reproduction*, vol. 126, no. 1, pp. 1–11, 2003 Jul.

137. J. A. Thomson, J. Itskovitz-Eldor, S. S. Shapiro, M. A. Waknitz, J. J. Swiergiel, V. S. Marshall, and J. M. Jones, Embryonic stem cell lines derived from human blastocysts., *Science*, vol. 282, no. 5391, pp. 1145–1147, 1998 Nov 6.

138. S. Ueda, M. Kawamata, T. Teratani, T. Shimizu, Y. Tamai, H. Ogawa, K. Hayashi, H. Tsuda, and T. Ochiya, Establishment of rat embryonic stem cells and making of chimera rats., *PLoS One*, vol. 3, no. 7, p. e2800, 2008.

139. Z. F. Fang, H. Gai, Y. Z. Huang, S. G. Li, X. J. Chen, J. J. Shi, L. Wu, A. Liu, P. Xu, and H. Z. Sheng, Rabbit embryonic stem cell lines derived from fertilized, parthenogenetic or somatic cell nuclear transfer embryos., *Exp Cell Res*, vol. 312, no. 18, pp. 3669–3682, 2006 Nov 1.

140. A. Honda, M. Hirose, K. Inoue, N. Ogonuki, H. Miki, N. Shimozawa, M. Hatori, N. Shimizu, T. Murata, M. Hirose, K. Katayama, N. Wakisaka, H. Miyoshi, K. K. Yokoyama, T. Sankai, and A. Ogura, Stable embryonic stem cell lines in rabbits: potential small animal models for human research., *Reprod Biomed Online*, vol. 17, no. 5, pp. 706–715, 2008 Nov.

141. E. Behboodi, A. Bondareva, I. Begin, K. Rao, N. Neveu, J. T. Pierson, C. Wylie, F. D. Piero, Y. J. Huang, W. Zeng, V. Tanco, H. Baldassarre, C. N. Karatzas, and I. Dobrinski, Establishment of goat embryonic stem cells from in vivo produced blastocyst-stage embryos., *Mol Reprod Dev*, vol. 78, no. 3, pp. 202–211, 2011 Mar.

142. J. A. Thomson, J. Kalishman, T. G. Golos, M. Durning, C. P. Harris, R. A. Becker, and J. P. Hearn, Isolation of a primate embryonic stem cell line., *Proc Natl Acad Sci U S A*, vol. 92, no. 17, pp. 7844–7848, 1995 Aug 15.

143. J. A. Thomson, V. S. Marshall, and J. Q. Trojanowski, Neural differentiation of rhesus embryonic stem cells., *APMIS*, vol. 106, no. 1, pp. 149–156, 1998 Jan.

144. K. H. Campbell, P. Loi, P. J. Otaegui, and I. Wilmut, Cell cycle co-ordination in embryo cloning by nuclear transfer., *Rev Reprod*, vol. 1, no. 1, pp. 40–46, 1996 Jan.

145. S. M. Willadsen, Nuclear transplantation in sheep embryos., *Nature*, vol. 320, no. 6057, pp. 63–65, 1986 Mar 6-12.

146. R. S. Prather and N. L. First, Developmental fate in chimeras derived from highly asynchronous murine blastomeres., *J Exp Zool*, vol. 242, no. 1, pp. 27–33, 1987 Apr.

147. I. Wilmut, A. E. Schnieke, J. McWhir, A. J. Kind, and K. H. Campbell, Viable offspring derived from fetal and adult mammalian cells., *Nature*, vol. 385, no. 6619, pp. 810–813, 1997 Feb 27.

148. K. J. McCreath, J. Howcroft, K. H. Campbell, A. Colman, A. E. Schnieke, and A. J. Kind, Production of gene-targeted sheep by nuclear transfer from cultured somatic cells., *Nature*, vol. 405, no. 6790, pp. 1066–1069, 2000 Jun 29.

149. T. Wakayama, A. C. Perry, M. Zuccotti, K. R. Johnson, and R. Yanagimachi, Full-term development of mice from enucleated oocytes injected with cumulus cell nuclei., *Nature*, vol. 394, no. 6691, pp. 369–374, 1998 Jul 23.

150. K. Shiga, T. Fujita, K. Hirose, Y. Sasae, and T. Nagai, Production of calves by transfer of nuclei from cultured somatic cells obtained from japanese black bulls., *Theriogenology*, vol. 52, no. 3, pp. 527–535, 1999 Aug.

151. K. H. Campbell, J. McWhir, W. A. Ritchie, and I. Wilmut, Sheep cloned by nuclear transfer from a cultured cell line., *Nature*, vol. 380, no. 6569, pp. 64–66, 1996 Mar 7.

152. D. N. Wells, P. M. Misica, A. M. Day, A. J. Peterson, and H. R. Tervit, Cloning sheep from cultured embryonic cells., *Reprod Fertil Dev*, vol. 10, no. 7-8, pp. 615–626, 1998.

153. Y. Dai, T. D. Vaught, J. Boone, S.-H. Chen, C. J. Phelps, S. Ball, J. A. Monahan, P. M. Jobst, K. J. McCreath, A. E. Lamborn, J. L. Cowell-Lucero, K. D. Wells, A. Colman, I. A. Polejaeva, and D. L. Ayares, Targeted disruption of the alpha1,3-galactosyltransferase gene in cloned pigs., *Nat Biotechnol*, vol. 20, no. 3, pp. 251–255, 2002 Mar.

154. A. Baguisi, E. Behboodi, D. T. Melican, J. S. Pollock, M. M. Destrempes, C. Cammuso, J. L. Williams, S. D. Nims, C. A. Porter, P. Midura, M. J. Palacios, S. L. Ayres, R. S. Denniston, M. L. Hayes, C. A. Ziomek, H. M. Meade, R. A. Godke, W. G. Gavin, E. W. Overstrom, and Y. Echelard, Production of goats by somatic cell nuclear transfer., *Nat Biotechnol*, vol. 17, no. 5, pp. 456–461, 1999 May.

155. J. Schenkel, *Transgene Tiere*. Spektrum Akademischer Verlag, 2nd ed., 2006.

156. A. J. Clark, S. Burl, C. Denning, and P. Dickinson, Gene targeting in livestock: a preview., *Transgenic Res*, vol. 9, no. 4-5, pp. 263–275, 2000.

157. G. A. McFarland and R. Holliday, Further evidence for the rejuvenating effects of the dipeptide l-carnosine on cultured human diploid fibroblasts., *Exp Gerontol*, vol. 34, no. 1, pp. 35–45, 1999 Jan.

158. S. J. Harrison, A. Guidolin, R. Faast, L. A. Crocker, C. Giannakis, A. J. F. D'Apice, M. B. Nottle, and I. Lyons, Efficient generation of alpha(1,3) galactosyltransferase knockout porcine fetal fibroblasts for nuclear transfer., *Transgenic Res*, vol. 11, no. 2, pp. 143–150, 2002 Apr.

159. I. Wilmut, N. Beaujean, P. A. de Sousa, A. Dinnyes, T. J. King, L. A. Paterson, D. N. Wells, and L. E. Young, Somatic cell nuclear transfer., *Nature*, vol. 419, no. 6907, pp. 583–586, 2002 Oct 10.

160. P. Hasty, J. Rivera-Perez, C. Chang, and A. Bradley, Target frequency and integration pattern for insertion and replacement vectors in embryonic stem cells., *Mol Cell Biol*, vol. 11, no. 9, pp. 4509–4517, 1991 Sep.

161. S. L. Mansour, K. R. Thomas, and M. R. Capecchi, Disruption of the proto-oncogene int-2 in mouse embryo-derived stem cells: a general strategy for targeting mutations to non-selectable genes., *Nature*, vol. 336, no. 6197, pp. 348–352, 1988 Nov 24.

162. T. Yagi, S. Nada, N. Watanabe, H. Tamemoto, N. Kohmura, Y. Ikawa, and S. Aizawa, A novel negative selection for homologous recombinants using diphtheria toxin a fragment gene., *Anal Biochem*, vol. 214, no. 1, pp. 77–86, 1993 Oct.

163. K. D. Hanson and J. M. Sedivy, Analysis of biological selections for high-efficiency gene targeting., *Mol Cell Biol*, vol. 15, no. 1, pp. 45–51, 1995 Jan.

164. G. Laible and L. Alonso-Gonzalez, Gene targeting from laboratory to livestock: current status and emerging concepts., *Biotechnol J*, vol. 4, no. 9, pp. 1278–1292, 2009 Sep.

165. K. R. Thomas, C. Deng, and M. R. Capecchi, High-fidelity gene targeting in embryonic stem cells by using sequence replacement vectors., *Mol Cell Biol*, vol. 12, no. 7, pp. 2919–2923, 1992 Jul.

166. C. Deng and M. R. Capecchi, Reexamination of gene targeting frequency as a function of the extent of homology between the targeting vector and the target locus., *Mol Cell Biol*, vol. 12, no. 8, pp. 3365–3371, 1992 Aug.

167. B. Mir and J. A. Piedrahita, Nuclear localization signal and cell synchrony enhance gene targeting efficiency in primary fetal fibroblasts., *Nucleic Acids Res*, vol. 32, no. 3, p. e25, 2004.

168. M. H. Porteus and D. Carroll, Gene targeting using zinc finger nucleases., *Nat Biotechnol*, vol. 23, no. 8, pp. 967–973, 2005 Aug.

169. J. Wu, K. Kandavelou, and S. Chandrasegaran, Custom-designed zinc finger nucleases: what is next?, *Cell Mol Life Sci*, vol. 64, no. 22, pp. 2933–2944, 2007 Nov.

170. A. M. Geurts, G. J. Cost, Y. Freyvert, B. Zeitler, J. C. Miller, V. M. Choi, S. S. Jenkins, A. Wood, X. Cui, X. Meng, A. Vincent, S. Lam, M. Michalkiewicz, R. Schilling, J. Foeckler, S. Kalloway, H. Weiler, S. Menoret, I. Anegon, G. D. Davis, L. Zhang, E. J. Rebar, P. D. Gregory, F. D. Urnov, H. J. Jacob, and R. Buelow, Knockout rats via embryo microinjection of zinc-finger nucleases., *Science*, vol. 325, no. 5939, p. 433, 2009 Jul 24.

171. T. Flisikowska, I. S. Thorey, S. Offner, F. Ros, V. Lifke, B. Zeitler, O. Rottmann, A. Vincent, L. Zhang, S. Jenkins, H. Niersbach, A. J. Kind, P. D. Gregory, A. E. Schnieke, and J. Platzer, Efficient immunoglobulin gene disruption and targeted replacement in rabbit using zinc finger nucleases., *PLoS One*, vol. 6, no. 6, p. e21045, 2011.

172. J. Hauschild, B. Petersen, Y. Santiago, A.-L. Queisser, J. W. Carnwath, A. Lucas-Hahn, L. Zhang, X. Meng, P. D. Gregory, R. Schwinzer, G. J. Cost, and H. Niemann, Efficient generation of a biallelic knockout in pigs using zinc-finger nucleases., *Proc Natl Acad Sci U S A*, vol. 108, no. 29, pp. 12013–12017, 2011 Jul 19.

173. Y. Doyon, J. M. McCammon, J. C. Miller, F. Faraji, C. Ngo, G. E. Katibah, R. Amora, T. D. Hocking, L. Zhang, E. J. Rebar, P. D. Gregory, F. D. Urnov, and S. L. Amacher, Heritable targeted gene disruption in zebrafish using designed zinc-finger nucleases., *Nat Biotechnol*, vol. 26, no. 6, pp. 702–708, 2008 Jun.

174. N. G. Copeland, N. A. Jenkins, and D. L. Court, Recombineering: a powerful new tool for mouse functional genomics., *Nat Rev Genet*, vol. 2, no. 10, pp. 769–779, 2001 Oct.

175. D. Yu, H. M. Ellis, E. C. Lee, N. A. Jenkins, N. G. Copeland, and D. L. Court, An efficient recombination system for chromosome engineering in escherichia coli., *Proc Natl Acad Sci U S A*, vol. 97, no. 11, pp. 5978–5983, 2000 May 23.

176. E. C. Lee, D. Yu, J. Martinez de Velasco, L. Tessarollo, D. A. Swing, D. L. Court, N. A. Jenkins, and N. G. Copeland, A highly efficient escherichia coli-based chromosome engineering system adapted for recombinogenic targeting and subcloning of bac dna., *Genomics*, vol. 73, no. 1, pp. 56–65, 2001 Apr 1.

177. P. Liu, N. A. Jenkins, and N. G. Copeland, A highly efficient recombineering-based method for generating conditional knockout mutations., *Genome Res*, vol. 13, no. 3, pp. 476–484, 2003 Mar.

178. T. Masek, V. Vopalensky, P. Suchomelova, and M. Pospisek, Denaturing rna electrophoresis in tae agarose gels., *Anal Biochem*, vol. 336, no. 1, pp. 46–50, 2005 Jan 1.

179. H. Niwa, K. Yamamura, and J. Miyazaki, Efficient selection for high-expression transfectants with a novel eukaryotic vector., *Gene*, vol. 108, no. 2, pp. 193–199, 1991 Dec 15.

180. M. Dominici, K. Le Blanc, I. Mueller, I. Slaper-Cortenbach, F. Marini, D. Krause, R. Deans, A. Keating, D. Prockop, and E. Horwitz, Minimal criteria for defining multipotent mesenchymal stromal cells. the international society for cellular therapy position statement., *Cytotherapy*, vol. 8, no. 4, pp. 315–317, 2006.

181. P. Bosch, S. L. Pratt, and S. L. Stice, Isolation, characterization, gene modification, and nuclear reprogramming of porcine mesenchymal stem cells., *Biol Reprod*, vol. 74, no. 1, pp. 46–57, 2006 Jan.

182. K. Bieback, S. Kern, H. Kluter, and H. Eichler, Critical parameters for the isolation of mesenchymal stem cells from umbilical cord blood., *Stem Cells*, vol. 22, no. 4, pp. 625–634, 2004.

183. C. De Bari, F. Dell'Accio, J. Vanlauwe, J. Eyckmans, I. M. Khan, C. W. Archer, E. A. Jones, D. McGonagle, T. A. Mitsiadis, C. Pitzalis, and F. P. Luyten, Mesenchymal multipotency of adult human periosteal cells demonstrated by single-cell lineage analysis., *Arthritis Rheum*, vol. 54, no. 4, pp. 1209–1221, 2006 Apr.

184. K. M. Vasquez, K. Marburger, Z. Intody, and J. H. Wilson, Manipulating the mammalian genome by homologous recombination., *Proc Natl Acad Sci U S A*, vol. 98, no. 15, pp. 8403–8410, 2001 Jul 17.

185. M. U. Fareed and F. L. Moolten, Suicide gene transduction sensitizes murine embryonic and human mesenchymal stem cells to ablation on demand– a fail-safe protection against cellular misbehavior., *Gene Ther*, vol. 9, no. 14, pp. 955–962, 2002 Jul.

186. C. Doucet, J. Giron-Michel, G. W. Canonica, and B. Azzarone, Human lung myofibroblasts as effectors of the inflammatory process: the common receptor gamma chain is induced by th2 cytokines, and cd40 ligand is induced by lipopolysaccharide, thrombin and tnf-alpha., *Eur J Immunol*, vol. 32, no. 9, pp. 2437–2449, 2002 Sep.

187. J. Schmidt, Targeting porcine interleukin-2 receptor gamma and janus kinase 3: production via recombineering, Master's thesis, Technische Universität München, 2008.

188. Y. Yang and B. Seed, Site-specific gene targeting in mouse embryonic stem cells with intact bacterial artificial chromosomes., *Nat Biotechnol*, vol. 21, no. 4, pp. 447–451, 2003 Apr.

189. K. M. Reindl, Immunodeficient pigs: cloning of a pcr control vector and shortening of a targeting vector, Master's thesis, Technische Universität München, 2010.

190. Y. H. Kim, J.-I. Chung, H. G. Woo, Y.-S. Jung, S. H. Lee, C.-H. Moon, H. Suh-Kim, and E. J. Baik, Differential regulation of proliferation and differentiation in neural precursor cells by the jak pathway., *Stem Cells*, vol. 28, no. 10, pp. 1816–1828, 2010 Oct.

191. J. W. Verbsky, E. A. Bach, Y. F. Fang, L. Yang, D. A. Randolph, and L. E. Fields, Expression of janus kinase 3 in human endothelial and other non-lymphoid and non-myeloid cells., *J Biol Chem*, vol. 271, no. 24, pp. 13976–13980, 1996 Jun 14.

192. G.-S. Wang, G.-S. Qian, D.-S. Zhou, and J.-Q. Zhao, Jak-stat signaling pathway in pulmonary arterial smooth muscle cells is activated by hypoxia., *Cell Biol Int*, vol. 29, no. 7, pp. 598–603, 2005 Jul.

193. K. S. Lai, Y. Jin, D. K. Graham, B. A. Witthuhn, J. N. Ihle, and E. T. Liu, A kinase-deficient splice variant of the human jak3 is expressed in hematopoietic and epithelial cancer cells., *J Biol Chem*, vol. 270, no. 42, pp. 25028–25036, 1995 Oct 20.

194. M. A. A. Al-Rawi, K. Rmali, G. Watkins, R. E. Mansel, and W. G. Jiang, Aberrant expression of interleukin-7 (il-7) and its signalling complex in human breast cancer., *Eur J Cancer*, vol. 40, no. 4, pp. 494–502, 2004 Mar.

195. X. Cao, E. W. Shores, J. Hu-Li, M. R. Anver, B. L. Kelsall, S. M. Russell, J. Drago, M. Noguchi, A. Grinberg, and E. T. Bloom, Defective lymphoid development in mice lacking expression of the common cytokine receptor gamma chain., *Immunity*, vol. 2, no. 3, pp. 223–238, 1995 Mar.

196. D. C. Thomis, C. B. Gurniak, E. Tivol, A. H. Sharpe, and L. J. Berg, Defects in b lymphocyte maturation and t lymphocyte activation in mice lacking jak3., *Science*, vol. 270, no. 5237, pp. 794–797, 1995 Nov 3.

197. P. E. Kovanen and W. J. Leonard, Cytokines and immunodeficiency diseases: critical roles of the gamma(c)-dependent cytokines interleukins 2, 4, 7, 9, 15, and 21, and their signaling pathways., *Immunol Rev*, vol. 202, pp. 67–83, 2004 Dec.

198. J. B. Gurdon and I. Wilmut, Nuclear transfer to eggs and oocytes., *Cold Spring Harb Perspect Biol*, vol. 3, no. 6, 2011.

199. Y. Kato, T. Tani, Y. Sotomaru, K. Kurokawa, J. Kato, H. Doguchi, H. Yasue, and Y. Tsunoda, Eight calves cloned from somatic cells of a single adult., *Science*, vol. 282, no. 5396, pp. 2095–2098, 1998 Dec 11.

200. A. Onishi, M. Iwamoto, T. Akita, S. Mikawa, K. Takeda, T. Awata, H. Hanada, and A. C. Perry, Pig cloning by microinjection of fetal fibroblast nuclei., *Science*, vol. 289, no. 5482, pp. 1188–1190, 2000 Aug 18.

201. H. T. Cheong, Y. Takahashi, and H. Kanagawa, Birth of mice after transplantation of early cell-cycle-stage embryonic nuclei into enucleated oocytes., *Biol Reprod*, vol. 48, no. 5, pp. 958–963, 1993 May.

202. A. Bortvin, K. Eggan, H. Skaletsky, H. Akutsu, D. L. Berry, R. Yanagimachi, D. C. Page, and R. Jaenisch, Incomplete reactivation of oct4-related genes in mouse embryos cloned from somatic nuclei., *Development*, vol. 130, no. 8, pp. 1673–1680, 2003 Apr.

203. T. Hiiragi and D. Solter, Reprogramming is essential in nuclear transfer., *Mol Reprod Dev*, vol. 70, no. 4, pp. 417–421, 2005 Apr.

204. J. Ramsoondar, M. Mendicino, C. Phelps, T. Vaught, S. Ball, J. Monahan, S. Chen, A. Dandro, J. Boone, P. Jobst, A. Vance, N. Wertz, I. Polejaeva, J. Butler, Y. Dai, D. Ayares, and K. Wells, Targeted disruption of the porcine immunoglobulin kappa light chain locus., *Transgenic Res*, vol. 20, no. 3, pp. 643–653, 2011 Jun.

205. R. Hickey, J. Lillegard, J. Fisher, T. McKenzie, S. Hofherr, M. Finegold, S. Nyberg, and M. Grompe, Efficient production of fah-null heterozygote pigs by chimeric adeno-associated virus-mediated gene knockout and somatic cell nuclear transfer., *Hepatology*, 2011 Jun 14.

206. I. A. Polejaeva, S. H. Chen, T. D. Vaught, R. L. Page, J. Mullins, S. Ball, Y. Dai, J. Boone, S. Walker, D. L. Ayares, A. Colman, and K. H. Campbell, Cloned pigs produced by nuclear transfer from adult somatic cells., *Nature*, vol. 407, no. 6800, pp. 86–90, 2000 Sep 7.

207. M. Kurome, R. Tomii, S. Ueno, K. Hiruma, S. Matsumoto, K. Okumura, K. Nakamura, M. Matsumoto, Y. Kaji, F. Endo, and H. Nagashima, Production of cloned pigs from salivary gland-derived progenitor cells., *Cloning Stem Cells*, vol. 10, no. 2, pp. 277–286, 2008 Jun.

208. N. Klymiuk, L. Mundhenk, K. Kraehe, A. Wuensch, S. Plog, D. Emrich, M. Langenmayer, M. Stehr, A. Holzinger, C. Kroner, A. Richter, B. Kessler, M. Kurome, M. Eddicks, H. Nagashima, K. Heinritzi, A. Gruber, and E. Wolf, Sequential targeting of cftr by bac vectors generates a novel pig model of cystic fibrosis., *J Mol Med (Berl)*, 2011 Dec 15.

209. B. M. Kumar, H.-F. Jin, J.-G. Kim, S.-A. Ock, Y. Hong, S. Balasubramanian, S.-Y. Choe, and G.-J. Rho, Differential gene expression patterns in porcine nuclear transfer embryos reconstructed with fetal fibroblasts and mesenchymal stem cells., *Dev Dyn*, vol. 236, no. 2, pp. 435–446, 2007 Feb.

210. R. Faast, S. J. Harrison, L. F. S. Beebe, S. M. McIlfatrick, R. J. Ashman, and M. B. Nottle, Use of adult mesenchymal stem cells isolated from bone marrow and blood for somatic cell nuclear transfer in pigs., *Cloning Stem Cells*, vol. 8, no. 3, pp. 166–173, 2006 Fall.

211. F. Moussavi-Harami, Y. Duwayri, J. A. Martin, F. Moussavi-Harami, and J. A. Buckwalter, Oxygen effects on senescence in chondrocytes and mesenchymal stem cells: consequences for tissue engineering., *Iowa Orthop J*, vol. 24, pp. 15–20, 2004.

212. M. Zscharnack, C. Poesel, J. Galle, and A. Bader, Low oxygen expansion improves subsequent chondrogenesis of ovine bone-marrow-derived mesenchymal stem cells in collagen type i hydrogel., *Cells Tissues Organs*, 2008 Nov 25.

213. L. L. Wei, K. Gao, P. Q. Liu, X. F. Lu, S. F. Li, J. Q. Cheng, Y. P. Li, and Y. R. Lu, Mesenchymal stem cells from chinese guizhou minipig by htert gene transfection., *Transplant Proc*, vol. 40, no. 2, pp. 547–550, 2008 Mar.

214. M. Kobune, Y. Kawano, Y. Ito, H. Chiba, K. Nakamura, H. Tsuda, K. Sasaki, H. Dehari, H. Uchida, O. Honmou, S. Takahashi, A. Bizen, R. Takimoto, T. Matsunaga, J. Kato, K. Kato, K. Houkin, Y. Niitsu, and H. Hamada, Telomerized human multipotent mesenchymal cells can differentiate into hematopoietic and cobblestone area-supporting cells., *Exp Hematol*, vol. 31, no. 8, pp. 715–722, 2003 Aug.

215. H. Cao, Y. Chu, H. Zhu, J. Sun, Y. Pu, Z. Gao, C. Yang, S. Peng, Z. Dou, and J. Hua, Characterization of immortalized mesenchymal stem cells derived from foetal porcine pancreas., *Cell Prolif*, vol. 44, no. 1, pp. 19–32, 2011 Feb.

216. W. Cui, D. Wylie, S. Aslam, A. Dinnyes, T. King, I. Wilmut, and A. J. Clark, Telomerase-immortalized sheep fibroblasts can be reprogrammed by nuclear transfer to undergo early development., *Biol Reprod*, vol. 69, no. 1, pp. 15–21, 2003 Jul.

217. H. te Riele, E. R. Maandag, and A. Berns, Highly efficient gene targeting in embryonic stem cells through homologous recombination with isogenic dna constructs., *Proc Natl Acad Sci U S A*, vol. 89, no. 11, pp. 5128–5132, 1992 Jun 1.

218. J. J. Ramsoondar, Z. Machaty, C. Costa, B. L. Williams, W. L. Fodor, and K. R. Bondioli, Production of alpha 1,3-galactosyltransferase-knockout cloned pigs expressing human alpha 1,2-fucosylosyltransferase., *Biol Reprod*, vol. 69, no. 2, pp. 437–445, 2003 Aug.

219. G. Testa, Y. Zhang, K. Vintersten, V. Benes, W. W. M. P. Pijnappel, I. Chambers, A. J. H. Smith, A. G. Smith, and A. F. Stewart, Engineering the mouse genome with bacterial artificial chromosomes to create multipurpose alleles., *Nat Biotechnol*, vol. 21, no. 4, pp. 443–447, 2003 Apr.

220. P. Hasty, J. Rivera-Perez, and A. Bradley, The length of homology required for gene targeting in embryonic stem cells., *Mol Cell Biol*, vol. 11, no. 11, pp. 5586–5591, 1991 Nov.

221. W. J. Montigny, S. F. Phelps, S. Illenye, and N. H. Heintz, Parameters influencing high-efficiency transfection of bacterial artificial chromosomes into cultured mammalian cells., *Biotechniques*, vol. 35, no. 4, pp. 796–807, 2003 Oct.

222. M. M. Marques, A. J. Thomson, K. J. McCreath, and J. McWhir, Conventional gene targeting protocols lead to loss of targeted cells when applied to a silent gene locus in primary fibroblasts., *J Biotechnol*, vol. 125, no. 2, pp. 185–193, 2006 Sep 1.

223. D.-I. Jin, S.-H. Lee, J.-H. Choi, J.-S. Lee, J.-E. Lee, K.-W. Park, and J.-S. Seo, Targeting efficiency of a-1,3-galactosyl transferase gene in pig fetal fibroblast cells., *Exp Mol Med*, vol. 35, no. 6, pp. 572–577, 2003 Dec 31.

224. R. P. Vazquez-Manrique, J. C. Legg, B. Olofsson, S. Ly, and H. A. Baylis, Improved gene targeting in c. elegans using counter-selection and flp-mediated marker excision., *Genomics*, vol. 95, no. 1, pp. 37–46, 2010 Jan.

225. K. R. Thomas and M. R. Capecchi, Targeted disruption of the murine int-1 proto-oncogene resulting in severe abnormalities in midbrain and cerebellar development., *Nature*, vol. 346, no. 6287, pp. 847–850, 1990 Aug 30.

226. M. Zijlstra, E. Li, F. Sajjadi, S. Subramani, and R. Jaenisch, Germ-line transmission of a disrupted beta 2-microglobulin gene produced by homologous recombination in embryonic stem cells., *Nature*, vol. 342, no. 6248, pp. 435–438, 1989 Nov 23.

227. L. Tesson, J.-M. Heslan, S. Menoret, and I. Anegon, Rapid and accurate determination of zygosity in transgenic animals by real-time quantitative pcr., *Transgenic Res*, vol. 11, no. 1, pp. 43–48, 2002 Feb.

228. J. Gomez-Rodriguez, V. Washington, J. Cheng, A. Dutra, E. Pak, P. Liu, D. W. McVicar, and P. L. Schwartzberg, Advantages of q-pcr as a method of screening for gene targeting in mammalian cells using conventional and whole bac-based constructs., *Nucleic Acids Res*, vol. 36, no. 18, p. e117, 2008 Oct.

229. V. P. Belancio, P. L. Deininger, and A. M. Roy-Engel, Line dancing in the human genome: transposable elements and disease., *Genome Med*, vol. 1, no. 10, p. 97, 2009.

230. D. Voehringer, D. Wu, H.-E. Liang, and R. M. Locksley, Efficient generation of long-distance conditional alleles using recombineering and a dual selection strategy in replicate plates., *BMC Biotechnol*, vol. 9, p. 69, 2009.

231. H. Song, S.-K. Chung, and Y. Xu, Modeling disease in human escs using an efficient bac-based homologous recombination system., *Cell Stem Cell*, vol. 6, no. 1, pp. 80–89, 2010 Jan 8.

232. S. F. Phelps, S. Illenye, and N. H. Heintz, Manipulating genes and gene copy number by bacterial artificial chromosomes transfection., *Methods Mol Biol*, vol. 383, pp. 153–163, 2007.

233. J. D. Heaney, A. N. Rettew, and S. K. Bronson, Tissue-specific expression of a bac transgene targeted to the hprt locus in mouse embryonic stem cells., *Genomics*, vol. 83, no. 6, pp. 1072–1082, 2004 Jun.

234. J. M. Sedivy, B. Vogelstein, H. J. Liber, E. A. Hendrickson, and A. Rosmarin, Gene targeting in human cells without isogenic dna, *Science*, vol. 283, p. 9a, 1999.

235. E. Giulotto and N. Israel, Dna-mediated gene transfer is more efficient during s-phase of the cell cycle., *Biochem Biophys Res Commun*, vol. 118, no. 1, pp. 310–316, 1984 Jan 13.

236. T. Yorifuji, S. Tsuruta, and H. Mikawa, The effect of cell synchronization on the efficiency of stable gene transfer by electroporation., *FEBS Lett*, vol. 245, no. 1-2, pp. 201–203, 1989 Mar 13.

237. M. Takahashi, T. Furukawa, K. Nikkuni, A. Aoki, N. Nomoto, T. Koike, Y. Moriyama, S. Shinada, and A. Shibata, Efficient introduction of a gene into hematopoietic cells in s-phase by electroporation., *Exp Hematol*, vol. 19, no. 5, pp. 343–346, 1991 Jun.

238. M. Takata, M. S. Sasaki, E. Sonoda, C. Morrison, M. Hashimoto, H. Utsumi, Y. Yamaguchi-Iwai, A. Shinohara, and S. Takeda, Homologous recombination and non-homologous end-joining pathways of dna double-strand break repair have overlapping roles in the maintenance of chromosomal integrity in vertebrate cells., *EMBO J*, vol. 17, no. 18, pp. 5497–5508, 1998 Sep 15.

239. L. Lai, D. Kolber-Simonds, K.-W. Park, H.-T. Cheong, J. L. Greenstein, G.-S. Im, M. Samuel, A. Bonk, A. Rieke, B. N. Day, C. N. Murphy, D. B. Carter, R. J. Hawley, and R. S. Prather, Production of alpha-1,3-galactosyltransferase knockout pigs by nuclear transfer cloning., *Science*, vol. 295, no. 5557, pp. 1089–1092, 2002 Feb 8.

240. C. S. Rogers, Y. Hao, T. Rokhlina, M. Samuel, D. A. Stoltz, Y. Li, E. Petroff, D. W. Vermeer, A. C. Kabel, Z. Yan, L. Spate, D. Wax, C. N. Murphy, A. Rieke, K. Whitworth, M. L. Linville, S. W. Korte, J. F. Engelhardt, M. J. Welsh, and R. S. Prather, Production of cftr-null and cftr-deltaf508 heterozygous pigs by adeno-associated virus-mediated gene targeting and somatic cell nuclear transfer., *J Clin Invest*, vol. 118, no. 4, pp. 1571–1577, 2008 Apr.

241. R. Tomii, M. Kurome, N. Wako, T. Ochiai, H. Matsunari, K. Kano, and H. Nagashima, Production of cloned pigs by nuclear transfer of preadipocytes following cell cycle synchronization by differentiation induction., *J Reprod Dev*, vol. 55, no. 2, pp. 121–127, 2009 Apr.

242. H. J. Oh, J. E. Park, M. J. Kim, S. G. Hong, J. C. Ra, J. Y. Jo, S. K. Kang, G. Jang, and B. C. Lee, Recloned dogs derived from adipose stem cells of a transgenic cloned beagle., *Theriogenology*, vol. 75, no. 7, pp. 1221–1231, 2011 Apr 15.

243. J. R. Hill, R. C. Burghardt, K. Jones, C. R. Long, C. R. Looney, T. Shin, T. E. Spencer, J. A. Thompson, Q. A. Winger, and M. E. Westhusin, Evidence for placental abnormality as the major cause of mortality in first-trimester somatic cell cloned bovine fetuses., *Biol Reprod*, vol. 63, no. 6, pp. 1787–1794, 2000 Dec.

244. A. Ogura, K. Inoue, N. Ogonuki, J. Lee, T. Kohda, and F. Ishino, Phenotypic effects of somatic cell cloning in the mouse., *Cloning Stem Cells*, vol. 4, no. 4, pp. 397–405, 2002.

245. Y. Ono and T. Kono, Irreversible barrier to the reprogramming of donor cells in cloning with mouse embryos and embryonic stem cells., *Biol Reprod*, vol. 75, no. 2, pp. 210–216, 2006 Aug.

246. X. Yang, S. L. Smith, X. C. Tian, H. A. Lewin, J.-P. Renard, and T. Wakayama, Nuclear reprogramming of cloned embryos and its implications for therapeutic cloning., *Nat Genet*, vol. 39, no. 3, pp. 295–302, 2007 Mar.

247. P. G. Shiels, A. J. Kind, K. H. Campbell, I. Wilmut, D. Waddington, A. Colman, and A. E. Schnieke, Analysis of telomere length in dolly, a sheep derived by nuclear transfer., *Cloning*, vol. 1, no. 2, pp. 119–125, 1999.

248. D. H. Betts, S. D. Perrault, J. Petrik, L. Lin, L. A. Favetta, C. L. Keefer, and W. A. King, Telomere length analysis in goat clones and their offspring., *Mol Reprod Dev*, vol. 72, no. 4, pp. 461–470, 2005 Dec.

249. R. P. Lanza, J. B. Cibelli, C. Blackwell, V. J. Cristofalo, M. K. Francis, G. M. Baerlocher, J. Mak, M. Schertzer, E. A. Chavez, N. Sawyer, P. M. Lansdorp, and M. D. West, Extension of cell life-span and telomere length in animals cloned from senescent somatic cells., *Science*, vol. 288, no. 5466, pp. 665–669, 2000 Apr 28.

250. W.-Q. Jiang, Z.-H. Zhong, J. D. Henson, A. A. Neumann, A. C.-M. Chang, and R. R. Reddel, Suppression of alternative lengthening of telomeres by sp100-mediated sequestration of the mre11/rad50/nbs1 complex., *Mol Cell Biol*, vol. 25, no. 7, pp. 2708–2721, 2005 Apr.

251. H. Y. Jeon, S. H. Hyun, G. S. Lee, H. S. Kim, S. Kim, Y. W. Jeong, S. K. Kang, B. C. Lee, J. Y. Han, C. Ahn, and W. S. Hwang, The analysis of telomere length and telomerase activity in cloned pigs and cows., *Mol Reprod Dev*, vol. 71, no. 3, pp. 315–320, 2005 Jul.

252. J. Fulka, H. Fulka, T. Slavik, K. Okada, and J. J. Fulka, Dna methylation pattern in pig in vivo produced embryos., *Histochem Cell Biol*, vol. 126, no. 2, pp. 213–217, 2006 Aug.

253. M. Monk, M. Boubelik, and S. Lehnert, Temporal and regional changes in dna methylation in the embryonic, extraembryonic and germ cell lineages during mouse embryo development., *Development*, vol. 99, no. 3, pp. 371–382, 1987 Mar.

254. J. Lee, K. Inoue, R. Ono, N. Ogonuki, T. Kohda, T. Kaneko-Ishino, A. Ogura, and F. Ishino, Erasing genomic imprinting memory in mouse clone embryos produced from day 11.5 primordial germ cells., *Development*, vol. 129, no. 8, pp. 1807–1817, 2002 Apr.

255. L. Jiang, P. Jobst, L. Lai, M. Samuel, D. Ayares, R. S. Prather, and X. C. Tian, Expression levels of growth-regulating imprinted genes in cloned piglets., *Cloning Stem Cells*, vol. 9, no. 1, pp. 97–106, 2007 Spring.

256. S. Choufani, C. Shuman, and R. Weksberg, Beckwith-wiedemann syndrome., *Am J Med Genet C Semin Med Genet*, vol. 154C, no. 3, pp. 343–354, 2010 Aug 15.

257. W. Dean, F. Santos, M. Stojkovic, V. Zakhartchenko, J. Walter, E. Wolf, and W. Reik, Conservation of methylation reprogramming in mammalian development: aberrant reprogramming

in cloned embryos., *Proc Natl Acad Sci U S A*, vol. 98, no. 24, pp. 13734–13738, 2001 Nov 20.

258. W. Dean, F. Santos, and W. Reik, Epigenetic reprogramming in early mammalian development and following somatic nuclear transfer., *Semin Cell Dev Biol*, vol. 14, no. 1, pp. 93–100, 2003 Feb.

259. C. Allegrucci, Y.-Z. Wu, A. Thurston, C. N. Denning, H. Priddle, C. L. Mummery, D. Ward-van Oostwaard, P. W. Andrews, M. Stojkovic, N. Smith, T. Parkin, M. E. Jones, G. Warren, L. Yu, R. M. Brena, C. Plass, and L. E. Young, Restriction landmark genome scanning identifies culture-induced dna methylation instability in the human embryonic stem cell epigenome., *Hum Mol Genet*, vol. 16, no. 10, pp. 1253–1268, 2007 May 15.

260. Y. K. Kang, D. B. Koo, J. S. Park, Y. H. Choi, H. N. Kim, W. K. Chang, K. K. Lee, and Y. M. Han, Typical demethylation events in cloned pig embryos. clues on species-specific differences in epigenetic reprogramming of a cloned donor genome., *J Biol Chem*, vol. 276, no. 43, pp. 39980–39984, 2001 Oct 26.

261. Y. K. Kang, D. B. Koo, J. S. Park, Y. H. Choi, A. S. Chung, K. K. Lee, and Y. M. Han, Aberrant methylation of donor genome in cloned bovine embryos., *Nat Genet*, vol. 28, no. 2, pp. 173–177, 2001 Jun.

262. Y. M. Han, Y. K. Kang, D. B. Koo, and K. K. Lee, Nuclear reprogramming of cloned embryos produced in vitro., *Theriogenology*, vol. 59, no. 1, pp. 33–44, 2003 Jan 1.

263. N. Beaujean, J. Taylor, J. Gardner, I. Wilmut, R. Meehan, and L. Young, Effect of limited dna methylation reprogramming in the normal sheep embryo on somatic cell nuclear transfer., *Biol Reprod*, vol. 71, no. 1, pp. 185–193, 2004 Jul.

264. A. J. Bonk, H.-T. Cheong, R. Li, L. Lai, Y. Hao, Z. Liu, M. Samuel, E. A. Fergason, K. M. Whitworth, C. N. Murphy, E. Antoniou, and R. S. Prather, Correlation of developmental differences of nuclear transfer embryos cells to the methylation profiles of nuclear transfer donor cells in swine., *Epigenetics*, vol. 2, no. 3, pp. 179–186, 2007 Sep.

265. D. Humpherys, K. Eggan, H. Akutsu, A. Friedman, K. Hochedlinger, R. Yanagimachi, E. S. Lander, T. R. Golub, and R. Jaenisch, Abnormal gene expression in cloned mice derived from embryonic stem cell and cumulus cell nuclei., *Proc Natl Acad Sci U S A*, vol. 99, no. 20, pp. 12889–12894, 2002 Oct 1.

266. Z. Beyhan, P. J. Ross, A. E. Iager, A. M. Kocabas, K. Cunniff, G. J. Rosa, and J. B. Cibelli, Transcriptional reprogramming of somatic cell nuclei during preimplantation development of cloned bovine embryos., *Dev Biol*, vol. 305, no. 2, pp. 637–649, 2007 May 15.

267. R. Vassena, Z. Han, S. Gao, D. A. Baldwin, R. M. Schultz, and K. E. Latham, Tough beginnings: alterations in the transcriptome of cloned embryos during the first two cell cycles., *Dev Biol*, vol. 304, no. 1, pp. 75–89, 2007 Apr 1.

268. S. L. Smith, R. E. Everts, X. C. Tian, F. Du, L.-Y. Sung, S. L. Rodriguez-Zas, B.-S. Jeong, J.-P. Renard, H. A. Lewin, and X. Yang, Global gene expression profiles reveal significant nuclear reprogramming by the blastocyst stage after cloning., *Proc Natl Acad Sci U S A*, vol. 102, no. 49, pp. 17582–17587, 2005 Dec 6.

269. J. Zhao, Y. Hao, J. W. Ross, L. D. Spate, E. M. Walters, M. S. Samuel, A. Rieke, C. N. Murphy, and R. S. Prather, Histone deacetylase inhibitors improve in vitro and in vivo developmental competence of somatic cell nuclear transfer porcine embryos., *Cell Reprogram*, vol. 12, no. 1, pp. 75–83, 2010 Feb.

270. J. Zhao, J. W. Ross, Y. Hao, L. D. Spate, E. M. Walters, M. S. Samuel, A. Rieke, C. N. Murphy, and R. S. Prather, Significant improvement in cloning efficiency of an inbred miniature pig by histone deacetylase inhibitor treatment after somatic cell nuclear transfer., *Biol Reprod*, vol. 81, no. 3, pp. 525–530, 2009 Sep.

271. K. Miyoshi, H. Mori, Y. Mizobe, E. Akasaka, A. Ozawa, M. Yoshida, and M. Sato, Valproic acid enhances in vitro development and oct-3/4 expression of miniature pig somatic cell nuclear transfer embryos., *Cell Reprogram*, vol. 12, no. 1, pp. 67–74, 2010 Feb.

272. Y. Huang, X. Tang, W. Xie, Y. Zhou, D. Li, C. Yao, Y. Zhou, J. Zhu, L. Lai, H. Ouyang, and D. Pang, Histone deacetylase inhibitor significantly improved the cloning efficiency of porcine somatic cell nuclear transfer embryos., *Cell Reprogram*, vol. 13, no. 6, pp. 513–520, 2011 Dec.

273. Y. Liu, O. Ostrup, J. Li, G. Vajta, L. Lin, P. M. Kragh, S. Purup, P. Hyttel, and H. Callesen, Increased blastocyst formation of cloned porcine embryos produced with donor cells pretreated with xenopus egg extract and/or digitonin., *Zygote*, vol. 20, no. 1, pp. 61–66, 2012 Feb.

274. A. J. Rathbone, P. A. Fisher, J.-H. Lee, J. Craigon, and K. H. S. Campbell, Reprogramming of ovine somatic cells with xenopus laevis oocyte extract prior to scnt improves live birth rate., *Cell Reprogram*, vol. 12, no. 5, pp. 609–616, 2010 Oct.

275. D. Biswas, E. M. Jung, E. B. Jeung, and S. H. Hyun, Effects of vascular endothelial growth factor on porcine preimplantation embryos produced by in vitro fertilization and somatic cell nuclear transfer., *Theriogenology*, vol. 75, no. 2, pp. 256–267, 2011 Jan 15.

276. D. Biswas and S. H. Hyun, Supplementation with vascular endothelial growth factor during in vitro maturation of porcine cumulus oocyte complexes and subsequent developmental competence after in vitro fertilization., *Theriogenology*, vol. 76, no. 1, pp. 153–160, 2011 Jul 1.

277. Y. Huang, X. Tang, W. Xie, Y. Zhou, D. Li, Y. Zhou, J. Zhu, T. Yuan, L. Lai, D. Pang, and H. Ouyang, Vitamin c enhances in vitro and in vivo development of porcine somatic cell nuclear transfer embryos., *Biochem Biophys Res Commun*, vol. 411, no. 2, pp. 397–401, 2011 Jul 29.

278. D. W. Russell and R. K. Hirata, Human gene targeting by viral vectors., *Nat Genet*, vol. 18, no. 4, pp. 325–330, 1998 Apr.

279. J. R. Chamberlain, D. R. Deyle, U. Schwarze, P. Wang, R. K. Hirata, Y. Li, P. H. Byers, and D. W. Russell, Gene targeting of mutant col1a2 alleles in mesenchymal stem cells from individuals with osteogenesis imperfecta., *Mol Ther*, vol. 16, no. 1, pp. 187–193, 2008 Jan.

280. Y. Luo, J. Li, Y. Liu, L. Lin, Y. Du, S. Li, H. Yang, G. Vajta, H. Callesen, L. Bolund, and C. B. Sorensen, High efficiency of brca1 knockout using raav-mediated gene targeting: developing a pig model for breast cancer., *Transgenic Res*, vol. 20, no. 5, pp. 975–988, 2011 Oct.

281. R. D. Hickey, J. B. Lillegard, J. E. Fisher, T. J. McKenzie, S. E. Hofherr, M. J. Finegold, S. L. Nyberg, and M. Grompe, Efficient production of fah-null heterozygote pigs by chimeric adeno-associated virus-mediated gene knockout and somatic cell nuclear transfer., *Hepatology*, vol. 54, no. 4, pp. 1351–1359, 2011 Oct.

282. A. Osiak, F. Radecke, E. Guhl, S. Radecke, N. Dannemann, F. Lutge, S. Glage, C. Rudolph, T. Cantz, K. Schwarz, R. Heilbronn, and T. Cathomen, Selection-independent generation of gene knockout mouse embryonic stem cells using zinc-finger nucleases., *PLoS One*, vol. 6, no. 12, p. e28911, 2011.

283. T. Mashimo, A. Takizawa, B. Voigt, K. Yoshimi, H. Hiai, T. Kuramoto, and T. Serikawa, Generation of knockout rats with x-linked severe combined immunodeficiency (x-scid) using zinc-finger nucleases., *PLoS One*, vol. 5, no. 1, p. e8870, 2010.

284. J. M. McCammon and S. L. Amacher, Using zinc finger nucleases for efficient and heritable gene disruption in zebrafish., *Methods Mol Biol*, vol. 649, pp. 281–298, 2010.

285. A. Lombardo, P. Genovese, C. M. Beausejour, S. Colleoni, Y.-L. Lee, K. A. Kim, D. Ando, F. D. Urnov, C. Galli, P. D. Gregory, M. C. Holmes, and L. Naldini, Gene editing in human

stem cells using zinc finger nucleases and integrase-defective lentiviral vector delivery., *Nat Biotechnol*, vol. 25, no. 11, pp. 1298–1306, 2007 Nov.

286. C. Mussolino, R. Morbitzer, F. Lutge, N. Dannemann, T. Lahaye, and T. Cathomen, A novel tale nuclease scaffold enables high genome editing activity in combination with low toxicity., *Nucleic Acids Res*, vol. 39, no. 21, pp. 9283–9293, 2011 Nov.

287. K. Takahashi and S. Yamanaka, Induction of pluripotent stem cells from mouse embryonic and adult fibroblast cultures by defined factors., *Cell*, vol. 126, no. 4, pp. 663–676, 2006 Aug 25.

288. K. Takahashi, K. Tanabe, M. Ohnuki, M. Narita, T. Ichisaka, K. Tomoda, and S. Yamanaka, Induction of pluripotent stem cells from adult human fibroblasts by defined factors., *Cell*, vol. 131, no. 5, pp. 861–872, 2007 Nov 30.

289. Y. Li, M. Cang, A. S. Lee, K. Zhang, and D. Liu, Reprogramming of sheep fibroblasts into pluripotency under a drug-inducible expression of mouse-derived defined factors., *PLoS One*, vol. 6, no. 1, p. e15947, 2011.

290. M.-Y. Chang, D. Kim, C.-H. Kim, H.-C. Kang, E. Yang, J.-I. Moon, S. Ko, J. Park, K.-S. Park, K.-A. Lee, D.-Y. Hwang, Y. Chung, R. Lanza, and K.-S. Kim, Direct reprogramming of rat neural precursor cells and fibroblasts into pluripotent stem cells., *PLoS One*, vol. 5, no. 3, p. e9838, 2010.

291. J. Okahara-Narita, R. Umeda, S. Nakamura, T. Mori, T. Noce, and R. Torii, Induction of pluripotent stem cells from fetal and adult cynomolgus monkey fibroblasts using four human transcription factors., *Primates*, 2011 Nov 11.

292. T. Ezashi, B. P. V. L. Telugu, A. P. Alexenko, S. Sachdev, S. Sinha, and R. M. Roberts, Derivation of induced pluripotent stem cells from pig somatic cells., *Proc Natl Acad Sci U S A*, vol. 106, no. 27, pp. 10993–10998, 2009 Jul 7.

293. B. P. V. L. Telugu, T. Ezashi, and R. M. Roberts, Porcine induced pluripotent stem cells analogous to naive and primed embryonic stem cells of the mouse., *Int J Dev Biol*, vol. 54, no. 11-12, pp. 1703–1711, 2010.

294. Z. Wu, J. Chen, J. Ren, L. Bao, J. Liao, C. Cui, L. Rao, H. Li, Y. Gu, H. Dai, H. Zhu, X. Teng, L. Cheng, and L. Xiao, Generation of pig induced pluripotent stem cells with a drug-inducible system., *J Mol Cell Biol*, vol. 1, no. 1, pp. 46–54, 2009 Oct.

295. M. A. Esteban, J. Xu, J. Yang, M. Peng, D. Qin, W. Li, Z. Jiang, J. Chen, K. Deng, M. Zhong, J. Cai, L. Lai, and D. Pei, Generation of induced pluripotent stem cell lines from tibetan miniature pig., *J Biol Chem*, vol. 284, no. 26, pp. 17634–17640, 2009 Jun 26.

296. N. Montserrat, E. G. Bahima, L. Batlle, S. Hafner, A. M. C. Rodrigues, F. Gonzalez, and J. C. Izpisua Belmonte, Generation of pig ips cells: a model for cell therapy., *J Cardiovasc Transl Res*, vol. 4, no. 2, pp. 121–130, 2011 Apr.

297. G. Wu, N. Liu, I. Rittelmeyer, A. D. Sharma, M. Sgodda, H. Zaehres, M. Bleidissel, B. Greber, L. Gentile, D. W. Han, C. Rudolph, D. Steinemann, A. Schambach, M. Ott, H. R. Scholer, and T. Cantz, Generation of healthy mice from gene-corrected disease-specific induced pluripotent stem cells., *PLoS Biol*, vol. 9, no. 7, p. e1001099, 2011 Jul.

298. G. Faust, Creation of immunodeficient pigs (rag1 and rag2 knockouts) using recombineering, 2008.

6. Abbreviations

APC	Antigen presenting cell
BAC	Bacterial artificial chromosome
BCR	B cell antigen receptor
BM	Bone marrow
BSA	Bovine serum albumin
BWS	Beckwith-Wiedemann-Syndrome
CCN	CAGGS-Cherry/ NLS
cDNA	Copy DNA
CFTR	Cystic fibrosis transmembrane conductance regulator
CMV	Cytomegalo virus
COL1A1	Collagen type1 α
Ct	Cycle threshold
DAPI	4,6-Diamidino-2-phenylindol
DL	German landrace
DMEM	Dulbecco's modified Eagle's medium
DMMB	1,9-dimethylmethylene blue
DMSO	Dimethyl sulfoxide
DNA	Desoxyribonucleic acid
DNase	Desoxyribonuclease
dNTP	Deoxynucleotide triphosphate
DPF	Designated pathogen-free
DSB	Double strand break
dTTP	Desoxythymidin-5'-triphosphate
dUTP	Desoxyuridin-5'-triphosphate
dsDNA	Double stranded DNA
DTT	Dithiothreitol
EDTA	Ethylenediamine tetracetic acid
eGFP	Enhanced green fluorescent protein
E. coli	Escherichia coli
ES cell	Embryonic stem cell

ET	Embryo transfer
FBS	Fetal bovine serum
FGF	Fibroblast growth factor
FISH	Fluorescence *in situ* hybridisation
FITC	Fluorescein-5-isothiocyanat
GGTA1	α-1,3-galactosyltransferase
HBS	HEPES buffered saline
HBSS	Hank's Buffered Salt Solution
HEPES	[4-(2-Hydroxyethyl)-piperazino]-ethansulfonicsaeureXXX
HIV	Human immunodeficiency virus
HLA	Human leukocyte antigen
HPRT	Hypoxanthine phosphoribosyl transferase
HSC	Hematopoietic stem cell
hTERT	Human telomerase reverse transcriptase
IL	Interleukin
IL2RG	Interleukin 2 receptor gamma
IFN	Interferon
iPS cell	Induced pluripotent stem cell
ITS	Insulin/ transferrin/ selenit
JAK	Janus kinase
JAK3	Janus kinase 3
LB	Luria-Bertani
SINE	Short interspersed element
MIX	3-methyl-isobutylxanthine
MSC	Mesenchymal stem cell
mRNA	Messenger RNA
NEAA	Non-essential amino acids
NK cell	Natural killer cell
p	Passage
pAD-MSC	Porcine adipose tissue mesenchymal stem cell
pBM-MSC	Porcine bone marrow mesenchymal stem cell
PBMC	Peripheral blood mononuclear cell
PBS	Phosphate buffered saline
PCR	Polymerase chain reaction
PD	Population doublings
Pen/ Strep	Penicillin/ streptomycin
PGK	Phosphoglycerate kinase

PNS	Positive negative selection
pMSC	Porcine mesenchymal stem cell
pKDNF	Porcine kidney fibroblast
poFF	Porcine fetal fibroblast
qPCR	Quantitative PCR
r	Recombinant
RAG	Recombination activating gene
RNA	Ribonucleic acid
RNase	Ribonuclease
rpm	Revolutions per minute
RT	Reverse transcription
RT	Reverse transcriptase
RT-PCR	Reverse transcriptase PCR
SCNT	Somatic cell nuclear transfer
SDS	Sodium dodecyl sulphate
SINE	Short interspersed element
STAT	Signal transducer and activator of transcription
SV 40	Simian virus 40
TAE	Tris acetate EDTA
TBE	Tris borate EDTA
TCR	T cell antigen receptor
TE	tris base/ EDTA buffer
TNF-α	Tumor necrosis factor α
TRIS	Tris(hydroxymethyl-)-aminomethan
X-Gal	5-Brom-4-chlor-3-indolyl-ß-D-galactopyranosid
X-SCID	X-linked severe combined immunodeficiency
ZFN	Zinc finger nuclease

A. Appendix

A.1. Molecular cloning of the JAK3 conventional targeting vector

The sequence of the conventional JAK3 targeting vector was derived from porcine BAC clone CH242-317A24. The BAC was modified by recombineering, in order to replace JAK3 exon 2 to exon 5 by a positive selection cassette flanked by two loxP sites. This cassette contains a neo resistance gene expressed both from a prokaryotic (em7) and eukaryotic (PGK) promoter. This loxP-PGK-em7-neo-loxP cassette is termed PGK-neo cassette for brevity.

First, a recombineering vector was cloned for the purpose of selection marker integration into the BAC. Figure A.1 shows a schematic overview of the important constructs and the restriction sites used. Table A.1 lists PCR details for amplified products used. 5' and 3' homology regions (HR2 and HR2b) were obtained by PCR amplification and then subcloned into pJET1.2/blunt and pGEM-T Easy, respectively. Excision of HR2 from *pJET1.2/blunt HR2* at the KpnI/EcoRI restriction sites introduced with the PCR primer overhangs was followed by subcloning into pL452 at the same sites. Subsequently, HR2b was obtained from *pGEM-T Easy HR2b* by NotI restriction digest and insertion into pL452 HR2. The linear recombineering cassette with the PGK-neo flanked by HR2 and HR2b was obtained by KpnI/SacII digestion of this newly cloned vector named *pL452 JAK3 HR2/2b*. Recombineering was performed by transformation of the heat-induced SW106 *E.coli* strain, which contained the JAK3 wildtype BAC. The modified construct was termed *JAK3-neo BAC* (Figure A.1A).

The JAK3 targeting vector was derived from this BAC. Short and long arm were obtained separately by PCR and long-range PCR amplification and subcloning into pJET1.2/blunt and pGEM-T Easy, respectively (Figure A.1B). JAK3 short arm PCR had a 5' KpnI and 3' EcoRI restriction site overhangs and was transferred into into pBluescriptIISK+. The PGK-neo cassette was cut from pL452 JAK3 HR2/2b and inserted in the same EcoRI restriction site. This new vector was named *pBlue2SK+ short/neo*. The vector was extended by introduction of CCN by PvuI digestion of *pSL1180 Amersham* CCN and ligation with the compatible DNA ends from PacI linearisation of JAK3 TV (Figures A.1 and A.2B). The long arm was transferred to this vector from pGEM-T Easy with a NotI digest. The completed vector was named *JAK3 TV CCN*.

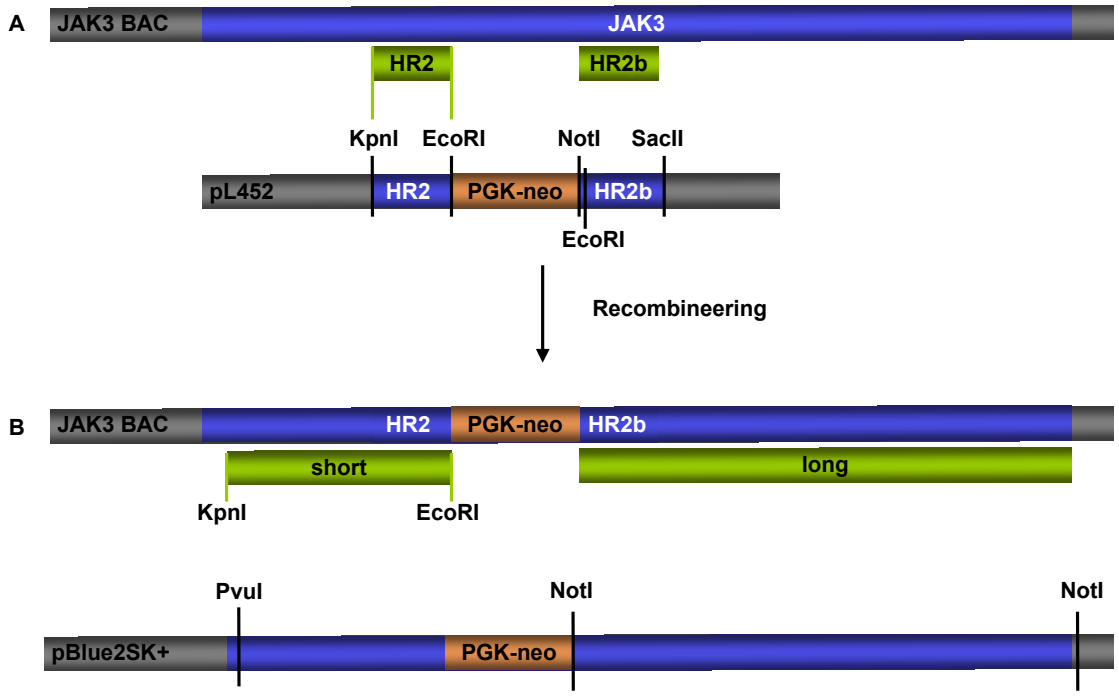

Figure A.1.: Molecular cloning of the JAK3 targeting vector schematic overview
A: Homology regions HR2 and HR2b were derived by PCR (green) from the JAK3 wildtype BAC. The regions were transferred into the recombineering vector pL452 after subcloning in pJET1.2/blunt and pGEM-T Easy, respectively. HR2 had KpnI and EcoRI restriction sites introduced by PCR primer overhangs. HR2b insertion into pL452 used NotI and SacII restriction sites from the multiple cloning site of pGEM-T Easy. Recombineering between this vector and the JAK3 BAC produced the JAK3-neo BAC. B: Short and long arm sequences for the targeting vector were obtained by PCR from JAK3-neo BAC and subcloned into pJET1.2/blunt and pGEM-T Easy, respectively (green). The short arm was transferred to pBluescriptIISK+ using KpnI and EcoRI primer derived overhangs. The PGK-neo cassette was obtained from the recombineering vector previously generated and joined to the short arm using a EcoRI restriction digest. Long arm insertion into the NotI site of pBluescriptIISK+ short/neo completed JAK3 TV. The CCN cassette was introduced into the PacI restriction site.

Table A.1.: PCR details for molecular cloning of JAK3 TV
Product and primer names, product sizes, vector names and important notes are listed.

Product	primers	size	vector	notes
HR2	P1_F, P2_R	591 bp	pJET1.2/blunt	KpnI and EcoRI overhangs
HR2b	HR2b_F, HR2b_R	510 bp	pGEM-T Easy	NotI/SacII digest from vector
Short	Short_F, P2_R	3.2 kb	pJET1.2/blunt	KpnI, EcoRI primer overhangs
Long arm	Long_F, Long_R	10 kb	pGEM-T Easy	NotI digest from vector
HR1	HR1_F, HR1_R	480 bp	pGEM-T Easy	BamHI/SacI digest from vector

A.2. Molecular cloning of the JAK3 PCR control vector

The PCR control vector was constructed in two steps. First, 400 bp of sequence were removed from pJET 1.2/blunt short by HincII digestion and re-ligation. Second, PGK-neo cut from pBluescriptIISK+ short/neo (see Section A.1) was ligated into the EcoRI restriction site of the previously shortened vector. This new vector was termed JAK3 PCR control.

A.3. Molecular cloning of the visual marker cassette

Introduction of the CCN cassette into the JAK3 conventional vector and the BAC backbones was performed with two approaches described in this section. The cloning strategy is depicted in Figure A.2 and primers are listed in Table A.2.

A.3.1. Cloning the CCN for the conventional vector

The 196 bp SV40 NLS sequence was amplified from pGL4.76 and cloned into pJET1.2/blunt. It was cut out with MluI, blunted and inserted into the blunted HindIII site of pCAGGS-Cherry Figure A.2A. This new CCN cassette was cut out by SpeI/BamHI digestion from pCAGGS Cherry NLS, blunted and inserted into the HpaI restriction site of pSL1180 Amersham (FigureA.2B). This vector pSL1180 Amersham CCN was used for introduction of the CCN cassette into JAK3 TV.

A.3.2. Cloning the CCN for BAC recombineering

The CCN cassette was introduced into the BAC backbones by recombineering. For easier selection of correct events, the recombineering vector was designed to carry an ampicilin resistance gene. It was introduced into the backbone at a site to disrupt the chloramphenicol resistance gene. Thus, screening for Amp^{+}/Cam^{-} clones could be performed.

The ampicilin resistance gene and its promoter were amplified by PCR from pGEM-T Easy and subcloned into pJET1.2/blunt (Figure A.2C). This vector, *pJET1.2/blunt Amp*, was digested with SwaI/PvuII, blunted and transferred into the EcoRV restriction site of pSL1180 Amersham CCN From this new vector the CCN-Amp cassette was cut with MluI/PsiI and blunted (Figure A.2D).

To generate the homology regions from the BAC backbone (BB) sequence, PCR amplification was performed on BAC DNA. The product was subcloned in pGEM-T Easy and digested with FaqI/MscI (Figure A.2E). The CCN-Amp cassette was ligated at this location. The linear recombineering cassette was obtained by SacII/BstXI digestion of this vector *pGEM-T Easy BAC BB rec*.

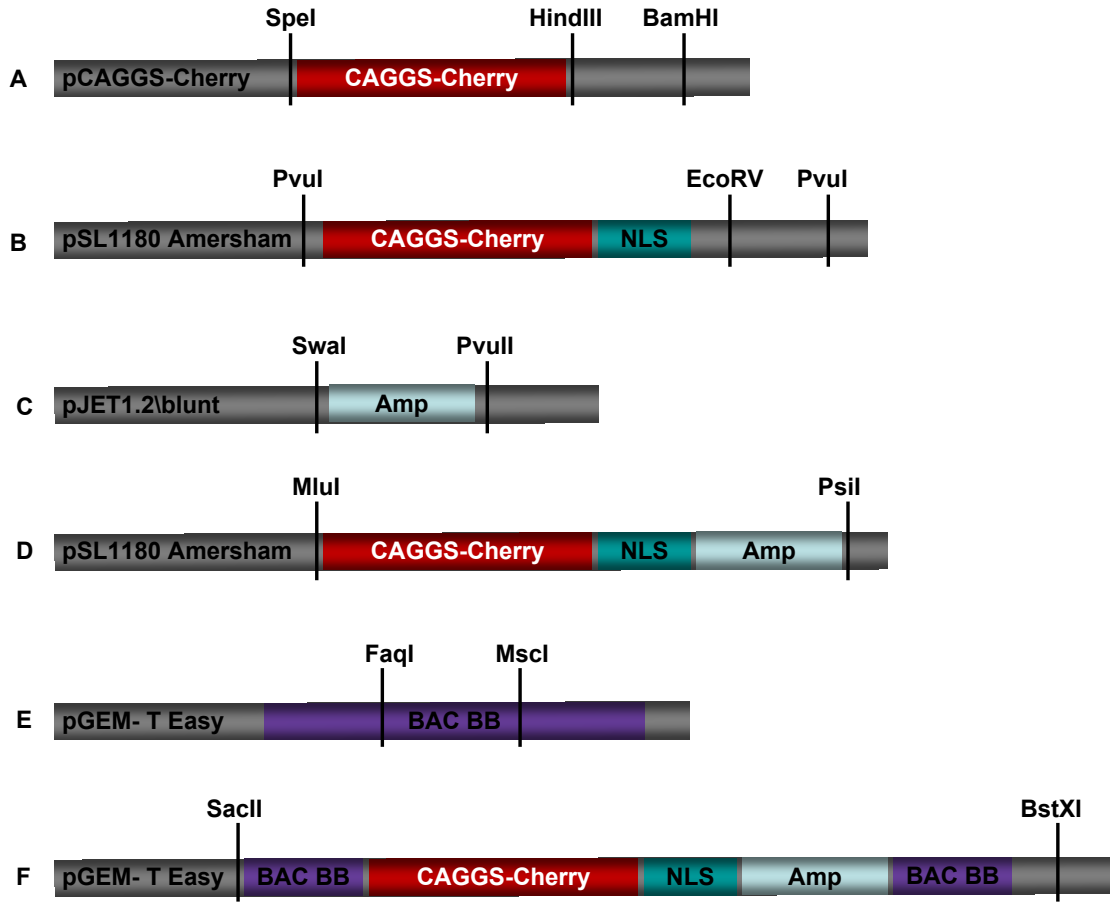

Figure A.2.: Molecular cloning of the JAK3 targeting vector schematic overview
A and B: The PCR amplified NLS was iserted at the HindIII site of pCAGGS-Cherry. CCN was transferred with SpeI/BamHI digestion and cloning into pSL1180 Amersham HpaI site. C and D: PCR amplified Amp resistance was subcloned into pJET1.2/blunt and transferred after SwaI/PvuII digestion and blunting into the pSL1180 CCN EcoRV site. E: Blunt cloning of CCN-Amp (MluI/PsiI) into pGEM-T Easy BAC BB (FaqI/MscI) produced the recombineering vector pGEM-T Easy BAC BB rec. The cassette was removed from the vector with SacII/BstXI digestion.

Table A.2.: PCR details for molecular cloning of JAK3 TV
Product and primer names, product sizes, vector names and important notes are listed.

Product	primers	size	vector	notes
NLS	NLS_F, NLS_R	196 bp	pJET1.2/blunt	MluI digest from vector
BAC BB	BB_F, BB_R	1.5/,kb	pGEM-T Easy	SacII/BstXI digest from vector
Amp	Amp_F, Amp_R	900 bp	pJET1.2/blunt	SwaI/PvuII

A.4. Molecular cloning of the PGK-geo based BACs

A.4.1. Molecular cloning of the PGK-geo cassette

The PGK-geo recombineering cassette was constructed by removal of neo sequence parts from pL452 with a NcoI restriction digest. NcoI cuts just in front of neo and within the gene. Partial transfer of lacZ-neo fusion gene geo from the vector pβ-geo was performed. Here, NcoI cuts again in front of the gene and in neo. This fragment was transferred to pL452, which was then named *pL452 geo*.

A.4.2. Molecular cloning of JAK3-geo-CCN BAC

Table A.1 lists PCR details for amplified products used. 5' and 3' homology regions (HR2 and HR1) were obtained by PCR amplification and then subcloned into pJET1.2/blunt and pGEM-T Easy, respectively. HR1 was obtained from *pGEM-T Easy HR2* by BamHI/SacI restriction digest and insertion into pL452 geo. Excision of HR2 from *pJET1.2/blunt HR2* at the KpnI/EcoRI restriction sites introduced with the PCR primer overhangs was followed by subcloning into pL452 geo HR1. The linear recombineering cassette with the PGK-geo flanked by HR2 and HR1 was obtained by KpnI/BstXI digestion of this newly cloned vector named *pL452 geo HR2/1*. Recombineering was performed by transformation of the heat-induced SW106 *E.coli* strain, which contained the JAK3 wildtype BAC. The modified construct was termed *JAK3-geo BAC*.

A.4.3. Molecular cloning of RAG2-geo BAC

Recombineering was performed by transformation of the heat-induced SW106 *E.coli* strain, which contained the JAK3 wildtype BAC. The modified construct was termed *RAG2-geo BAC*. The recombineering cassette was generated according to Faust (2008) [298]. Instead of using pL452, pL452-geo was applied for insertion of the homology arms.

A.5. Molecular cloning of pPGK-TK/PGK-neo

To test the function of HSV-TK in pMSC, stable clones expressing TK had to be generated. For this purpose PGK-neo was cut from pL452 with EcoRI/BamHI and inserted into pBluescriptIISK+ PGK-TK. The final vector was named *pPGK-TK/PGK-neo*.

Acknowledgement

This project was funded by the Bayerische Forschungsstiftung.

I would like to thank my supervisor Prof. Dr. Angelika Schnieke for the opportunity to work on this exciting project and for her supervision, the guidance and the support throughout my work.

I would like to thank Dr. Alex Kind for the discussion and his support during my work and the helpful suggestions on my thesis. Furthermore I would like to thank Prof. Dr. Oswald Rottmann and everyone else at the animal research station at Thalhausen for taking care of the animals. I also would like to thank Prof. Dr. Eckhard Wolf, Dr. Barbara Keßler and everyone involved in the nuclear and embryo transfers at the Institute for Molecular Animal Breeding and Biotechnology in Oberschleißheim.

I would like to express my deepest gratitude to all members of the Institute for Livestock Biotechnology. I would like to thank Dr. Tatiana Flisikowska, Dr. Claudia Merkl and Dr. Nooshin Rezaei for their suggestions and their scientific and non- scientific support. I would like to thank Peggy Müller, Marlene Edlinger, Angela Zaruba, Kristina Mosandl, Dr. Simone Kraner, Dr. Krzysztof Flisikowski, Tobias Kranz, Simon Seleneit and Barbara Bauer for all their help and the fun during the past years. Thanks to my fellow Ph.D. students Tobias Richter, Anja Saalfrank, Konrad Fischer, Benedikt Baumer and Xinxin Cui, for their input and the exchange of ideas. I also want to thank my students Johannes Schmidt, Silke Seißenberger, Katrin Reindl, Anne Richter, Fabian Hansen, Denise Nguyen, and Monika Gostic. I want to say a special thank you to Margret Bahnweg, Sulith Christan and Steffen and Viola Löbnitz for their outstanding support and their patience in the lab and in the stable. Huge thanks to Simon Leuchs for the great time, the professional and moral support and our friendship. It was great to work with you all!

Finally, I want to thank Flo and my family for all their love and unlimited support during these years.